acceleration power spectral density represents the objective function to be minimized over the speed range of interest. Finally, the recommendations proposed for improvement in the bounce response of the MAGLEV vehicle are represented numerically in terms of a modified suspension system with optimum elements for design adaptation.

ACKNOWLEDGEMENTS

The author is deeply indebted to her supervisor, Dr. T.S. Sankar, and her co-supervisor, Dr. M. Samaha, for their continued guidance and encouragement throughout the course of this investigation.

The author is grateful to her husband, Mr. Ehab Kotb, for preparing the graphs and illustrations and to Mrs. L. Saab, for her timely effort in typing this manuscript.

Thanks are also due to the Computer Center at Concordia University for their support.

The author gratefully acknowledges the research fellowship provided to her through the Natural Sciences and Engineering Research Council of Canada Grant No. A7104.

TABLE OF CONTENTS

LIST OF FIGURES

Fig. 6.6 The Power Spectral Density of the Vehicle Bounce Acceleration with Guideway Span of 50 m for Optimal Suspension Values.

LIST OF TABLES

NOMENCLATURE

$\underset{\sim}{a}$	Lower bound of the design variables defined as the suspension parameters.
A	Guideway roughness parameter.
$\underset{\sim}{A}_F$	The system matrix corresponding to the filter equations.
$\underset{\sim}{A}_O$	The overall system matrix (filter + vehicle).
A_0, A_n	Standard Fourier coefficients.
$\underset{\sim}{b}$	Upper bound of the design variables defined as the suspension parameters.
$\underset{\sim}{B}_F$	The associated system matrix for the vehicle.
$\underset{\sim}{B}_O$	The associated overall system matrix (Filter + vehicle).
$\underset{\sim}{B}_V$	The associated matrix for the vehicle.
C_i	Viscous damping coefficient of the shock absorbers.
$\underset{\sim}{D}$	Constant covariance matrix for the equivalent white noise input.
$E[\ ]$	Ensemble averaging.
$\underset{\sim}{F}$	The vehicle system matrix
F_{p_i}	Suspension force of the ith magnetic suspension system.
F_{s_i}	Suspension force of the system connecting the vehicle body to the ith levitation magnet.
$\underset{\sim}{G}$	Guideway input disturbance vector.
$H(s)$	Dynamic filter transfer function.
$\underset{\sim}{I}$	Identity matrix.
I_s	Mass moment of inertia of the vehicle body.
K_i	Stiffness of springs connecting the shock absorbers to the vehicle body (in series).
K_{0_i}	Stiffness of springs connected in parallel with the shock absorbers.

K_{p_i}	Equivalent stiffness of the ith magnetic suspension.
L	Half the guideway span length.
M_{p_i}	Mass of the ith levitation magnet.
M_s	Mass of the vehicle body.
PSD	Power Spectral Density.
$\underset{\sim}{q}_0$	Overall system state vector (Filter + vehicle).
$\underset{\sim}{Q}$	Modified input covariance matrix.
s	Laplace domain variable.
$S(\omega)$	Power spectral density with appropriate subscript to denote particular cases.
t	Time domain variable.
$\underset{\sim}{U}$	Filtered white noise vector.
V	vehicle velocity.
W	White noise input.
$\underset{\sim}{W}$	White noise Gaussian disturbance vector.
$\underset{\sim}{X}$	Vehicle state vector.
$\underset{\sim}{X}_d$	Vector of design variables.
Z_G	Guideway displacement in the vertical direction (vertical misalignment).
Z_0	Magnitude of the maximum guideway displacement in the Z direction.
Z_{p_i}	Vertical displacement of the center of the ith levitation magnet.
Z_s	Vertical displacement of the center of gravity of the vehicle body.
$\delta(\tau)$	Dirac delta function.
Δq_{p_i}	Deflection of the ith, primary, magnetic suspension system.
Δq_{s_i}	Deflection of the ith, secondary, mechanical suspension system.

η_i Auxiliary state variable defined for the ith mechanical suspension system.

θ_s Pitch angle of the center of gravity of the vehicle body.

π 3.14.

ℓ_{s_i} Distance between the ith levitation magnet and the center of gravity of the vehicle body.

$\underline{\psi}$ State vector of the overall linear filter representing the input excitations.

ω Frequency of vibration.

CHAPTER 1

INTRODUCTION AND BACKGROUND LITERATURE

1.1 Preliminaries

The turn of this century has witnessed an evolution in the development of the different means of transport to meet with the rising need of the people for fast and efficient urban and interurban movement. Due to energy problems and social consciousness for environmental protection, high speed vehicle design is now receiving increased attention for fast, economical, and comfortable mass transportation. A number of advanced public transportation system have been proposed including air cushion, magnetic suspension, and advanced railway systems.

There appears to be no physical reason why the speed of the conventional railway system based on steel wheels rolling on steel rails should not be further extended. However, at high speeds, the noise and wear problems arising from the wheel-rail contact become acute and would have to be overcome. Also, since most existing tracks are designed presently for slower freight transportation and some passenger service, extending the speed of passenger trains would require the building and construction of new separate rail tracks for the use of rapid transit systems. Even though the technology of contact free suspension systems requires extensive research and refinement and the implementation of such systems for mass transport will be associated with a very high initial capital cost. However, the ever rising cost of fuel and the need for conservation of energy make electrically propelled type vehicles an appealing option in one way for achieving dependable high speed urban

transportation.

A number of advanced contact free suspension systems are now being developed in different countries. France has developed an 80 passenger Tracked Air Cushion Vehicle (TACV) which cruises at 248 km/hr (155 mph) on an elevated guideway. The U.S. Department of Transportation has conducted extensive research on tracked air cushion vehicles for speeds up to 480 km/hr (300 mph). Germany is developing an intercity magnetically levitated vehicle capable of up to 480 km/hr (300 mph) operational speeds over an elevated guideway, and research on similar systems is well underway in U.S., Canada and Japan [1]. Dynamic analysis and performance of such magnetically levitated vehicle system is the objective of this thesis.

There are two different systems of magnetic levitation: the attraction system which suspends a vehicle by means of the attractive force generated between a controlled electromagnet and a ferromagnetic rail [2], and the repulsion system which utilizes the repulsive levitation force generated by the current induced in a normal conducting guideway as a result of the motion of a superconducting coil carried onboard the vehicle [3]. The power needed to activate the levitation system is relatively low for the attraction system and particularly the magnetic drag in the low speed range is relatively low. However, at high speeds it has been theoretically predicted that induced electromagnetic currents will cause a decrease in the suspension forces and hence stability problems may arise [4] for this type of magnetic levitation. In the repulsion system, the power needed to suspend the vehicle is derived from the forward motion of the vehicle. The levitation performance for such system at the proposed cruising speed of up to 480 km/hr (300 mph)

is adequate, but large breaking forces are developed at low speeds due to the high magnetic drag forces [4].

Canada is presently developing a conceptual design for a high speed, repulsive type, magnetically levitated vehicle. One of the problems associated with the design of any new mass transport system is the design of the vehicle suspension that would yield an acceptable ride quality and conform closely with certain recommended specifications. The ride quality specifications are usually expressed in terms of limits of the maximum allowable acceleration levels of the passenger compartment. The investigation reported in this thesis is concerned with the design of the mechanical suspension systems that control the bounce dynamics of the Canadian MAGLEV so that acceptable ride quality can be achieved. The main design features of the Canadian MAGLEV vehicle are briefly described in the following section.

1.2 The Canadian MAGLEV Vehicle

The Canadian MAGLEV vehicle, designed and developed by the Canadian MAGLEV group at the Canadian Institute of Guided Ground Transport and the National Research Council of Canada uses a repulsion levitation system. The proposed design for this vehicle [5] consists of a single 100 passenger car electrodynamically suspended and laterally guided relative to a pier supported elevated guideway as illustrated in Figs. 1.1, 1.2 and 1.3. The vehicle is propelled at a cruise velocity of about 480 km/hr (300 mph) by means of an air core linear synchronous motor (LSM). An array of superconducting magnets contained within seven cryogenically independent pods located along the entire underside of the vehicle couple magnetically with a travelling magnetic wave that

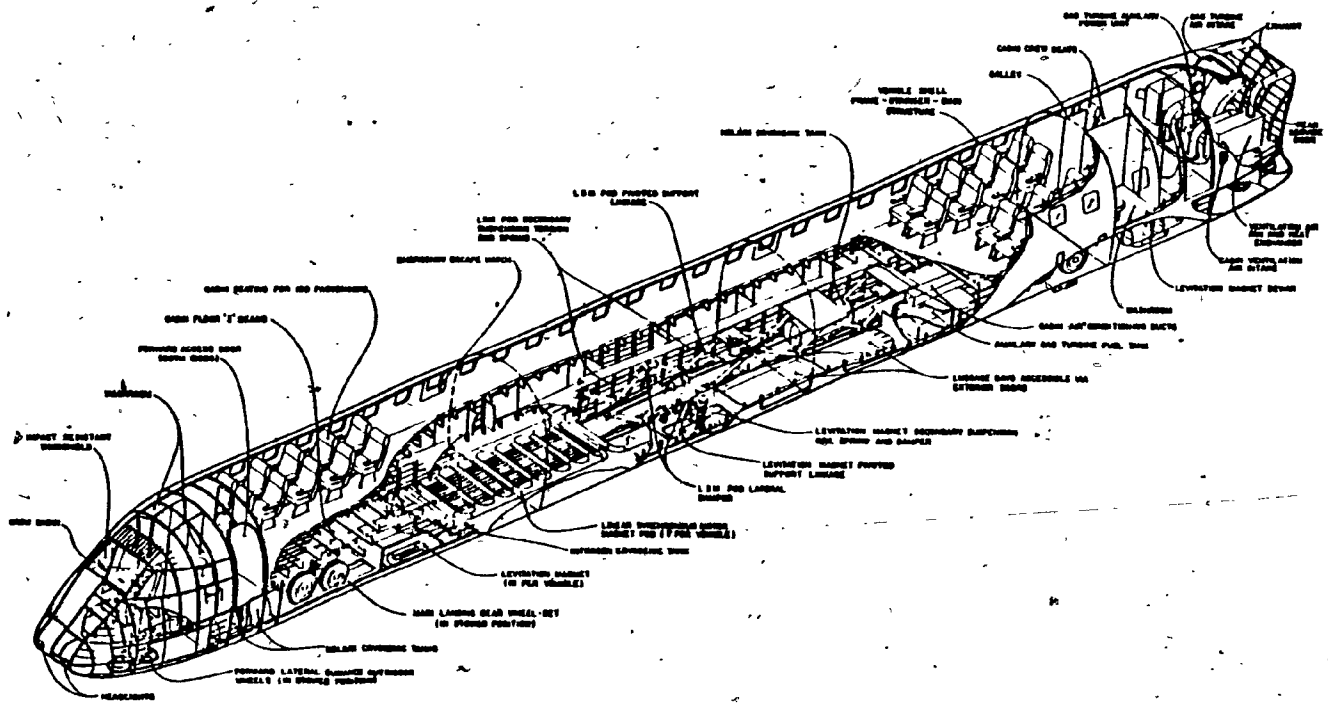

Fig. 1.1. Canadian MAGLEV Vehicle Conceptual Design.
(Courtesy: Division of Mechanical Engineering,
National Research Council Laboratories [5]).

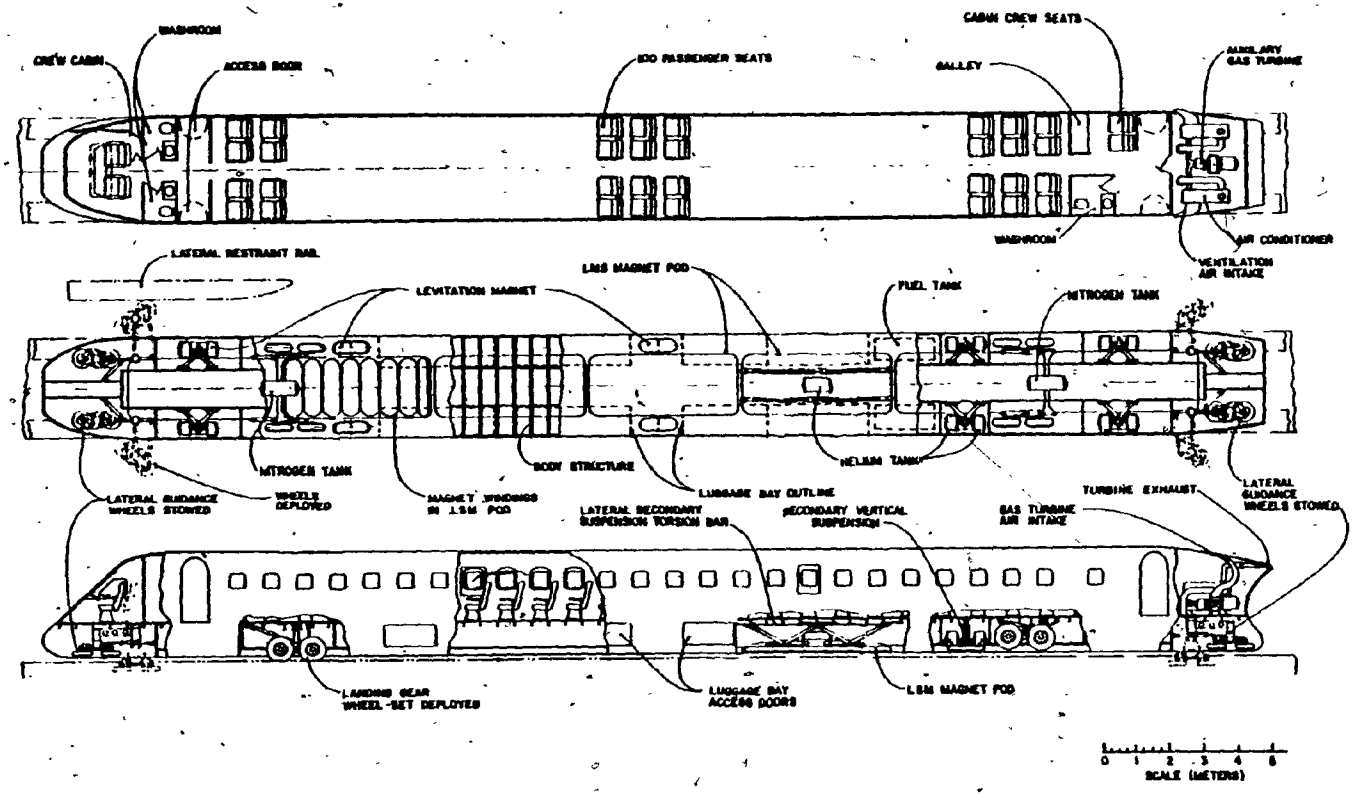

Fig. 1.2. Proposed MAGLEV Vehicle Layout.
(Courtsey: Division of Mechanical Engineering,
National Research Council Laboratories [5]).

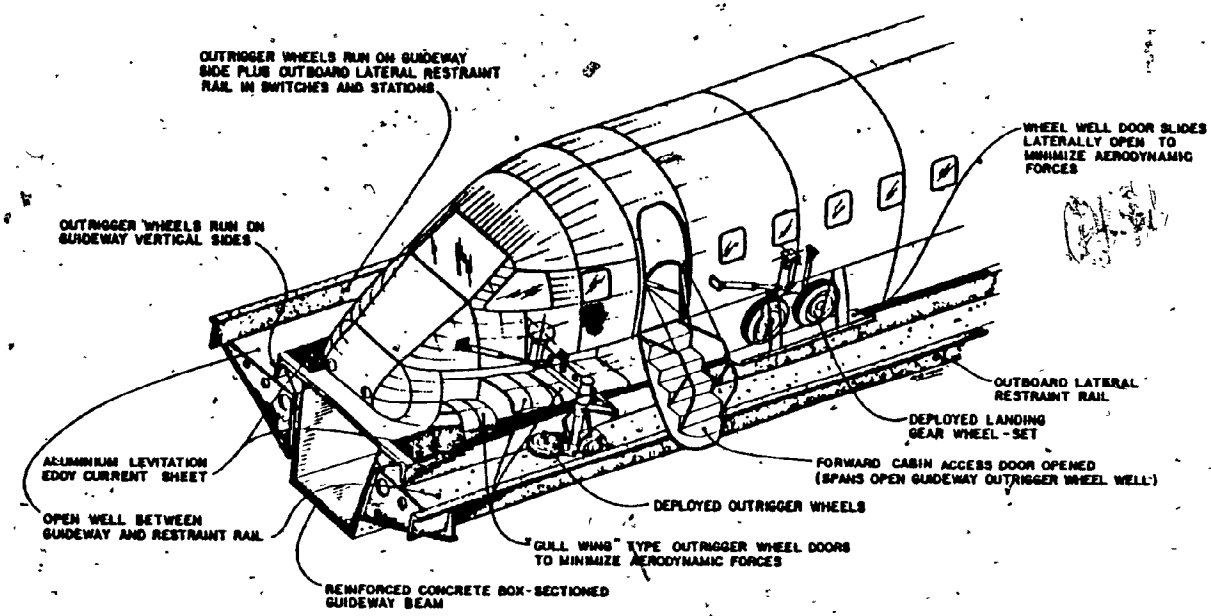

Fig. 1.3. MAGLEV Vehicle Forward Section.
(Courtsey: Division of Mechanical Engineering,
National Research Council Laboratories [5]).

is generated by a split three phase winding on the guideway surface to produce the desired vehicle thrust. The LSM guideway winding is excited in a 5 km block length by wayside located variable frequency inverter. Vehicle speed is directly controlled by frequency regulation of the guideway winding input. Vehicle lift is electrodynamically generated by the magnetic fields of ten moderate ampere - turn rated superconducting levitation magnets inducing eddy currents within two aluminum sheet conductor strips on the guideway surface.

Vehicle lateral guidance is electrodynamically generated by the magnetic fields of the LSM superconducting magnet arrays inducing eddy currents within "figure-of-eight" shaped null-flux loop conductors on the guideway surface overlaying the LSM windings as illustrated in Fig. 1.4. Additional back up guidance is provided by electrodynamic interaction between the LSM magnet windings and the edges of the lift inducing conductor strips when the vehicle lateral displacement becomes substantial. The vehicle is designed in such a way that the electromagnetic guidance force and accordingly the guidance induced drag is negligible when the vehicle is centered on the guideway.

The MAGLEV vehicle is supported on retractable tired wheels running on the guideway strips, at low velocities at which the generated electrodynamic lift and guidance forces are inadequate, that is the velocity is below 50 km/hr (31 mph), and is guided by small retractable tired on trigger wheels running on the vertical side surfaces of the guideway beam, as shown in Fig. 1.3.

Several options of the suspension systems design are still being explored and studied by the National Research Council of Canada, and

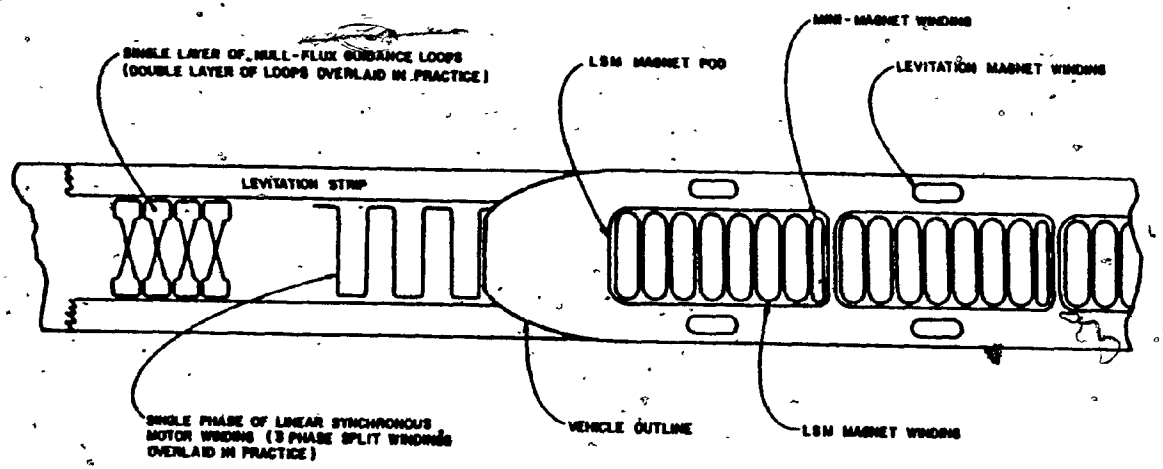

Fig. 1.4. Schematic of Guideway and Vehicle Magnet Windings.
(Courtsey: Division of Mechanical Engineering,
National Research Council Laboratories [5]).

the Canadian MAGLEV group at the Institute of Guided Ground Transport [6]. These options are: passive electrodynamic primary suspension damping, active electrodynamic primary suspension damping, passive mechanical secondary suspension, and active mechanical secondary suspension. Investigations of the first two primary suspension options do not favor the use of active primary suspensions because of reliability considerations in case of control feedback circuit failure. The investigation carried out by the National Research Council of Canada [5] recommends the use of an active secondary suspension system in order to achieve acceptable ride quality without compromising on the primary suspension system design. This active suspension system design was only recommended for the vertical suspension systems which control the bounce dynamics of the vehicle, while adequate lateral dynamic response was found possible to achieve by both passive primary and secondary suspension systems. On the other hand, it has been found that controlling the vehicle bounce dynamics with the use of passive vertical suspension systems offers a higher degree of reliability potential in its being analogous to conventional automobile and railway logic wheelset suspension system design practice.

In this investigation, analytical techniques are employed for the determination of the bounce dynamic response of the Canadian MAGLEV vehicle, and it is attempted to show how acceptable ride quality can be achieved with the use of passive vertical secondary suspension systems. It is shown that the amplitude of the passenger compartment bounce acceleration can be controlled through appropriate modifications to the design specification of the vertical suspension system. Addition

of suspension elements are also considered, and the design of optimum suspension system elements to reduce the vibrations transmitted to the vehicle body is also investigated.

1.3 Literature Review

During the past decade, there has been a marked increase in the attention devoted to achieving noiseless, smooth and efficient suspension systems for use on high speed ground vehicles. Previous investigations in high speed vehicle dynamic include a diversity of emphasis concerning the analytical and experimental determination of the dynamics of high speed guided vehicles.

In his book, Laithwaite [7] gave a review of the development of high speed ground transportation and the different vehicle systems designed in Canada, Japan and France. Ward [8] identified the future roles for Tracked Levitated Vehicle (TLV) systems by comparing the advantages and disadvantages of developing such systems as opposed to the improvement of passenger rail systems and short route air systems. This comparison concluded that when developed, tracked levitated vehicle systems will be better than rail systems in terms of travel times and operational cost per seat mile; as for the comparison with air systems, tracked levitated vehicle systems were found to have higher fixed costs than air because of the large investment in guideway and other infrastructure. However, TLV systems were found superior to air systems with respect to total trip time and vehicle productivity and as a result, TLV systems are preferred for trip distances of about 800 km (500 miles).

The Canadian MAGLEV group Contract Reports [9, 10, 6] give

detailed description of the different design aspects of the Canadian MAGLEV vehicle including the proposed guideway design, the vehicle-guideway interaction, and bounce and lateral dynamic response analyses. The MAGLEV design was later modified by the National Research Council of Canada, and Hayes [5] and Atherton et al. [11] analysed the dynamics of the MAGLEV vehicle by considering a very simple vehicle model, which neglects the actual geometry of the vehicle, subjected to an input process which neglects the periodicity of the guideway and only accounts for some of the random aspects of the guideway surface. Similar dynamic analysis on different types of magnetically levitated vehicle models were conducted by Howell [12], and by Bélanger and Guillemette [13] and arrived at partial conclusions.

The vehicle-guideway interaction problem and the effect of the vehicle-guideway system parameters on the vehicle dynamic response as well as the guideway deflections have also been given some thought and attention. Biggers and Wilson [14], Chung and Genin [15], Smith et al. [16], Doran and Mingori [17], Chiu et al. [18], Snyder and Wormley [19], and Richardson and Wormley [1], analysed the responses of both the vehicle and the guideway structure for vehicles travelling over multi-span-beam elevated guideways. All of them studied the influences of critical system parameters, such as the vehicle to guideway stiffness and mass ratio on guideway deflection and vehicle vibrational accelerations based on idealized vehicle-guideway models to allow for certain simplifications to be made. The results derived from these investigations are useful only in giving an insight into how some of the vehicle and guideway parameters affect the motion dynamics and further investi-

gations are necessary in order to come up with specific design recommendations for the different vehicle and guideway configurations and physical models.

Controlling dynamic characteristics of high speed vehicles have also received a great deal of interest in the last decade. Active secondary suspension system design with a feedback control was investigated by the National Research Council of Canada [5] for possible implementation in the Canadian MAGLEV vehicle design. Wilkie [20] analysed the dynamics of high speed magnetically levitated vehicle for five alternative guideway configurations and discussed the use of some feedback control guidance schemes. Limbert et al. [2] proposed a guidance controller that can be used to improve the dynamic characteristics of ferromagnetic vehicle suspensions providing simultaneous lift and guidance. Katz et al. [21] described the simulation of attractive and repulsive types of MAGLEV vehicle models and explored the effects of active suspension control elements on the vehicle performance. Hullender et al. [22] showed how to achieve near optimum performance of a flexible-skirted air cushion suspension using active control systems. Margolis et al. [23] used bond graph modeling techniques to analyse the heave mode dynamics of a nonlinear tracked air cushion vehicle incorporating a semi-active air bag secondary suspension. Crosby and Karnopp [24] investigated the performance of an active damper on a single and a two degree of freedom isolation systems and considered the use of the active damper in vehicle suspension design. Since the dynamic performance of the Canadian MAGLEV vehicle suspension systems have not been sufficiently investigated based on a reliable and appropriate vehicle model and since

the use of passive suspension systems is heavily favored over active suspension systems, it is premature to recommend the implementation of feedback control systems before conclusive investigations on the vehicle dynamics under all track inputs are carried out. An attempt to solve this problem is made in this thesis.

Optimization studies of the vehicle suspensions have also received a great deal of interest. Hedrick et al. [25] proposed optimal vertical and lateral linear suspension systems for a high speed vehicle subjected to guideway and aerodynamic inputs. In their analysis the random aspect of the guideway surface was modeled through a power spectral density expression which is only representative of a single span guideway. Also, the dynamic analysis was carried out by considering independently the deterministic and stochastic input processes rather than the real case of a combination of periodic and stochastic random excitations. Samaha and Sankar [26, 27] successfully optimized the non-linear suspension system controlling the rocking response of a freight car vehicle under the effect of periodic excitations from the rail tracks. Elmaraghy et al. [28] applied methods of multivariable optimization to a linear model of a locomotive to find the minimax response of the system in a critical frequency range of interest. Samaha [29] utilized the minimax principle together with some search algorithms for multivariable optimization to evaluate the optimum design variables for a nonlinear freight car model. In the present investigation, a similar minimax princple together with some available search algorithms [28, 30] are utilized to evaluate the optimum design variables for the secondary mechanical suspension system using a linear model of a high speed magnetically levitated vehicle.

The objective function of the optimization is taken to minimize the passenger compartment vertical accelerations. The optimization is done for the case when the vehicle is subjected to periodic deterministic inputs, and the vehicle response, for the same optimum suspension parameters, is determined for the case when the vehicle is subjected to a combination of periodic and random inputs generated from the guideway.

1.4 Scope of the Present Investigation

In this study, the dynamic bounce response of the Canadian MAGLEV vehicle is completely investigated. A parameter sensitivity analysis on the effect of varying the suspension system parameters on the vehicle bounce response and a multivariable optimization study for an optimal set of parameters of a modified suspension model to minimize the maximum vehicle body bounce acceleration, when the system is subjected to either periodic or a combination of periodic and random excitations from the guideway, are presented.

The improved mathematical model proposed in this investigation is constructed in such a way to describe completely the bounce and pitch modes of vibrations of the vehicle body as well as the bounce modes of vibrations of the levitation magnets. The equations of motion of the vehicle model are solved numerically using a digital computer, and the results obtained are used to generate plots showing the variations in the vehicle body bounce acceleration, pitch angle, and the bounce accelerations of the levitation magnets in both time and frequency domains.

In Chapter 2, the physical model of the system is described, the purpose of each of the main components of the vehicle is defined, and

the possible modes of vibrations of the vehicle system are identified. The major assumptions and limitations of the model considered are also discussed.

In Chapter 3, the guideway input excitations acting on the vehicle are described. A Fourier analysis is employed to describe the periodic input process generated due to the segmented nature of the elevated guideway structure over equi-distant pier supports. Power spectral density in the form of a filtered white noise is used for describing the simultaneous combination of periodic and random excitations from the guideway irregularities. This total excitation spectral density is then modeled as the output of a linear filter having a white noise input for simpler stochastic analysis. The dynamic state equations of the designed filter are derived to aid solution of the system response under a purely stochastic input process or a combination of periodic and stochastic input processes.

In Chapter 4, the equations of motion of the system are developed using d'Alembert's principle of force and moment analysis. The system response in time domain is obtained using numerical integration techniques. A procedure is developed to generate the response curves in the frequency domain from a series of time response curves for later use to carry out a parameter sensitivity analysis for all the mechanical suspension elements of the vehicle model. Although some useful results are obtained from this investigation, it is argued that the solution to the limitation of bounce acceleration requires further study through multivariable optimization techniques. Optimization techniques are employed in Chapter 5, to evaluate the suspension parameters that would minimize the maximum

steady state bounce acceleration response in the frequency range of interest.

In Chapter 6, a scheme is described to evaluate the mean square value and the power spectral density of the response process. The bounce acceleration power spectral density response is generated for different sets of suspension parameters. Ride quality specifications are set and the actual ride quality achieved with the optimal set of suspension parameters is evaluated.

Finally, a discussion of the results, conclusions and recommendations for future work are presented in Chapter 7.

CHAPTER 2

THE PHYSICAL MODEL OF THE MAGLEV VEHICLE

2.1 Preliminaries

In this Chapter, an idealized model for the high speed magnetically levitated vehicle is formulated. Since the objective is to evaluate the vehicle ride quality in terms of the bounce or vertical acceleration response of the passenger compartment, the main features of the model are to be based on the proper representation of those major components of the vehicle which influence the system's bounce dynamic response. The physical model is, therefore, developed through identification of the mechanical characteristics of these major components by idealized elements such as masses, springs and damping elements. The model developed in this Chapter assumes only small oscillations of the system about its equilibrium position and hence all the suspension forces of the system are considered to be linear. The model will also be employed later in this investigation to evaluate and optimize the parameters of a modified mechanical suspension system that would yield a minimum response acceleration under the action of both the periodic as well as a combination of the periodic and the random guideway excitation inputs to the vehicle.

2.2 Main Elements of the Vehicle

The main element of a magnetically levitated vehicle which affects the vertical dynamic response is the main vehicle body which is supported by some vertical mechanical suspension systems connected to the levitation magnets which in turn interact with the levitation strip along the guideway to provide lift for the whole system. The vertical

arrangement of the vehicle is shown in Fig. 2.1. The mass of the vehicle body is much greater than the mass of all levitation magnets combined. The main purpose of the mechanical suspension systems is to isolate the passenger's compartment on the main vehicle body from the motion of the levitation magnets, and provide maximum passenger comfort. The main mechanical properties of the vehicle components and the corresponding idealized elements are listed in Table 2.1.

Throughout this thesis, the vehicle body will be referred to as the secondary mass, the levitation magnets as the primary masses, the mechanical suspension systems as the secondary suspension, and the magnetic suspension elements as the primary suspension.

The passive mechanical suspension system model shown in Fig. 2.2a was used for the dynamic analysis carried out by the National Research Council of Canada [5], which concluded that ride quality specifications cannot be met with the use of purely passive vertical suspension systems, and recommended the possibility of the use of active suspensions. In the present investigation, a logically modified mechanical suspension system model, as shown in Fig. 2.2b, in which the viscous damper is elastically coupled with the vehicle body, is used to analyse and study the system dynamic response. This suspension model is believed to reduce comparatively the vibration transmitted to the vehicle body, and will be shown later how acceptable ride quality can be achieved by proper design and optimization of the mechanical suspension elements.

As the vehicle travels on the guideway, input excitations due to guideway irregularities produce vertical displacements of the levitation magnets. The input displacements are in turn transmitted to the

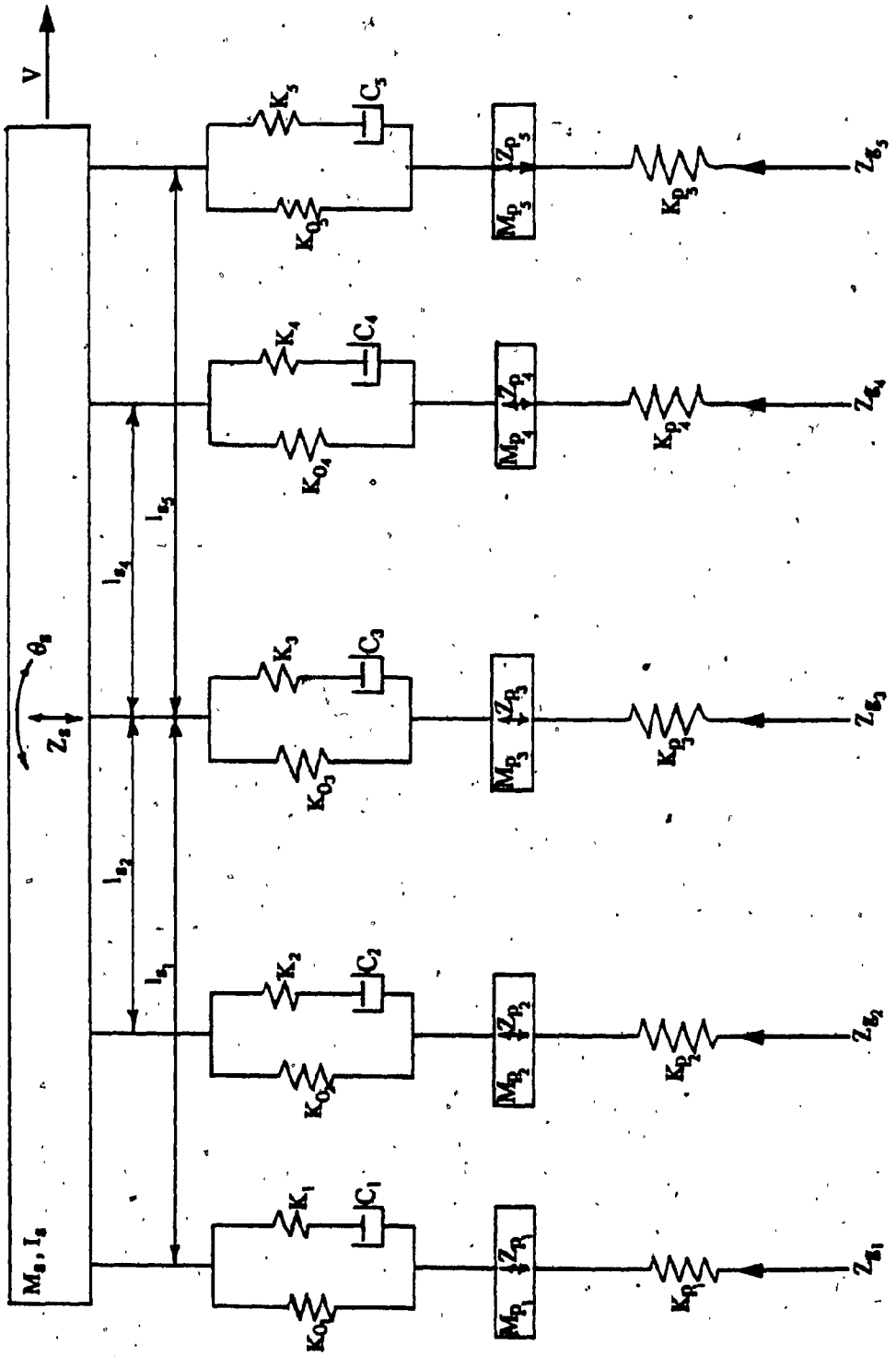

Fig. 2.1. Vertical Suspension Arrangement of the Vehicle.

No.	Components of the MAGLEV Vehicle	Idealized Representation in the Model
1	Mass and mass moment of inertia of the vehicle body	Represented by M_s and I_s of a rigid body
2	Masses of the five levitation magnets distributed along one side of the vehicle	Represented by five equal discrete masses, m_p of a rigid body
3	Force of interaction between the five levitation magnets and the guideway levitation strip	Represented by five linear springs with equal individual stiffnesses K_p
4	Vertical action of the five mechanical suspension systems connecting the levitation magnets with the vehicle body	Each system is represented by a viscous damper C connected in series with a spring with stiffness K, and the combination is connected in parallel with a spring with stiffness K_0, all linear

Table 2.1. List of Vehicle Mechanical Components.

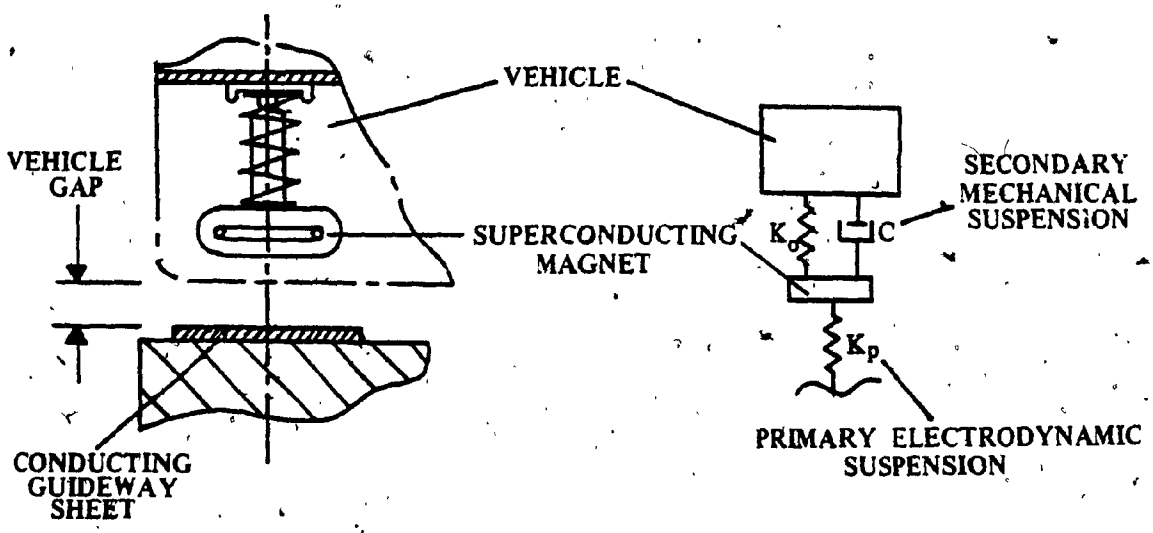

Fig. 2.2a. Passive Mechanical Suspension Model.

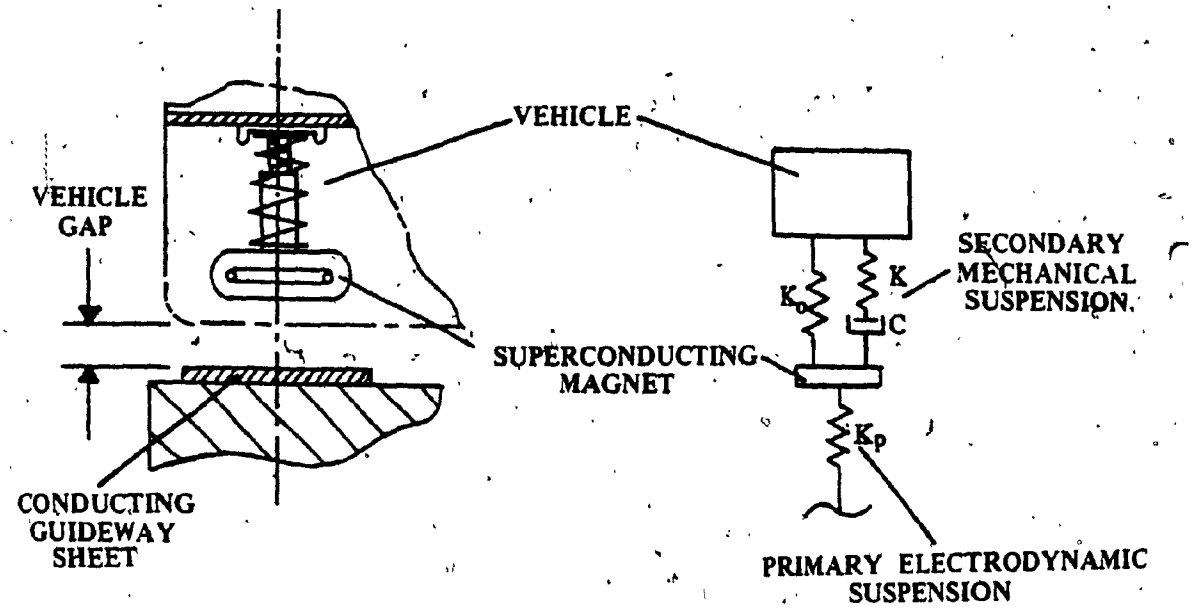

Fig. 2.2b. Modified Mechanical Suspension Model.

vehicle body through the secondary suspension systems causing bounce and pitch responses in the vehicle system. Since vertical ride quality is measured by the magnitude of the bounce acceleration of the vehicle body, it is important to control the amplitude of the bounce acceleration by designing suspension systems which provide maximum isolation of the vehicle body from the input excitations. The types of excitations to the system which cause bounce vibration basically arise from the vehicle guideway relative motion and can be modeled either as a purely periodic process, purely random process, or a combination of periodic and random processes. These types of excitation are discussed in detail in Chapter 3.

2.3 Assumptions and Limitations of the Model

The main assumptions implied in the modeling process together with the limitations of the derived model may be stated in the following manner:

i) The input forcing function to the right and left levitation magnets are assumed to be identical. This assumption is justifiable because of the symmetry of the vehicle and the guideway beam about the x-axis. A planar model of the vehicle can sufficiently describe the vehicle bounce response under deterministic as well as stochastic inputs.

ii) It is assumed that the excitation on the bounce model of the vehicle system is only due to guideway irregularities. Some previous investigations [25, 31] recommended the inclusion of the effect of the aerodynamic force on the vehicle bounce dynamics, however the only significant aerodynamic force in terms of the total vehicle dynamics

is the one due to cross wind effects [5]. Thus the effect of the aerodynamic force on the vehicle bounce dynamics can be assumed insignificant and hence neglected.

iii) The vertical mode of vibration is analysed independently of the lateral or rocking mode. This assumption is valid for the vehicle-guideway configuration such as that proposed for the Canadian MAGLEV vehicle. The guideway induced excitations are transmitted to the vehicle body through the levitation magnets which are restricted to move only in the vertical plane. Thus the levitation magnets displacements are not at all affected by any input excitations except those causing the vehicle bounce vibration.

iv) The model developed for the vehicle system assumes small oscillations of the vehicle system about its equilibrium position. Therefore, both primary and secondary suspension forces can be taken to be linearly varying. A more general modeling procedure could account for any nonlinear behavior of both the magnetic and the mechanical suspension systems and should be considered in future investigations.

v) As the vehicle travels over the guideway, it induces a motion in the guideway beam spans which in turn develop reaction forces to act on the levitation magnets. This coupling effect between the vehicle and guideway motion is neglected in this model. The inclusion of the guideway flexibility will yield a complicated set of coupled vehicle - guideway system equations in which the motion of the guideway will have to be described on the basis of Euler-Bernoulli beam theory. For the purpose of this thesis, and according to the guideway design described in [5], the guideway span is assumed to be on a rigid foun-

dation and consequently the vehicle is considered to be travelling over a rigid guideway. The inclusion of the vehicle-guideway system elastic coupling can be useful in assessing the sensitivity of the vehicle dynamic response to different guideway structures and could be possibly considered in future investigations.

2.4 Requirements for an Appropriate Mathematical Model

The vehicle model proposed in this study is chosen in such a way that the car bounce dynamics under the action of guideway induced excitations can be simulated and analysed. In this section, the requirements for developing an appropriate mathematical model are set so that methods of solution can be given.

For the system model shown in Fig. 2.1, the complete set of equations of motion are to be derived to include the following points:

i) The equations of motion are to describe the coupled bounce and pitch motions of the vehicle body, and the bounce displacements of the five levitation magnets.

ii) The dynamic interactions between the vehicle body and the levitation magnets and between the levitation magnets and the guideway must be included.

Based on the available information, the vehicle bounce dynamics can be completely described by a set of seven linear second order equations corresponding to the seven generalized coordinates of the system. The solution for the system response under periodic excitation can be conveniently obtained by expressing the system equations into state variable form and then applying numerical integration techniques

to solve the system state equations using a digital computer. This method can be used in solving for the system transient response in time and frequency domains. However, to optimize the system response, a great saving in computer time can be achieved by taking advantage of the linearity of the system and approximating the input periodic excitations by harmonic excitations, and then the method of complex algebra can be used to solve the state equations for the system steady state response and for optimization. A modified system state equations are also used to determine the system stochastic dynamic response when subjected to combined periodic and random excitations.

2.5 Summary

In this Chapter, the physical model representing the MAGLEV vehicle bounce dynamics is proposed and explained. The main components of the vehicle are identified and represented through idealized linear elements in the form of masses, springs, and damping elements. The assumptions and limitations of the model are also summarized.

The basis for the formulation of the mathematical model used for determining the system response under deterministic and periodic excitation from the guideways is also described.

CHAPTER 3

VEHICLE INPUT EXCITATIONS

3.1 Basic Types of Input Excitation to MAGLEV Car

There are essentially two basic types of input excitation that affect the dynamic response of a high speed vehicle:

i) Wind gust induced excitation, and

ii) Guideway induced excitation.

The wind gust or aerodynamic input on the vehicle has to be described statistically on the basis of reliable measured data. Some earlier attempts [25, 31] to represent these in terms of PSD have been made on the basis of some experimental data, and influence of this on the bounce response of high speed vehicles have been reported. These investigations considered a very simple and elementary vehicle model for their dynamic analysis and hence their results are not representative of the actual dynamic behavior of the vehicle. It is not clear how much influence the wind gust contributes particularly to the bounce response of the vehicle but it is possible to expect that such aerodynamic forces are purely secondary compared to the major input to the vehicle derived from guideway misalignment and irregularities. Since the present investigation is aimed at a reliable and accurate representation of the MAGLEV vehicle it is justified to concentrate on the major problem of mainly the influence of the guideway input excitation. Further, the investigation carried out by the National Research Council of Canada [5] on the dynamics of this particular type of vehicle found that the only aerodynamically derived vehicle input excitation which has any significant

relation to ride quality considerations is that induced by random cross-wind gusts which affects only the lateral dynamic response of the vehicle. Hence, for the purpose of this investigation the wind gust induced disturbance is neglected since the analysis concerns only the vehicle bounce dynamics.

The guideway induced excitations, that significantly affect the bounce dynamics of the vehicle, are due to periodic disturbances resulting from flexing of the guideway beams between equally spaced pier supports as well as random disturbances due to the guideway beams surface roughness and misalignment. These types of guideway irregularities are indicated in Fig. 3.1 and are described in detail in the following section.

3.2 Basic Types of Guideway Irregularities

There are two distinct input processes which can be used as the basis for defining the guideway irregularities. They are:

i) A periodic deterministic excitation process, and

ii) A stationary random excitation process.

The periodic input is principally due to the dynamic flexure of the equally spaced elevated guideway beams during the passage of the vehicle as well as any self-weight static deflection of the beam which is not appropriately compensated by built-in pre-camber.

The other input waveform representation of the guideway irregularity is essentially through a random process which is generated from various sources such as the random fluctuations in the guideway elevation and the irregularities and surface roughness of the guideway beams

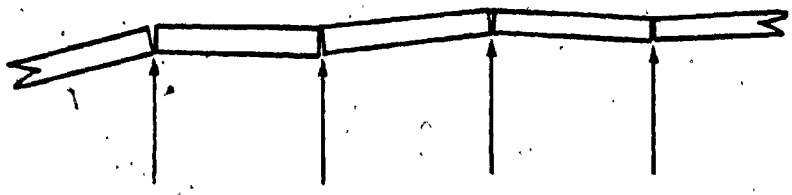

MISALIGNED ROUGH BEAMS (ELEVATED GUIDEWAY)

(a). Guideway Roughness Due to Misalignment.

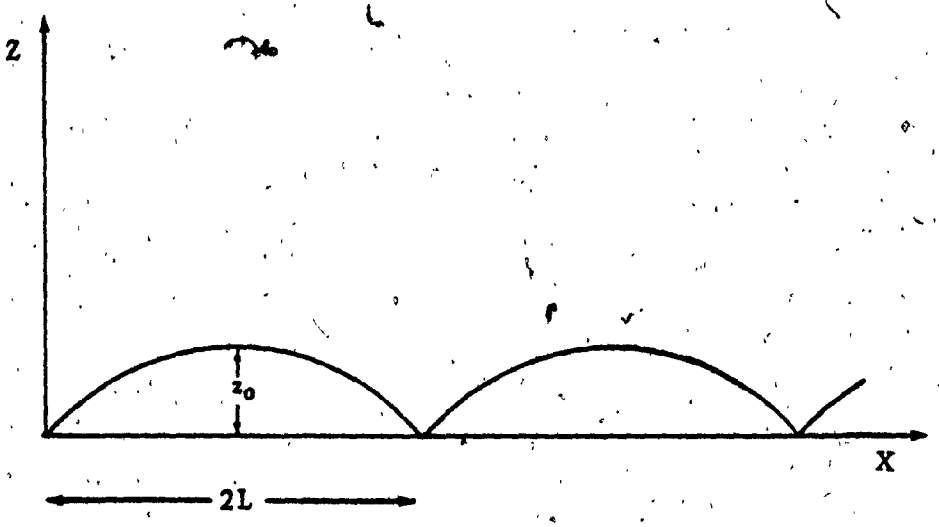

(b). Periodic Model of Irregularities.

Fig. 3.1. Basic Types of Guideway Irregularities.

[32]. These random irregularities are originally present when the guideways were first constructed and they combine with the dynamics of the vehicle travel and with the variations arising due to the flexibiility of the guideway pier supports to introduce additional random disturbances to the system.

Samaha [29] was the first to recognize and take into account an input process that combines both the periodic and the random processes in describing the total irregularities of the rail-tracks. This procedure is found to be the most appropriate way of modelling the guideway induced excitations and can be adapted to the present description of the guideway irregularities.

3.3. Deterministic Guideway Periodic Excitations

As described above, the input forcing function to the sytem may be represented only by a periodic deterministic process that neglects the random irregularities of the guideway. In such a case the forcing function can be properly described as a spatial function and then transformed into a time function for ease of analysis.

Periodic irregularities of simply supported guideway spans modeled as uniform beams are shown in Fig. 3.1 in the z-direction. These guideway irregularities can be expressed in terms of a harmonic series employing a Fourier analysis as follows.

From Fig. 3.1 , the guideway irregularity can be expressed as a harmonic function of the variable x in the form:

$$Z_G(x) = Z_0 \sin(\frac{\pi x}{2L}) \qquad \text{for} \quad 0 < x < 2L$$

where 2L is the standard guideway span length (25 m), and Z_0 is a constant

depending on the guideway class. Hayes [5] estimates the value of Z_0, for the Canadian MAGLEV vehicle guideway system, to be less than 2 mm, thus imposing very stringent conditions on the guideway construction. However, for the purpose of this investigation, maximum guideway deflections of up to 1 cm is considered for enabling one to study the effect of guideway flexibility on the vehicle dynamics. $Z_G(x)$ is an even function with a period 2L and can be expanded as a Fourier cosine series in the form:

$$Z_G(x) = A_0 + \sum_{n=1}^{\infty} A_n \cos\left(\frac{n\pi x}{2L}\right) \qquad (3.1)$$

where A_0, A_n are the standard Fourier coefficients and are evaluated to be:

$$A_0 = \frac{1}{2L}\int_0^{2L} Z_G(x)\, dx = \frac{2}{\pi} Z_0$$

$$A_n = \frac{2}{2L}\int_0^{2L} Z_G(x) \cos\frac{n\pi x}{2L}\, dx = \frac{2Z_0(1+\cos n\pi)}{\pi(1-n^2)}, \quad n = 2,4,6,\ldots$$

$$Z_G(x) = \frac{2Z_0}{\pi}\left[1 - \frac{2}{3}\cos\frac{\pi x}{L} - \frac{2}{15}\cos\frac{2\pi x}{L} \ldots.\right] \qquad (3.2)$$

The guideway induced input relation (3.2) can be expressed as a time function using the time-distance relationship

$$\frac{x}{2L} = \frac{t}{\tau} = \frac{\omega t}{2}$$

or

$$\omega t = \frac{\pi x}{L}$$

where ω (rad/sec) is given by:

$$\omega = \frac{2\pi}{t} = \frac{2\pi}{2L/V} = \left(\frac{\pi}{L}\right)V$$

V being the vehicle velocity in (m/sec)

Therefore the periodic deterministic excitation process acting on the

system is given by the final expression:

$$Z_G(t) = \frac{2Z_0}{\pi}\left[1 - \frac{2}{3}\cos\omega t - \frac{2}{15}\cos 2\omega t - \frac{2}{35}\cos 3\omega t \ .....\right]$$

3.4 Randomness of Guideway Irregularities

Early measurements of the power spectral density (PSD) identified purely random waveforms for various types of road and track surfaces and were approximately expressed through a simple form

$$S(\omega) = \frac{A}{\omega^2} \qquad (3.3)$$

where A is defined as a constant roughness parameter depending on the type of surface measured [5]. For an elevated-beam/pier-supported guideway such a surface roughness is only applicable to individual beam spans. More accurate description of the PSD of rough elevated guideway beams can be given by the modified expression:

$$S(\omega) = \frac{AV}{\omega^2 + \omega_0^2} \qquad (3.4)$$

where ω_0 is the breakpoint frequency for the roughness spectrum calculated from the vehicle velocity V and guideway span length [5].

The expressions in Equations (3.3) and (3.4) identify only the random aspects of the guideway irregularities. Since a complete dynamic analysis should include the effect of both the periodic and the random input processes on the vehicle response, the guideway irregularities can be accurately described through an expression which identifies the random aspects of the guideway surface and also takes into consideration the effect of the guideway periodicity by introducing and controlling a variable h in Equation (3.4) where $h \leq 1$, [29]. For smaller values of h, the PSD expression indicates a relatively large amount of energy

present at frequency ω_0 showing a strong presence of the periodic part of the guideway irregularity also, as can be seen in Fig. 3.2b. The modified expression for the spectra is then defined by:

$$S(\omega) = \frac{AV(\omega^2 + \omega_0{}^2)}{[\omega^4 - 2(1-2h^2)\omega^2\omega_0{}^2 + \omega_0{}^4]} \qquad (3.5)$$

for h = 1, Equation (3.5) reduces to (3.4) describing the contribution due to the random surface irregularity only as shown in Fig. 3.2a.

3.4.1 Design of a Linear Filter for White Noise Input. To simplify the analysis and to reduce the mathematical complexities due to integration of stochastic differential equations, it is preferable to have the stochastic input to the system represented in terms of an equivalent white noise. Samaha [29] suggests that in order to achieve this, the PSD expression (3.5) can be modeled as the output of a linear filter having a white noise input. The filter dynamic equations are derived, and the overall system equations, as derived and given later in Chapter 6, can then be determined by incorporating the filter dynamic equations with the vehicle dynamic equations. The overall system can then be considered to have a white noise input and analytical solutions can be obtained. The transfer function H(s) of the filter, and the filter dynamic equations are derived through the following procedure.

Let, in Equation (3.5), $s = j\omega$, where s is the Laplace transform variable. Then, Equation (3.5) in Laplace domain is given by:

$$S(s) = \frac{AV(\omega_0{}^2 - s^2)}{[s^4 + 2(1-2h^2)s^2\omega_0{}^2 + \omega_0{}^4]}$$

$$= AV\left|\frac{(\omega_0 + s)}{(s^2 + 2h\omega_0 s + \omega_0{}^2)}\right|^2 \qquad (3.6)$$

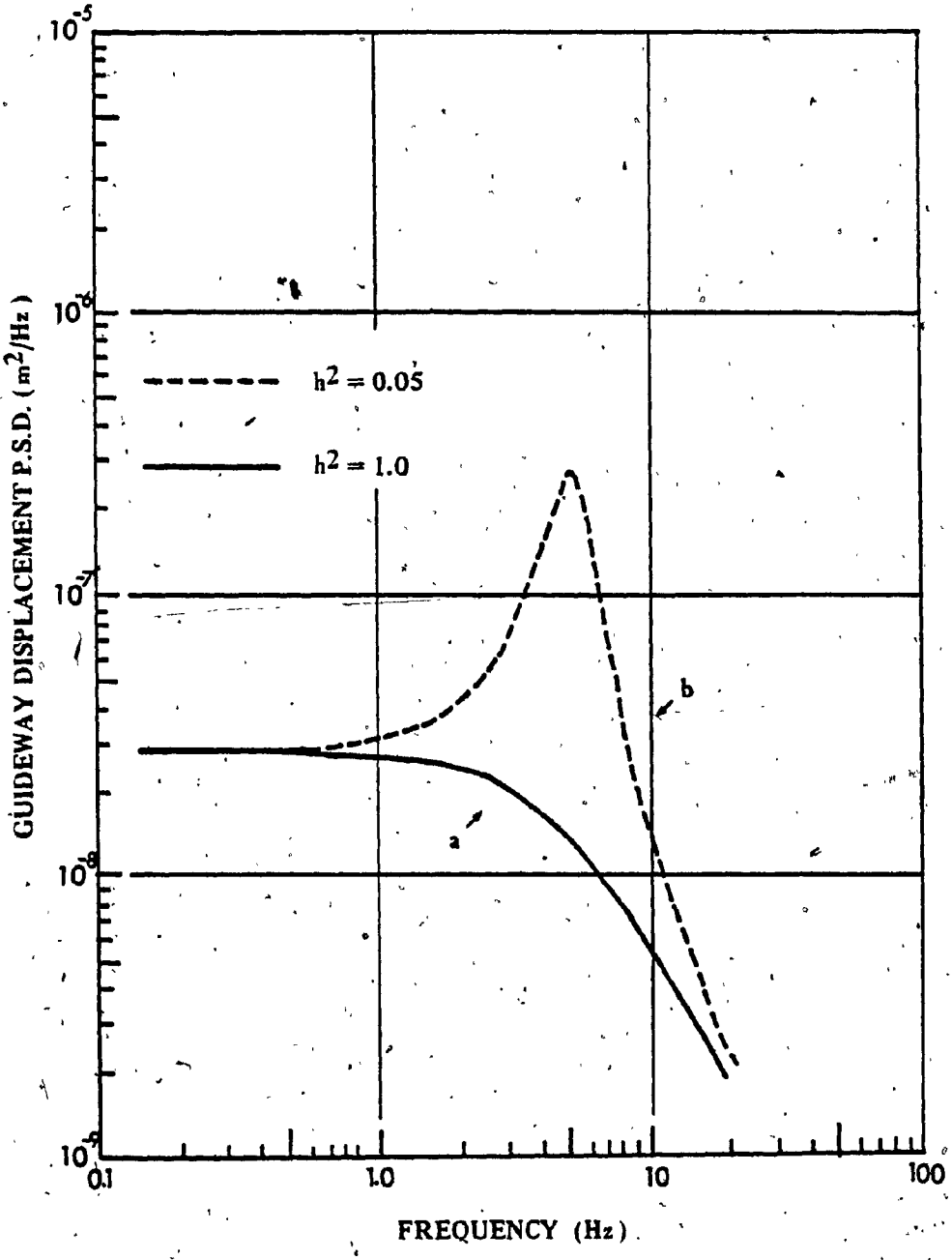

Fig. 3.2. Guideway Displacement Power Spectral Density.

For a linear system with white noise input, shown in Fig. 3.3:

$$S(s) = S_W|H(s)||H(-s)| = S_W|H(s)|^2 \qquad (3.7)$$

where S_W is the white noise input spectra, $S(s)$ is the filtered white noise spectra (output of the filter), and $H(s)$ is the linear filter transfer function. By comparing Equations (3.6) and (3.7), the input white noise spectral density to the filter will be:

$$S_W = AV$$

indicating a delta-correlated input defined by

$$E[W(t)W(t+\tau)] = 2\pi AV\delta(\tau)$$

where $\delta(\tau)$ is the Dirac delta function.

The transfer function of the linear filter system is then

$$H(s) = \frac{(\omega_0 + s)}{(s^2 + 2h\omega_0 s + \omega_0^2)} = \frac{U(s)}{W(s)} \qquad (3.8)$$

To find the filter equations of motion, Equation (3.8) is transformed into the time domain in the form:

$$\ddot{U}(t) + 2h\omega_0 \dot{U}(t) + \omega_0^2 U(t) = \dot{W}(t) + \omega_0 W(t) \qquad (3.9)$$

Equation (3.9) is of second order and can be realized in terms of state variables with the following set of equations:

$$\begin{aligned} \dot{\underline{\psi}}_{Gi} &= \underline{A}_{Gi}\,\underline{\psi}_{Gi} + \underline{B}_{Gi}\,\underline{W}_{Gi}(t) \\ \underline{U}_{Gi}(t) &= \underline{C}_{Gi}\,\underline{\psi}_{Gi} \end{aligned} \qquad (3.10)$$

These can also be written as:

$$\begin{bmatrix} \dot{\psi}_1 \\ \dot{\psi}_2 \end{bmatrix} = \begin{bmatrix} 0 & 1 \\ -\omega_0 & -2h\omega_0 \end{bmatrix} \begin{bmatrix} \psi_1 \\ \psi_2 \end{bmatrix} + \begin{bmatrix} 0 \\ 1 \end{bmatrix} \underline{W}_{Gi}$$

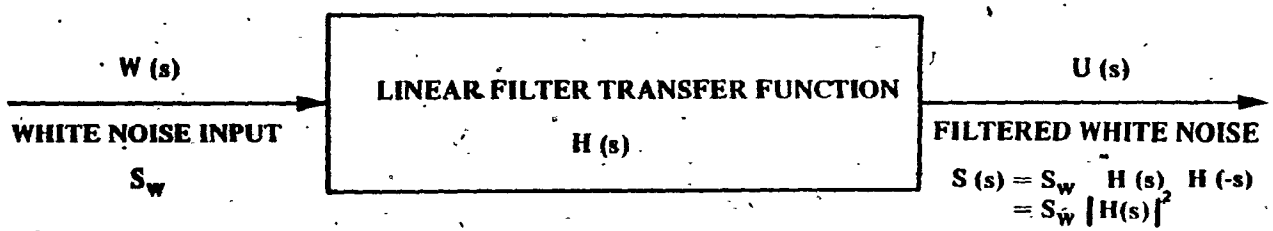

Fig. 3.3. Linear Filter with White Noise Input.

and

$$\left[U(t)\right] = \left[\omega_0 \qquad 1\right]_{Gi} \begin{bmatrix} \psi_1 \\ \psi_2 \end{bmatrix}_{Gi}$$

Equations (3.10) represent the dynamic equations of the constructed linear filter, shown in Fig. 3.3, which when combined with the vehicle dynamic equations will represent a complete system equivalent to the problem of the vehicle subjected to only a white noise input W(t).

3.4.2 Overall Filter-Vehicle Input Excitations. Since there are five levitation magnets supporting the vehicle there are five input excitations to the system all having the same frequency and each excitation being the same as that of the leading magnet input excitation except for a time delay. The correlation terms can thus be neglected [25], and the dynamic equations for the overall shaping filter representing all five input excitations will have the form:

$$\begin{aligned} \underset{\sim}{\dot{\psi}}_{(10x1)} &= \underset{\sim}{A}_{F(10x10)}\underset{\sim}{\psi}_{(10x1)} + \underset{\sim}{B}_{F(10x5)}\underset{\sim}{W}_{(5x1)} \\ \underset{\sim}{U}_{(5x1)} &= \underset{\sim}{C}_{F(5x10)}\underset{\sim}{\psi}_{(10x1)} + \underset{\sim}{D}_{F(5x5)}\underset{\sim}{W}_{(5x1)} \end{aligned} \tag{3.11}$$

where

$\underset{\sim}{\psi}$ is the state vector for the overall linear filter,

$\underset{\sim}{W}$ is white noise Gaussian disturbance vector,

$\underset{\sim}{U}$ is the vector specifying the input forcing functions to the system

and

$$E[\underset{\sim}{W}(t)\underset{\sim}{W}(t+\tau)] = \underset{\sim}{D}\delta(\tau).$$

$\underset{\sim}{D}$ is the constant covariance matrix for the equivalent white noise input and is given by:

$$\underset{\sim}{D} = 2\pi AV\ \underset{\sim}{I}$$

and

$$\underset{\sim}{v}^T = [Z_{G1} \quad Z_{G2} \quad Z_{G3} \quad Z_{G4} \quad Z_{G5}]$$

Further,

$$\underset{\sim}{A}_{F(10\times10)} = \begin{bmatrix} \underset{\sim}{A}_{F_{G1}} & \underset{\sim}{0} & \underset{\sim}{0} & \underset{\sim}{0} & \underset{\sim}{0} \\ \underset{\sim}{0} & \underset{\sim}{A}_{F_{G2}} & \underset{\sim}{0} & \underset{\sim}{0} & \underset{\sim}{0} \\ \underset{\sim}{0} & \underset{\sim}{0} & \underset{\sim}{A}_{F_{G3}} & \underset{\sim}{0} & \underset{\sim}{0} \\ \underset{\sim}{0} & \underset{\sim}{0} & \underset{\sim}{0} & \underset{\sim}{A}_{F_{G4}} & \underset{\sim}{0} \\ \underset{\sim}{0} & \underset{\sim}{0} & \underset{\sim}{0} & \underset{\sim}{0} & \underset{\sim}{A}_{F_{G5}} \end{bmatrix}$$

$$\underset{\sim}{B}_{F(10\times5)} = \begin{bmatrix} \underset{\sim}{B}_{F_{G1}} & \underset{\sim}{0} & \underset{\sim}{0} & \underset{\sim}{0} & \underset{\sim}{0} \\ \underset{\sim}{0} & \underset{\sim}{B}_{F_{G2}} & \underset{\sim}{0} & \underset{\sim}{0} & \underset{\sim}{0} \\ \underset{\sim}{0} & \underset{\sim}{0} & \underset{\sim}{B}_{F_{G3}} & \underset{\sim}{0} & \underset{\sim}{0} \\ \underset{\sim}{0} & \underset{\sim}{0} & \underset{\sim}{0} & \underset{\sim}{B}_{F_{G4}} & \underset{\sim}{0} \\ \underset{\sim}{0} & \underset{\sim}{0} & \underset{\sim}{0} & \underset{\sim}{0} & \underset{\sim}{B}_{F_{G5}} \end{bmatrix}$$

$$\underset{\sim}{C}_{F(5\times10)} = \begin{bmatrix} \underset{\sim}{C}_{F_{G1}} & \underset{\sim}{0} & \underset{\sim}{0} & \underset{\sim}{0} & \underset{\sim}{0} \\ \underset{\sim}{0} & \underset{\sim}{C}_{F_{G2}} & \underset{\sim}{0} & \underset{\sim}{0} & \underset{\sim}{0} \\ \underset{\sim}{0} & \underset{\sim}{0} & \underset{\sim}{C}_{F_{G3}} & \underset{\sim}{0} & \underset{\sim}{0} \\ \underset{\sim}{0} & \underset{\sim}{0} & \underset{\sim}{0} & \underset{\sim}{C}_{F_{G4}} & \underset{\sim}{0} \\ \underset{\sim}{0} & \underset{\sim}{0} & \underset{\sim}{0} & \underset{\sim}{0} & \underset{\sim}{C}_{F_{G5}} \end{bmatrix}$$

$$\underset{\sim}{D}_{F(5\times2)} = \underset{\sim}{0}$$

where A is the guideway roughness parameter, V is the vehicle velocity, and I is the identity matrix.

The dynamic equations of the filter given in Equation (3.11) are combined with the vehicle equations in Chapter 6 to form the overall system equations. The overall system will then be subjected to an equivalent white noise input and analysis of the stochastic response will then be carried out.

3.5 Proposed Analytical Investigation for the Vehicle Dynamic Response

In order to evaluate the ride quality of the MAGLEV vehicle in terms of the bounce response of the passengers' compartment, the solution for the bounce response of the vehicle when subjected to guideway irregularities is attempted in the following chapters using digital solutions.

In Chapter 4, the excitation is assumed to be purely periodic and vehicle responses in time and frequency domain are evaluated. Parametric study and optimization of the system response is then carried out in Chapter 5. Finally, the system response when subjected to a combination of periodic and random inputs is evaluated in Chapter 6.

CHAPTER 4

VEHICLE RESPONSE DUE TO PERIODIC INPUTS

4.1 Preliminaries

In Chapters 4 and 5, the vehicle bounce response, when subjected to purely periodic excitation from the guideways is investigated. Numerical integration techniques are found convenient for solving the system equations using a digital computer. However, because of the lengthy computations and the constraint due to computer time limitations, the response can only be evaluated for a limited time period hence it is not possible to anticipate whether or not the system response would have reached a steady state value within the allocated time period. The time required for a system to reach its steady state response depends on the values of the system parameters. The response of the system in time domain presented here shows how the bounce vibration of the vehicle builds up to a maximum value before it reaches steady state. Hence, the response plots shown may be termed quasi steady state or even transient.

In this particular Chapter, the "transient" response of the system is evaluated by numerical integration of the equations of motion on a digital computer. The system equations for the MAGLEV vehicle are derived using d'Alembert's principle for force and moment equilibrium. The results obtained from this are used to generate plots showing the variations in the vehicle body bounce acceleration, pitch angle, and the bounce accelerations of the levitation magnets. Maximum deflections of the suspension systems, for the purposes of design, are also evaluated. Series of system response curves in time domain are generated for

different vehicle speeds in order to obtain transient response results in the frequency domain. These results are used in Chapter 5 to carry out a parametric study on the different elements of the mechanical suspension systems.

4.2 The Equations of Motion of the Vehicle Model

The vehicle model shown in Fig. 4.1 was described in detail in Chapter 2. The derivation of the complete equations of motion is done through a detailed force analysis carried out to determine the relationships of the forces acting between the levitation magnets and the vehicle body and of those acting between the guideway and the levitation magnets. From this force analysis, the following sets of equilibrium conditions can be developed:

i) By considering the free body equilibrium of the vehicle configuration, Fig. 4.2, the secondary, or mechanical, suspension forces can be evaluated.

ii) By considering the free body equilibrium of each one of the levitation magnets, Fig. 4.3, the vehicle-guideway interaction forces can also be evaluated.

4.2.1. Force and Moment Analysis. All the forces shown on the free body diagrams in Figs. 4.2 and 4.3 are defined as follows:

i) the suspension forces for the systems connecting the vehicle body to the levitation magnets are

$$F_{s_i} = f(K_i, K_{0_i}, C_i, \Delta q_{s_i}), \qquad i = 1,2,.....5$$

Δq_{s_i} being the deflection of the ith secondary suspension system.

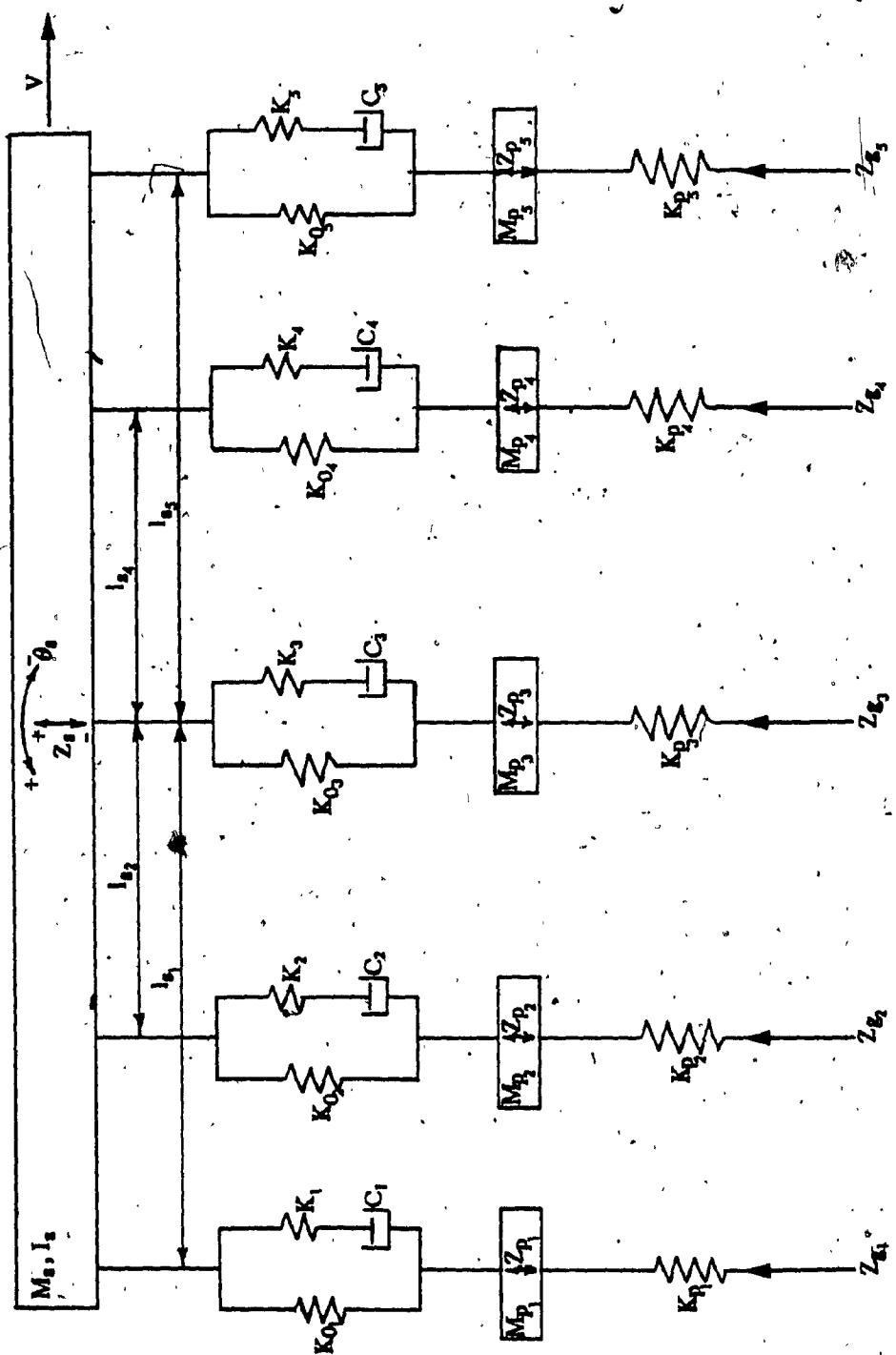

Fig. 4.1: Vehicle Suspension System Model.

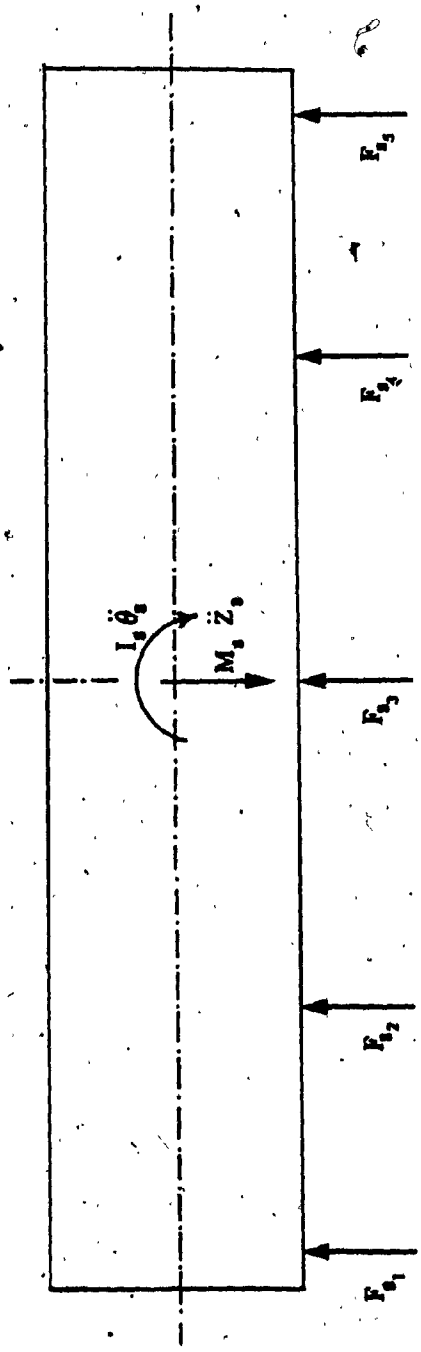

Fig. 4.2. Free Body Diagram of the Vehicle Body.

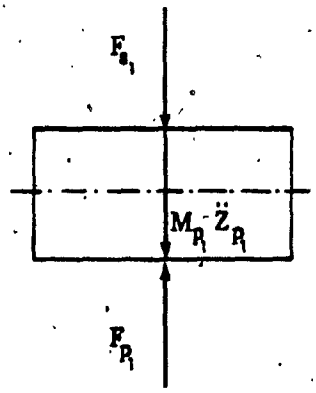

LEVITATION MAGNET 1

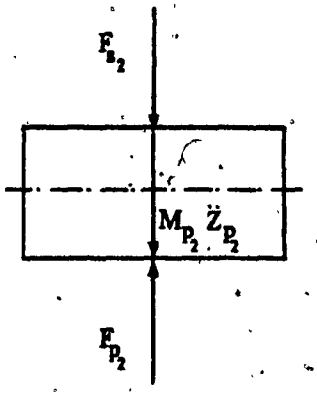

LEVITATION MAGNET 2

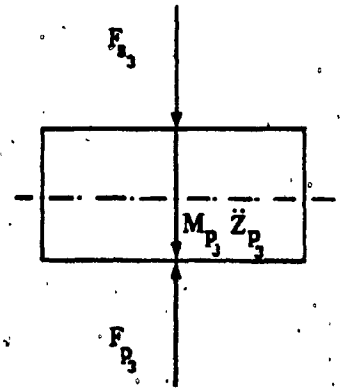

LEVITATION MAGNET 3

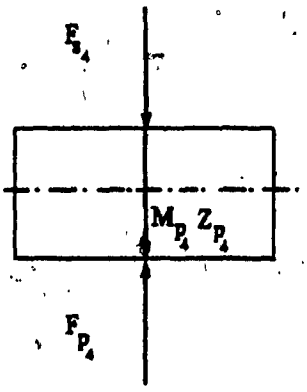

LEVITATION MAGNET 4

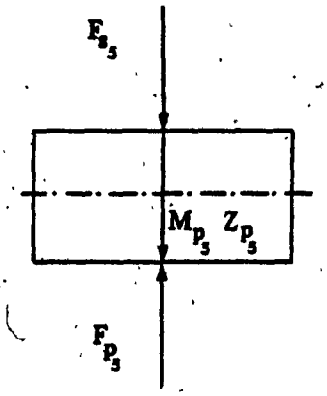

LEVITATION MAGNET 5

Fig. 4.3. Free Body Diagrams for the Five Levitation Magnets.

ii) the force acting on the ith levitation magnets due to the vehicle guideway interaction is

$$F_{p_i} = f(K_{p_i}, \Delta q_{p_i}), \quad i = 1,2,.....5$$

Δq_{p_i} being the deflection of the ith primary suspension system.

Here, the secondary and primary suspension systems are respectively the mechanical and magnetic support systems as previously defined.

Considering the vehicle body equilibrium in Fig. 4.2, the set of equations of motion can be stated as follows:

$$M_s \ddot{Z}_s = F_{s_1} + F_{s_2} + F_{s_3} + F_{s_4} + F_{s_5} \tag{4.1}$$

$$I_s \ddot{\theta}_s = F_{s_5} \ell_{s_5} + F_{s_4} \ell_{s_4} - F_{s_2} \ell_{s_2} - F_{s_1} \ell_{s_1} \tag{4.2}$$

Considering the equilibrium of each one of the levitation magnets, the following additional equations are also valid.

$$M_{p_1} \ddot{Z}_{p_1} = F_{p_1} - F_{s_1} \tag{4.3}$$

$$M_{p_2} \ddot{Z}_{p_2} = F_{p_2} - F_{s_2} \tag{4.4}$$

$$M_{p_3} \ddot{Z}_{p_3} = F_{p_3} - F_{s_3} \tag{4.5}$$

$$M_{p_4} \ddot{Z}_{p_4} = F_{p_4} - F_{s_4} \tag{4.6}$$

$$M_{p_5} \ddot{Z}_{p_5} = F_{p_5} - F_{s_5} \tag{4.7}$$

Equations (4.1) to (4.7) describe completely the dynamic behavior of the vehicle under consideration.

4.2.2. Derivation of the Suspension Force Transfer Function. The suspension force transfer function relates the suspension force to the suspension deflection through the different components of the suspension system. In this section, an expression for the transfer function of the

general suspension system, shown in Fig. 4.4, is derived. Then, from this general expression, suspension force transfer functions for simpler models of suspension systems such as those representing the primary suspension systems, can be easily deduced by appropriate substitutions.

Consider the suspension model shown in Fig. 4.4. This model assumes that the suspension system can be adequately represented by a point contact model, although most actual suspension systems have a finite contact length. The general equations of motion for this model is:

$$M\ddot{q}_1 = -F \tag{4.8}$$

where F is the suspension force which can be expressed in terms of K, C, and K_0 by assuming that a lumped mass with displacement q_3 acts between the spring K and the damper C, then it can be written

$$M\ddot{q}_1 + K_0(q_1 - q_2) + K(q_1 - q_3) = 0 \tag{4.9a}$$

$$K(q_3 - q_1) + C(\dot{q}_3 - \dot{q}_2) = 0 \tag{4.9b}$$

Equations (4.9a) and (4.9b) can be combined to yield a third order equation in the form

$$\frac{M}{K}\dddot{q}_1 + \frac{M}{C}\ddot{q}_1 + (\frac{K_0}{K} + 1)(\dot{q}_1 - \dot{q}_2) + \frac{K_0}{C}(q_1 - q_2) = 0 \tag{4.10}$$

Defining the suspension deflection to be

$$\Delta q = q_1 - q_2$$

and combining Equations (4.8) and (4.10)

$$-\frac{1}{K}\dot{F} - \frac{1}{C}F + (\frac{K_0}{K} + 1)\Delta\dot{q} + \frac{K_0}{C}\Delta q = 0 \tag{4.11}$$

Assuming a force free initial configuration, Equation (4.11) can be written in the Laplace domain as:

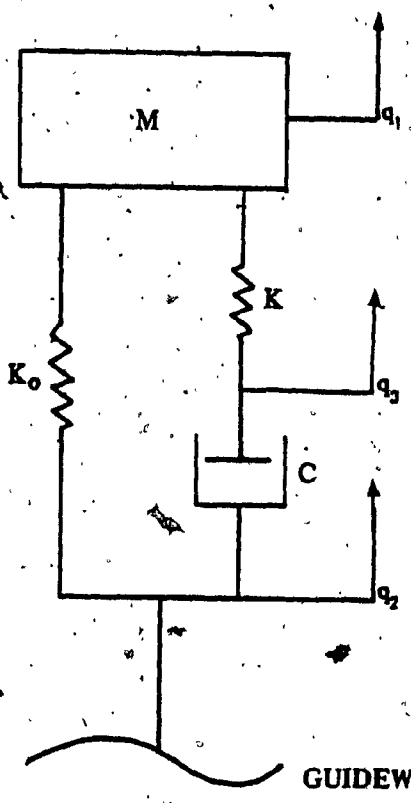

Fig. 4.4. General Model of a Mechanical Suspension System.

$$-\frac{1}{K}sF(s) - \frac{1}{C}F(s) + \left(\frac{K_0}{K} + 1\right)s\,\Delta q(s) + \frac{K_0}{C}\Delta q(s) = 0$$

or

$$\frac{F(s)}{\Delta q(s)} = \frac{K_0[1 + \tau_1 s]}{[1 + \tau_2 s]} \qquad (4.11a)$$

where τ_1 and τ_2 are defined as follows:

$$\tau_2 = C/K$$

$$\tau_1 = \frac{C}{K} + \frac{C}{K_0}$$

Equation (4.11a) defines the transfer function relating the suspension force and the suspension deflection for a general type of suspension model in question. This model and analysis is representative of the secondary suspension systems of the vehicle and the primary suspension systems transfer functions can be obtained by considering just a special case of this general suspension model by setting τ_1 and τ_2 both equal to zero.

The primary suspension forces can then be simply defined by:

$$F_p = K_p\,\Delta q_p \qquad (4.12)$$

4.2.3. State Variable Form. In order to be able to incorporate the expressions for the suspension forces into the system equations, Equations (4.1) to (4.7), the suspension forces transfer functions should be expressed in the time domain. For the primary suspension systems described by

$$F_p = K_p\,\Delta q_p$$

the inverse Laplace transformation can be simply carried out. However, for the secondary suspension system transfer function,

$$\frac{F_s(s)}{\Delta q_s(s)} = \frac{K_0[1 + \tau_1 s]}{[1 + \tau_2 s]}$$

and due to the complexity of the model, some mathematical manipulations are needed to be carried out. An auxiliary state variable η[25] can be defined such that

$$\dot{\eta} = -\frac{\eta}{\tau_2} + \Delta q_s \tag{4.13}$$

This can be transformed in the Laplace domain as:

$$s\eta(s) = -\frac{\eta(s)}{\tau_2} + \Delta q_s(s)$$

or

$$s = -\frac{1}{\tau_2} + \frac{\Delta q_s(s)}{\eta(s)} \tag{4.14}$$

Substituting for s from Equation (4.14) into Equation (4.11a)

$$F_s(s) = K_0 \frac{\tau_1}{\tau_2} \Delta q_s(s) + K_0 \frac{\tau_1}{\tau_2} \eta(s) \left[\frac{1}{\tau_1} - \frac{1}{\tau_2}\right]$$

which can be written in time domain as:

$$F_s = K_0 \frac{\tau_1}{\tau_2} \Delta q_s + K_0 \frac{\tau_1}{\tau_2} \eta \left[\frac{1}{\tau_1} - \frac{1}{\tau_2}\right] \tag{4.15}$$

The system Equations (4.1) to (4.7) can now be written in terms of the suspension systems parameters by substituting for F_{s_i} and F_{p_i} by

$$F_{p_i} = K_{p_i} \Delta q_{p_i} \qquad i = 1,2,\ldots,5$$

and

$$F_{s_i} = K_{0_i} \frac{\tau_{1i}}{\tau_{2i}} \Delta q_{s_i} + K_{0_i} \frac{\tau_{1i}}{\tau_{2i}} \eta_i \left[\frac{1}{\tau_{1i}} - \frac{1}{\tau_{2i}}\right] \quad i = 1,2,\ldots,5$$

The system equations are then written in terms of the following set:

$$M_s \ddot{Z}_s = \sum_{i=1}^{5} K_{T_i} \Delta q_s + \sum_{i=1}^{5} (K_{T_i})(T_i)\eta_i \tag{4.1a}$$

$$I_s\ddot{\theta}_s = -\sum_{i=1}^{2}(\ell_{s_i})(K_{T_i})\Delta q_{s_i} - \sum_{i=1}^{2}(\ell_{si})(K_{Ti})(T_i)n_i + \sum_{i=4}^{5}(\ell_{s_i})(K_{T_i})\Delta q_{s_i} + \sum_{i=4}^{5}(\ell_{si})(K_{Ti})(T_i)n_i \qquad (4.2a)$$

$$M_{p_1}\ddot{Z}_{p_1} = K_{p_1}\Delta q_{p_1} - K_{T_1}\Delta q_{s_1} - (K_{T_1})(T_1)n_1 \qquad (4.3a)$$

$$M_{p_2}\ddot{Z}_{p_2} = K_{p_2}\Delta q_{p_2} - K_{T_2}\Delta q_{s_2} - (K_{T_2})(T_2)n_2 \qquad (4.4a)$$

$$M_{p_3}\ddot{Z}_{p_3} = K_{p_3}\Delta q_{p_3} - K_{T_3}\Delta q_{s_3} - (K_{T_3})(T_3)n_3 \qquad (4.5a)$$

$$M_{p_4}\ddot{Z}_{p_4} = K_{p_4}\Delta q_{p_4} - K_{T_4}\Delta q_{s_4} - (K_{T_4})(T_4)n_4 \qquad (4.6a)$$

$$M_{p_5}\ddot{Z}_{p_5} = K_{p_5}\Delta q_{p_5} - K_{T_5}\Delta q_{s_5} - (K_{T_5})(T_5)n_5 \qquad (4.7a)$$

where K_{Ti} and T_i are given by

$$K_{Ti} = K_{0_i}\frac{\tau_{1i}}{\tau_{2i}} \qquad i = 1,2,\ldots,5$$

and

$$T_i = \frac{1}{\tau_{1i}} - \frac{1}{\tau_{2i}} \qquad i = 1,2,\ldots,5$$

The system equations can now be written in terms of the following state variables of the system:

$\dot{Z}_s$, the linear velocity of the vehicle body at its center of gravity,

$\dot{\theta}_s$, the angular velocity of the secondary mass M_s,

$\dot{Z}_{p_1}, \dot{Z}_{p_2}, \dot{Z}_{p_3}, \dot{Z}_{p_4}, \dot{Z}_{p_5}$, the linear velocities of the five primary masses,

n_1, n_2, n_3, n_4, and n_5, the five auxiliary state variables,

$\Delta q_{s_1}, \Delta q_{s_2}, \Delta q_{s_3}, \Delta q_{s_4}$, and Δq_{s_5}, the deflections of the five secondary suspension systems,

and finally,

$\Delta q_{p_1}, \Delta q_{p_2}, \Delta q_{p_3}, \Delta q_{p_4}$, and Δq_{p_5}, the deflections of the five primary suspension systems.

The state equation of the system is now expressed as:

$$\dot{\underline{X}} = \underline{\underline{F}}\underline{X} + \underline{G}(t) \tag{4.16}$$

where $\underline{X}$ is the state vector defined by:

$$\underline{X}^T = [\dot{Z}_s, \dot{\theta}_s, \dot{Z}_{p_1}, \dot{Z}_{p_2}, \dot{Z}_{p_3}, \dot{Z}_{p_4}, \dot{Z}_{p_5}, \eta_1, \eta_2, \eta_3, \eta_4, \eta_5, \Delta q_{s_1}, \Delta q_{s_2}, \Delta q_{s_3}, \Delta q_{s_4}, \Delta q_{s_5}, \Delta q_{p_1}, \Delta q_{p_2}, \Delta q_{p_3}, \Delta q_{p_4}, \Delta q_{p_5}]$$

and $\underline{G}(t)$ is the guideway input disturbance vector defined by:

$$\underline{G}(t)^T = [0, 0, 0, 0, 0, 0, 0, 0, 0, 0, 0; 0, 0, 0, 0, 0, 0, \dot{Z}_{g_1}, \dot{Z}_{g_2}, \dot{Z}_{g_3}, \dot{Z}_{g_4}, \dot{Z}_{g_5}]$$

Further, $\underline{\underline{F}}$ is a 22 by 22 system matrix and the elements of matrix F are given in Table 4.1.

The bounce response of the vehicle model can now be obtained by solving the above derived state equation of the system. The method employed for solving the system state equation is given in detail in the next section.

4.3 The Method of Solution

The complete equations of motion derived in Section 4.2 is solved for the time response. For a deterministic input, the periodic guideway profile described in Section 3.3 is considered. The dynamic system equations in state form, Equation (4.16), with zero initial conditions, are integrated numerically. Hamming [33] modified predictor corrector method with a fourth order Runge-Kutta starter integration package is employed. This method is a fourth order method, using four preceeding values for the computation of a new vector of the dependent variable. Fourth order Runge-Kutta method is used in the algorithm for adjustment of the initial increment for the integration step size and for the

$$F = \begin{bmatrix}
0 & 0 & 0 & 0 & 0 & 0 & 0 & -\left(\frac{K_{T_1}T_{s_1}}{K_{p_1}}\right) & \left(\frac{K_{T_1}T_{s_1}}{K_{p_2}}\right) & \left(\frac{K_{T_1}T_{s_1}}{K_{p_3}}\right) & \left(\frac{K_{T_1}T_{s_1}}{K_{p_4}}\right) & \left(\frac{K_{T_1}T_{s_1}}{K_{p_5}}\right) & \frac{K_{T_1}}{K_{p_1}} & \frac{K_{T_2}}{K_{p_2}} & \frac{K_{T_3}}{K_{p_3}} & \frac{K_{T_4}}{K_{p_4}} & \frac{K_{T_5}}{K_{p_5}} & 0 & 0 & 0 & 0 \\
0 & 0 & 0 & 0 & 0 & 0 & 0 & -\left(\frac{K_{T_2}T_{s_2}}{I_{s_1}}\right) & -\left(\frac{K_{T_2}T_{s_2}}{I_{s_2}}\right) & 0 & \left(\frac{K_{T_2}T_{s_2}}{I_{s_3}}\right) & \left(\frac{K_{T_2}T_{s_2}}{I_{s_4}}\right) & \frac{K_{T_1}s_{s_1}}{I_{s_1}} & \frac{K_{T_2}s_{s_2}}{I_{s_2}} & 0 & \frac{K_{T_4}s_{s_4}}{I_{s_3}} & \frac{K_{T_5}s_{s_5}}{I_{s_4}} & 0 & 0 & 0 & 0 \\
0 & 0 & 0 & 0 & 0 & 0 & 0 & -\left(\frac{K_{T_1}T_{s_1}}{K_{p_1}}\right) & 0 & 0 & 0 & 0 & -\frac{K_{T_1}}{K_{p_1}} & 0 & 0 & 0 & 0 & \frac{K_{p_1}}{K_{p_1}} & 0 & 0 & 0 \\
0 & 0 & 0 & 0 & 0 & 0 & 0 & 0 & -\left(\frac{K_{T_2}T_{s_2}}{K_{p_2}}\right) & 0 & 0 & 0 & 0 & \frac{K_{T_2}}{K_{p_2}} & 0 & 0 & 0 & 0 & \frac{K_{p_2}}{K_{p_2}} & 0 & 0 \\
0 & 0 & 0 & 0 & 0 & 0 & 0 & 0 & 0 & -\left(\frac{K_{T_3}T_{s_3}}{K_{p_3}}\right) & 0 & 0 & 0 & 0 & \frac{K_{T_3}}{K_{p_3}} & 0 & 0 & 0 & \frac{K_{p_3}}{K_{p_3}} & 0 & 0 \\
0 & 0 & 0 & 0 & 0 & 0 & 0 & 0 & 0 & 0 & -\left(\frac{K_{T_4}T_{s_4}}{K_{p_4}}\right) & 0 & 0 & 0 & 0 & -\frac{K_{T_4}}{K_{p_4}} & 0 & 0 & \frac{K_{p_4}}{K_{p_4}} & 0 \\
0 & 0 & 0 & 0 & 0 & 0 & 0 & 0 & 0 & 0 & 0 & -\left(\frac{K_{T_5}T_{s_5}}{K_{p_5}}\right) & 0 & 0 & 0 & 0 & \frac{K_{T_5}}{K_{p_5}} & 0 & 0 & \frac{K_{p_5}}{K_{p_5}} \\
0 & 0 & 0 & 0 & 0 & 0 & 0 & -1/\tau_{11} & 0 & 0 & 0 & 0 & 1 & 0 & 0 & 0 & 0 & 0 & 0 & 0 & 0 \\
0 & 0 & 0 & 0 & 0 & 0 & 0 & 0 & -1/\tau_{22} & 0 & 0 & 0 & 0 & 1 & 0 & 0 & 0 & 0 & 0 & 0 & 0 \\
0 & 0 & 0 & 0 & 0 & 0 & 0 & 0 & 0 & -1/\tau_{33} & 0 & 0 & 0 & 0 & 1 & 0 & 0 & 0 & 0 & 0 & 0 \\
0 & 0 & 0 & 0 & 0 & 0 & 0 & 0 & 0 & 0 & -1/\tau_{44} & 0 & 0 & 0 & 0 & 1 & 0 & 0 & 0 & 0 & 0 \\
0 & 0 & 0 & 0 & 0 & 0 & 0 & 0 & 0 & 0 & 0 & -1/\tau_{55} & 0 & 0 & 0 & 0 & 1 & 0 & 0 & 0 & 0 \\
-1 & s_{s_1} & 1 & 0 & 0 & 0 & 0 & 0 & 0 & 0 & 0 & 0 & 0 & 0 & 0 & 0 & 0 & 0 & 0 & 0 & 0 \\
-1 & s_{s_2} & 0 & 1 & 0 & 0 & 0 & 0 & 0 & 0 & 0 & 0 & 0 & 0 & 0 & 0 & 0 & 0 & 0 & 0 & 0 \\
-1 & 0 & 0 & 0 & 1 & 0 & 0 & 0 & 0 & 0 & 0 & 0 & 0 & 0 & 0 & 0 & 0 & 0 & 0 & 0 & 0 \\
-1 & s_{s_4} & 0 & 0 & 0 & 1 & 0 & 0 & 0 & 0 & 0 & 0 & 0 & 0 & 0 & 0 & 0 & 0 & 0 & 0 & 0 \\
-1 & s_{s_5} & 0 & 0 & 0 & 0 & 1 & 0 & 0 & 0 & 0 & 0 & 0 & 0 & 0 & 0 & 0 & 0 & 0 & 0 & 0 \\
0 & 0 & -1 & 0 & 0 & 0 & 0 & 0 & 0 & 0 & 0 & 0 & 0 & 0 & 0 & 0 & 0 & 0 & 0 & 0 & 0 \\
0 & 0 & 0 & -1 & 0 & 0 & 0 & 0 & 0 & 0 & 0 & 0 & 0 & 0 & 0 & 0 & 0 & 0 & 0 & 0 & 0 \\
0 & 0 & 0 & 0 & -1 & 0 & 0 & 0 & 0 & 0 & 0 & 0 & 0 & 0 & 0 & 0 & 0 & 0 & 0 & 0 & 0 \\
0 & 0 & 0 & 0 & 0 & -1 & 0 & 0 & 0 & 0 & 0 & 0 & 0 & 0 & 0 & 0 & 0 & 0 & 0 & 0 & 0 \\
0 & 0 & 0 & 0 & 0 & 0 & -1 & 0 & 0 & 0 & 0 & 0 & 0 & 0 & 0 & 0 & 0 & 0 & 0 & 0 & 0
\end{bmatrix}$$

Table 4.1. Elements of the System Matrix F.

computation of starting values. The subroutine automatically adjusts the increment during the whole computation by either doubling or halfing its original value. The automatic step size correction feature of the algorithm was found to be essential for numerical solution stability. However, a considerable saving in computer time was established by ensuring that the initial guess of the integration step size Δt is less than $(1/20)f$ where f is the highest natural frequency of the system. The system natural frequencies are determined by solving for the eigenvalues of the system matrix F defined in Equation (4.16). The eigenvalues of the system matrix F are considerably important as the values of their real parts give strong indications about the stability of the system. The system equations are then solved in order to determine the linear and angular accelerations, velocities, and displacements of the vehicle body, as well as the accelerations and displacements of the five levitation magnets. The numerical integration process is terminated when the time reaches a certain predetermined value. For this investigation, this time measure is fixed at 12 seconds as to allow for some of the interesting aspects of the dynamic response of the system to be illustrated.

4.4 System Response in the Time Domain

Typical plots of the time response obtained in this analysis are generated for further critical study. These are given in Figs. 4.5, 4.6 and 4.7, for a periodic input excitation resulting from a guideway vertical misalignment variation of 1.0 cm (0.4 in). Plotted in these figures are respectively the linear acceleration of the secondary mass, i.e. vehicle body, the pitching angle of the vehicle body, and the

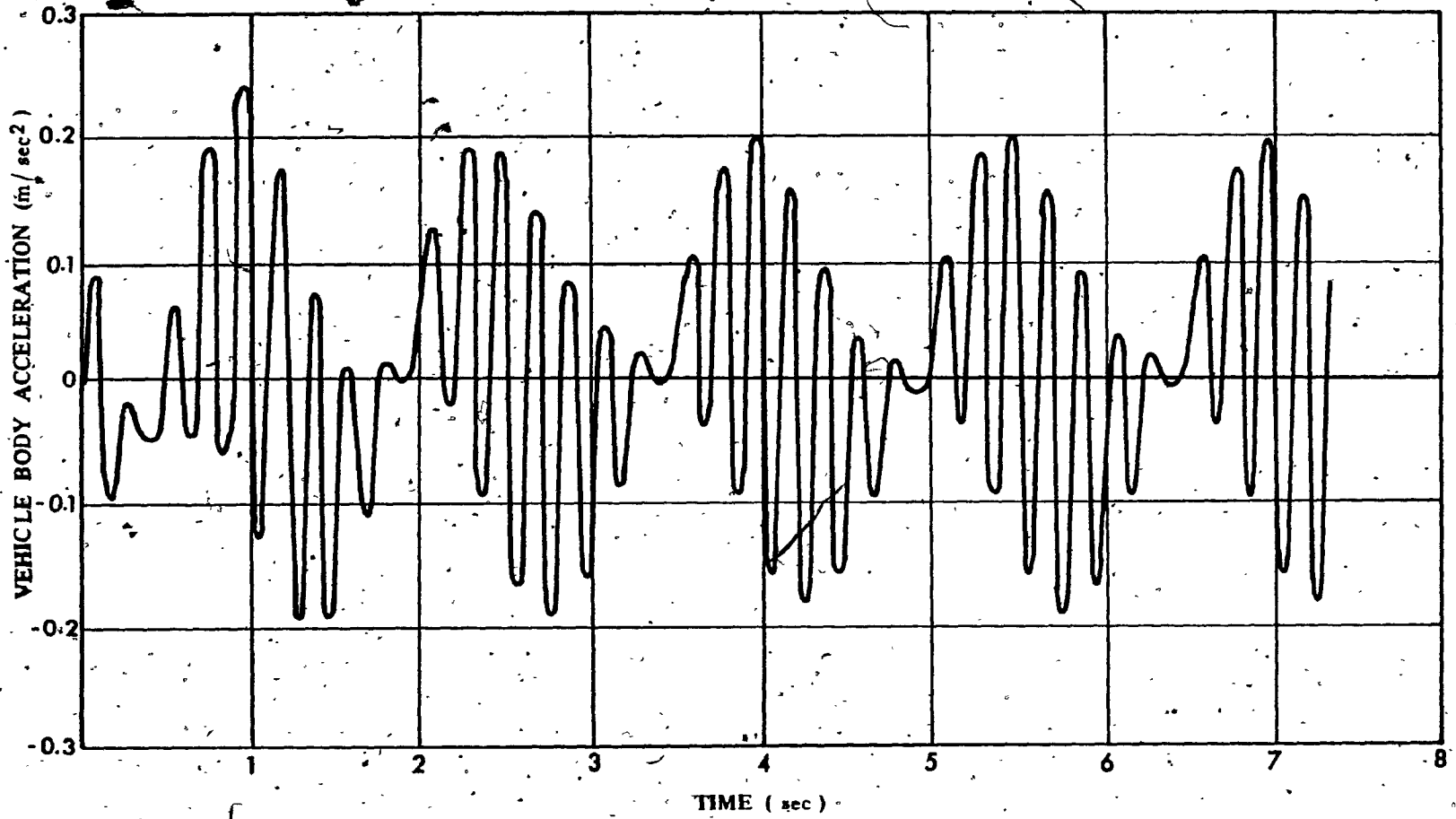

Fig. 4.5. Vehicle Body Bounce Acceleration in the Time Domain.

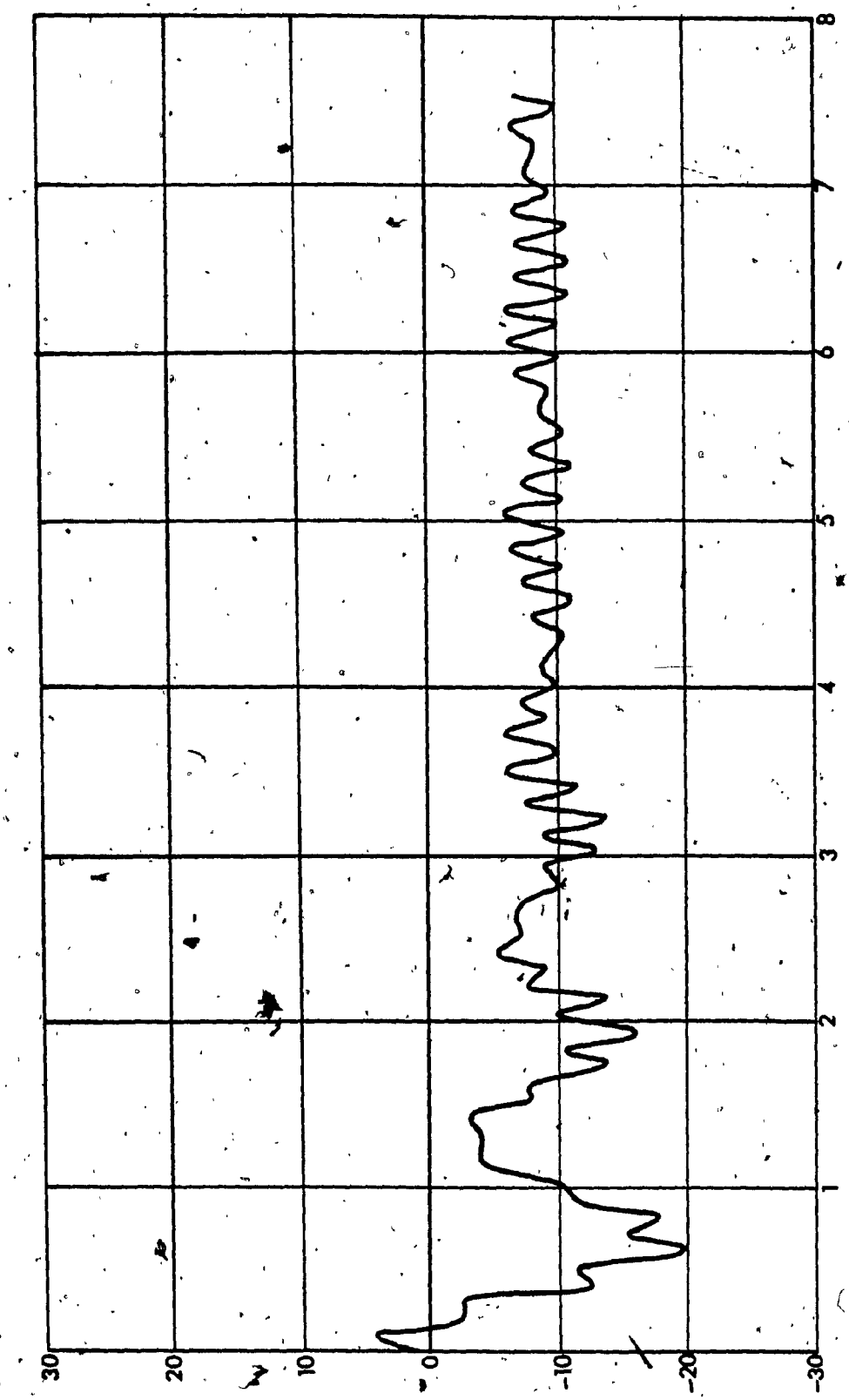

Fig. 4.6. Vehicle Body Pitch Response in the Time Domain.

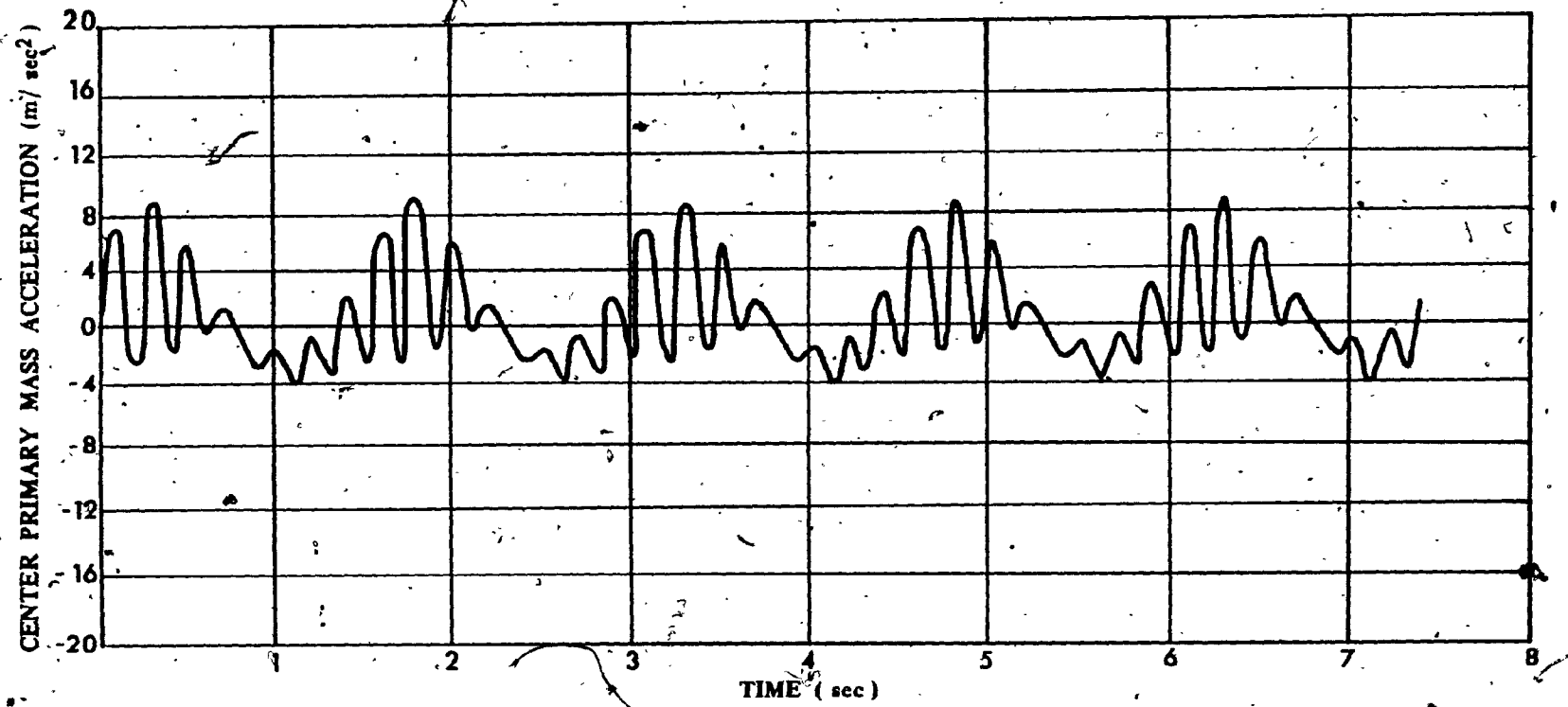

Fig. 4.7. Center Levitation Magnet Bounce Acceleration in the Time Domain.

acceleration of the center levitation magnet. It may be seen from Figs. 4.5 and 4.6 that the vehicle body bounce acceleration and pitching angle time responses grow rapidly from the given initial conditions to peak values in about 0.8 second and then these responses decay. This beating cycle phenomenon is repeated until the system response has reached a relative steady state after approximately 5 seconds. The oscillation of the pitching angle of the vehicle about a negative value could not be physically justified and requires further investigation. By observing the pitching response of the vehicle for different guideway span lengths, it was found that the pitching response oscillates about a negative value in all cases when the guideway span length is smaller than the distance between the leading and the trailing levitation magnets. As for the acceleration response of the center levitation magnet, it can be seen from Fig. 4.7 that the response reaches a peak value in about 0.3 second and that steady state is also reached in about 5 seconds. Also, it can be observed from Figs. 4.5 and 4.7 that the vehicle system exhibits the beat phenomenon. There is a transfer of energy from the bounce mode of vibration of the vehicle body to that of the levitation magnet, this phenomenon is attributed to the fact that the bounce natural frequencies of the vehicle body and those of the levitation magnets are very close in value. A series of time response curves are generated for different vehicle velocities and are employed to generate plots of the system response in the frequency domain as shown in the next section.

4.5 System Response in the Frequency Domain

The system dynamic response in the frequency domain is obtained from a series of time response curves plotted for different vehicle speeds. The system response in frequency domain is used to show the

critical frequency range in which peak amplitudes of vibration occur.

Bounce and pitch responses data in the frequency domain are summarized in Figs. 4.8, 4.9 and 4.10. In these figures the maximum response amplitudes are plotted against the vehicle speed which is linearly proportional to the exciting frequency, for a speed range from 50 to 480 km/hr (31 to 300 mph). The approach used in obtaining the system response in the frequency domain, plotted in Figs. 4.8, 4.9 and 4.10, assumes that the vehicle enters the frequency ω_i with zero initial conditions corresponding to a stationary position at the frequency ω_{i-1}. The advantage of using this approach is that the system response plots in the frequency domain generated using this approach describe the system performance at the required range of exciting frequencies independent from the initial conditions and the time required for the system to reach steady state conditions.

Figure 4.8 shows that the vehicle bounce acceleration response reaches a peak value at a frequency of about 6 rad/sec, which is found to correspond to the pitch natural frequency of the system, after which the response decreases to a minimum aplitude, fluctuates about this amplitude and thereafter starts increasing as vehicle velocity increases. The vehicle bounce natural frequency is calculated to be about 59 rad/sec which corresponds to a vehicle speed of about twice the maximum operating speed. Thus, the increase of the bounce response with increasing frequency can be accordingly explained. Fig. 4.9 shows that the vehicle pitching angle builds up to a maximum at a frequency corresponding to the pitch natural frequency of the system, thereafter it decays with the increasing vehicle velocity. From Fig. 4.10, one can see that, as expected, the levitation magnet response is not affected by the pitching

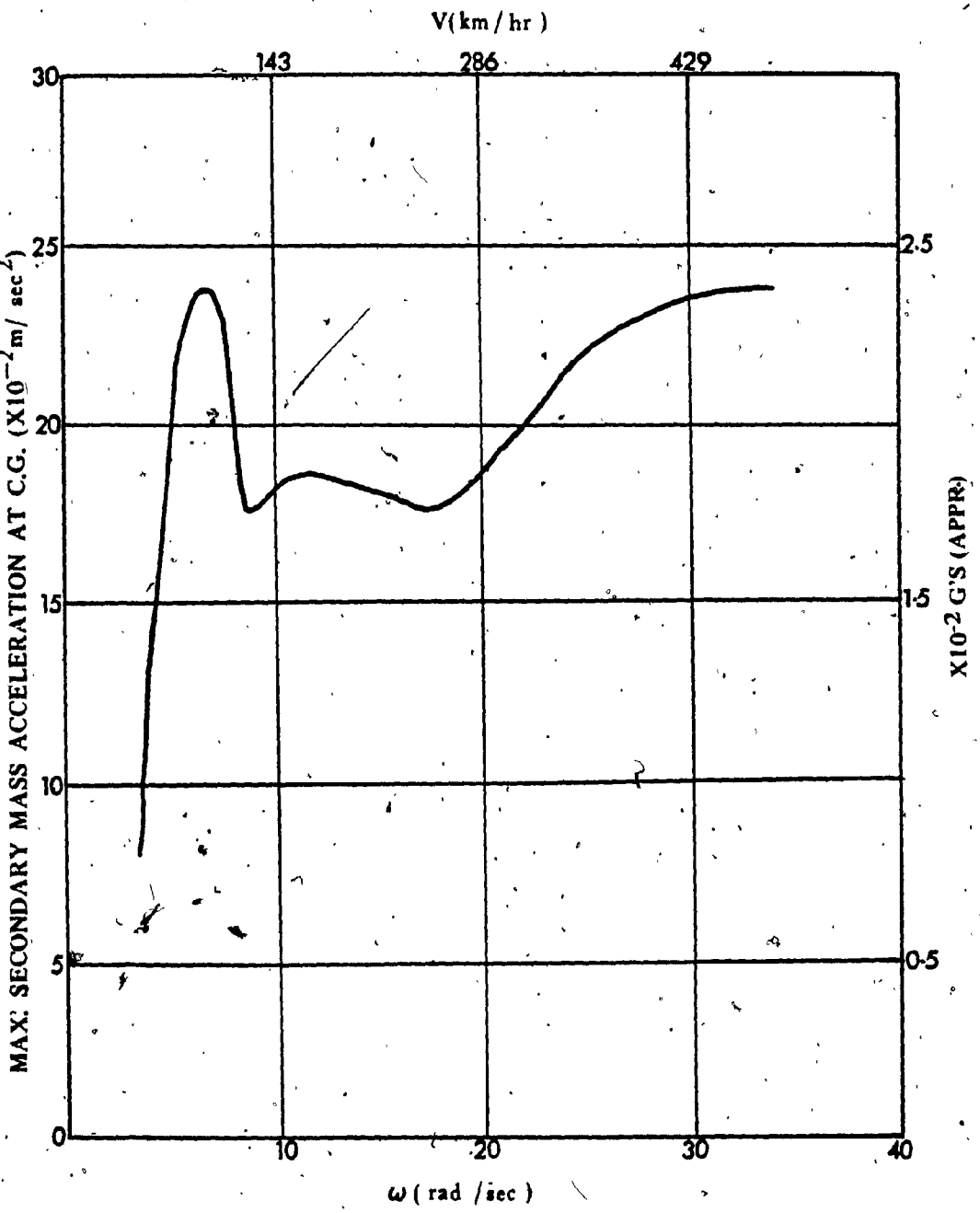

Fig. 4.8. Vehicle Body Bounce Acceleration in the Frequency Domain.

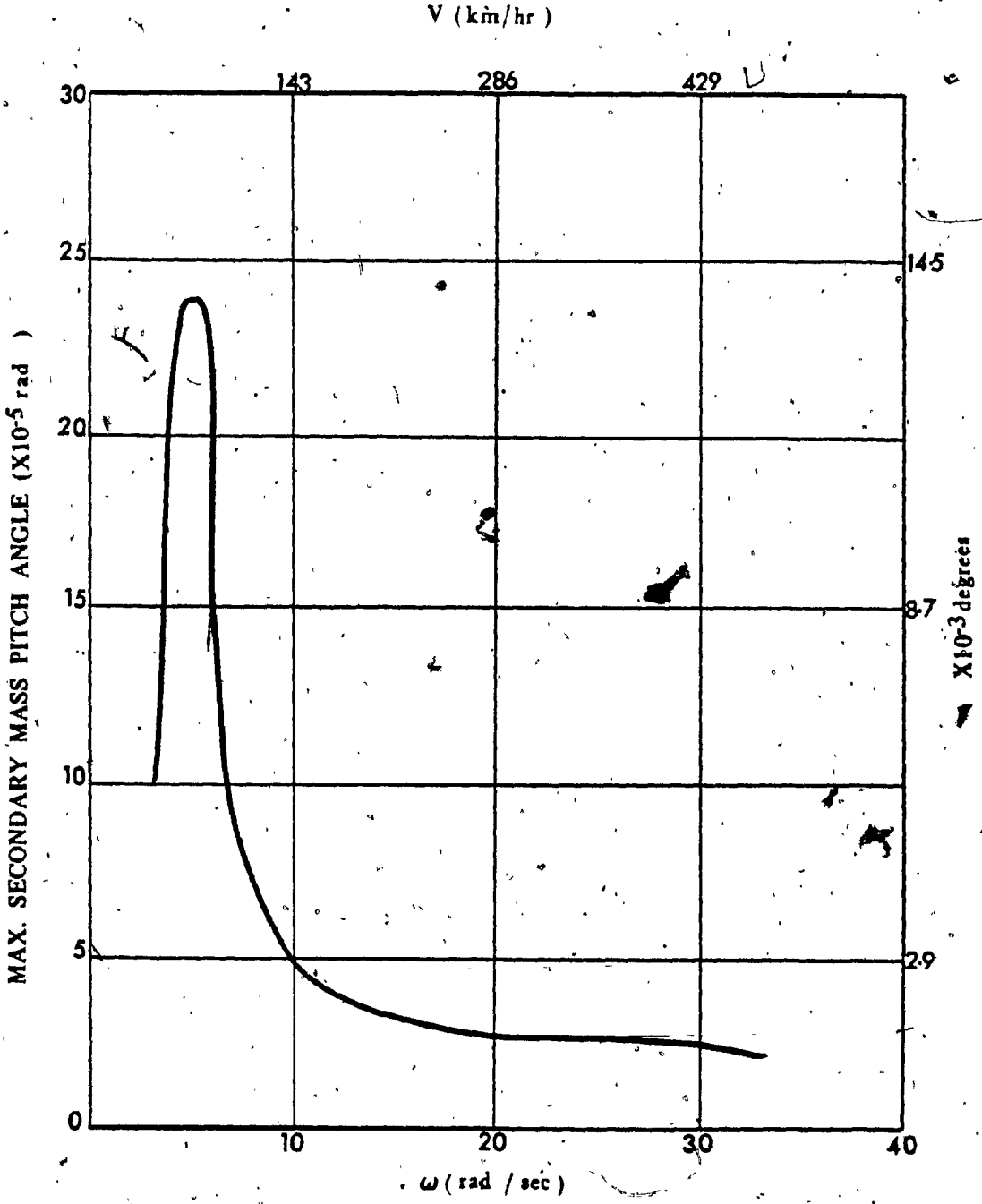

Fig. 4.9. Vehicle Body Pitch Response in the Frequency Domain.

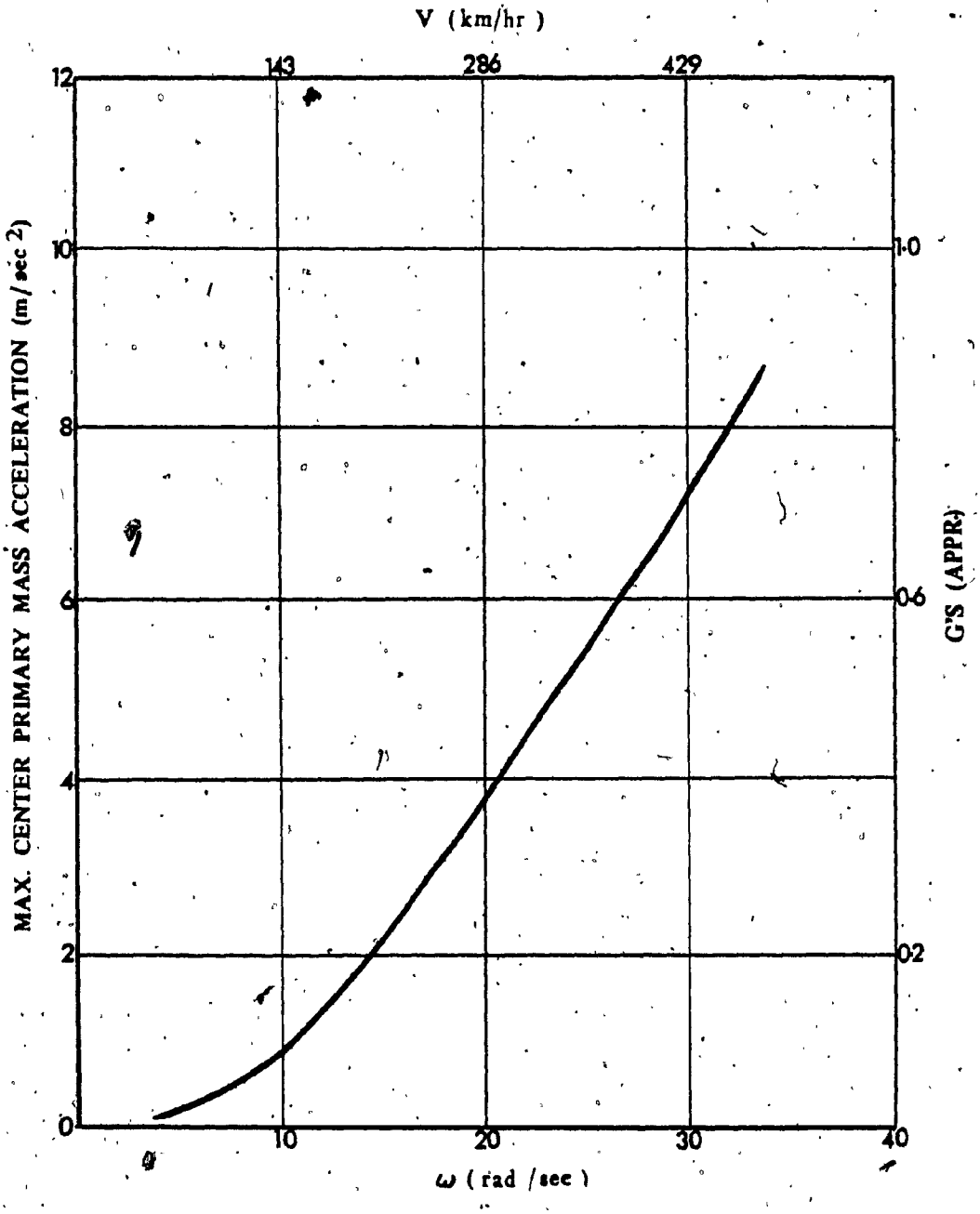

Fig. 4.10. Center Levitation Magnet Bounce Acceleration in the Frequency Domain.

natural frequency of the system since the levitation magnets are only restricted to motions in the vertical plane and do not have any rotational degree of freedom. Their response builds up with increasing vehicle speed toward a maximum value at about 60 rad/sec which corresponds to the bounce natural frequency of the primary mass.

The system behavioral characteristics described by the frequency response curves are utilized in the next chapter to carry out a parameter sensitivity study and a subsequent optimization of the vehicle mechanical suspension elements.

4.6 Summary

In this Chapter, the vehicle bouncing and pitching dynamic responses are evaluated in time as well as in the frequency domains. The system equations of motion, under a purely periodic guideway excitation, are derived. Numerical integration techniques are used to solve the system equations on a digital computer. The solution yields the vehicle time response curves, from which the vehicle response in frequency domain can be obtained. Even though the time response curves could only be generated for a limited time period, solely due to computer time limitations, it is found that steady state conditions for the response were reached. In the next chapter, a parametric study is carried out on the transient system response in the frequency domain. Here, another mathematical approach, using complex algebra analysis, is also utilized to determine the steady state responses of the system, and the results obtained from this approach are compared with those obtained from the solution of the system equations using numerical integration techniques.

CHAPTER 5

PARAMETRIC STUDY AND OPTIMIZATION OF THE SUSPENSION SYSTEM FOR BEST BOUNCE CHARACTERISTICS

5.1 Introduction

The frequency response plot of the vehicle body linear acceleration in Fig. 4.8 shows a strong peak indicating excessive bouncing occurring at a vehicle speed range of 75 to 125 km/hr (46.9 to 78.1 mph). This speed at which excessive bouncing occurs was found to correspond to the pitching natural frequency of the vehicle system. The vehicle frequency response plot also shows that the bounce response of the vehicle increases as the vehicle approached its maximum operating speed of 480 km/hr (300 mph). Since the vehicle body bouncing acceleration gives a true indication of the vehicle ride quality, it is important to study critically and understand the effects of those suspension elements which affect this bounce response and such an understanding can be obtained only through a parameter sensitivity study for the suspension constants. Through this parametric study, the sensitivity of the vehicle body bounce response to variations in the different suspension parameters is analysed, and methods of reducing the vehicle body bouncing acceleration are investigated. Even though the main objective of this analysis is to minimize the bouncing response of the vehicle, the effect of changing the suspension system parameters on the vehicle body pitching motion as well as the bouncing motions of the levitation magnets are also taken into consideration.

In order to conduct a parametric study, certain function of the bouncing response should be chosen to represent truly the performance

of the vehicle. This objective function may be chosen to be either the maximum value of the transient or the steady state bouncing responses in the frequency domain. Chapter 4 gives the system response in the time domain from which the transient frequency response was obtained. The transient response in the frequency domain was established assuming that the car enters a frequency ω_i with zero initial conditions corresponding to an instantaneous stationary state at the previous frequency ω_{i-1}. Such system behavior was employed in Figs. 4.8, 4.9, and 4.10 to give the corresponding maximum vehicle body bouncing acceleration, pitching angle, and the center levitation magnet bouncing acceleration respectively, as a single value for each input frequency. This representation provides a good basis for comparing the system performance at the required range of frequencies independent of the initial conditions and therefore it is found to be suitable for use in carrying out the parametric study proposed.

5.2 Objectives

A detailed parametric study is described in this Chapter utilizing the transient frequency response of the system with an objective to minimize the maximum value of the vehicle body bounce acceleration. The parametric study involves finding the effect of changing a single suspension parameter on the vehicle response when the vehicle is subjected to a purely periodic excitation from the guideway. The results of this study, in the form of trial solutions, show that further advanced investigation using multivariable optimization techniques is required. Through an optimization procedure, it would then be possible to find the optimum combination of the different suspension elements that would

minimize the maximum bounce acceleration in the frequency range of interest.

5.3 Parametric Study of the Vehicle Mechanical Suspension

Here, sensitivity analysis of the system responses to variations in each suspension parameter, one at a time, is carried out in order to determine the near optimum suspension parameters which would produce a minimum vehicle body bounce response over the frequency range specified. The effect on this response due to variation in the values of the coefficient of the viscous dampers, stiffness of the springs, changes in the guideway allowable maximum deflections, and the effect of adding another spring in series with the damper, thus introducing an elastic coupling between the viscous dampers and the vehicle body are particularly studied in detail. Initially, each secondary suspension system is considered to consist of a stiffness element K_{0_i} in parallel with a viscous damper C_i with the damper rigidly coupled to the vehicle body as shown in Fig. 5.1a. Then, the suspension system can be considered to consist of a stiffness element K_{0_i} in parallel with a viscous damper C_i, with the damper elastically coupled to the vehicle body through a series connection with a stiffness element K_i as in Fig. 5.1b. The results of the different parametric sensitivity on response is presented in the following subsections.

5.3.1 Viscous Dampers Rigidly Coupled to the Vehicle Body. Fig. 5.2 shows all the suspension elements of the vehicle consisting of the existing elements (K_{0_i}, C_i) and the additional stiffness elements (K_i) connected in series with the shock absorbers. The original values of the mechanical parameters of the MAGLEV vehicle used to generate the

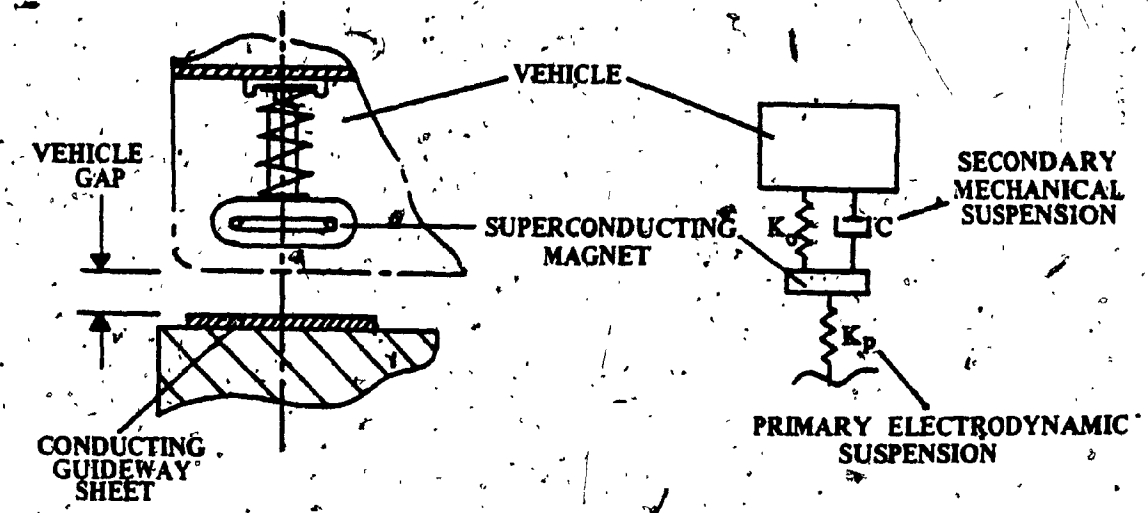

Fig. 5.1a. Passive Mechanical Suspension Model.

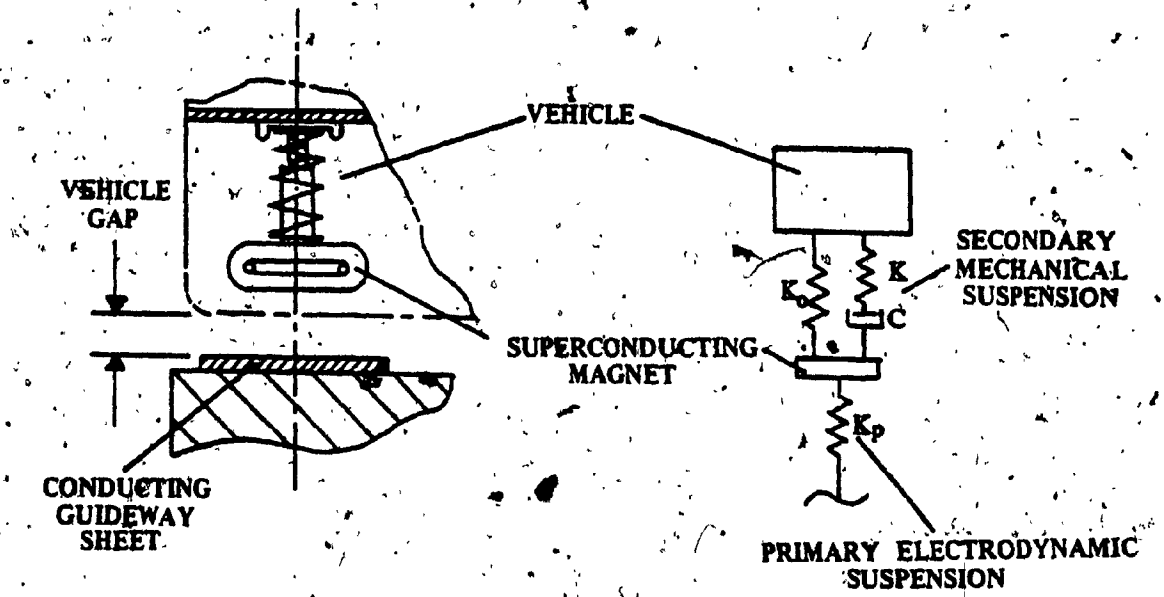

Fig. 5.1b. Modified Mechanical Suspension Model.

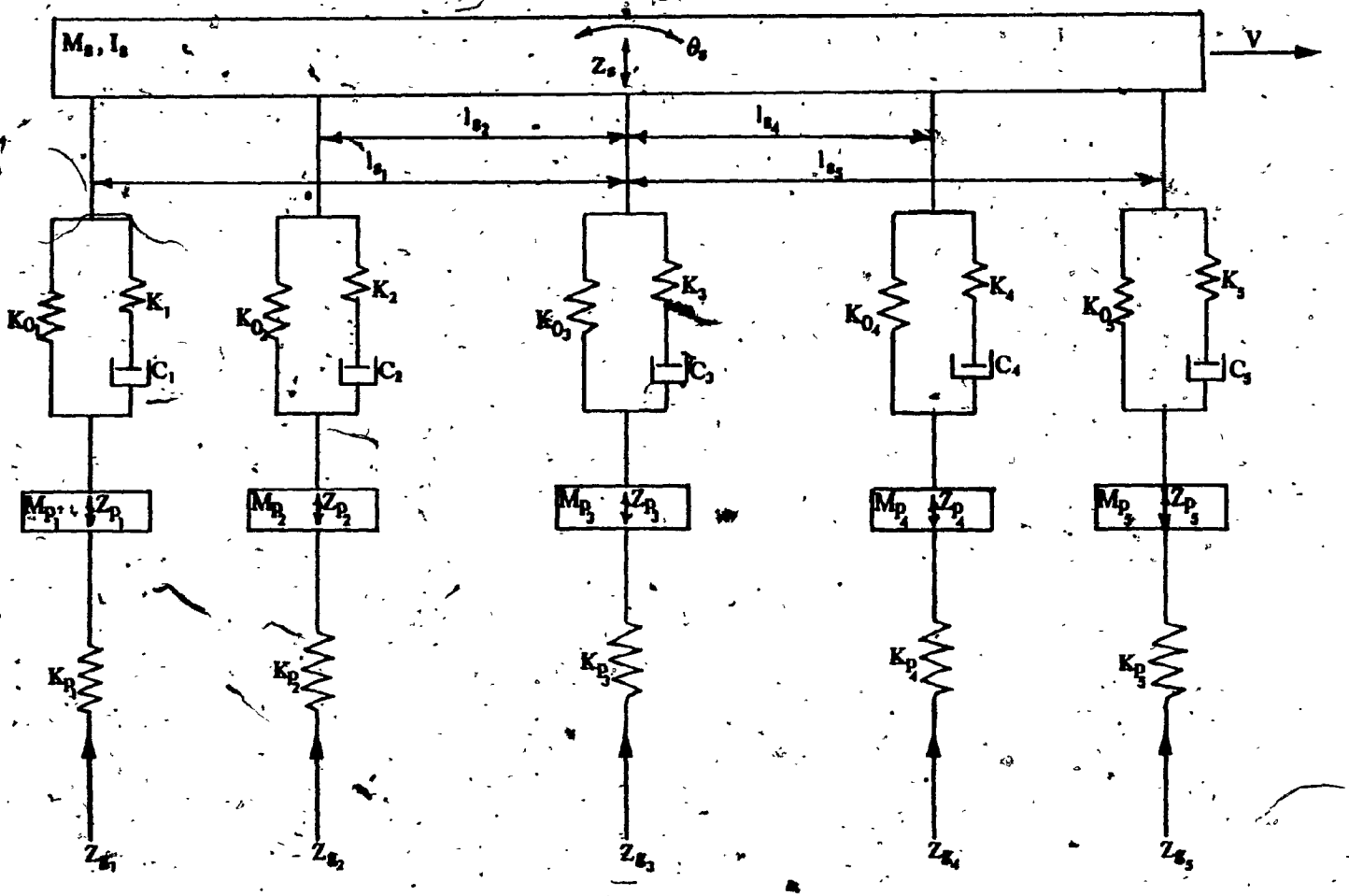

Fig. 5.2. Vertical Suspension Arrangement of the Vehicle.

system dynamic response are listed in Table 5.1. The response curves of the system generated using this set of parameters form the basis of comparison for the parameter sensitivity analysis. This analysis is carried out by comparing the transient response of the system in the frequency domain for different sets of suspension system parameters. The plots of the system response in the frequency domain are obtained from a series of time response curves generated for different vehicle speeds.

The effect of varying the viscous damper coefficients, C_i, of the shock absorbers mounted between the levitation magnets and the vehicle body on the frequency response of the vehicle body (secondary mass) bounce acceleration, pitching angle, and the center levitation magnet (primary mass) acceleration is shown in Figs. 5.3, 5.4, and 5.5 respectively. From Fig. 5.3, it can be seen that increasing the viscous damper coefficients to one and a half time its original value reduces the peak bounce acceleration occurring at a frequency of about 6 rad/sec; however it causes higher bounce acceleration response to occur for frequency values higher than 8 rad/sec. From Figs. 5.4 and 5.5 it can be seen that a higher value of C_i yields a lower vehicle body pitching response as well as a lower center levitation magnet bounce response for all the frequency levels of interest. Also, by observing the suspension system deflections for both the magnetic (primary) and the mechanical (secondary) suspension systems, it is found that a lower value of C_i causes higher deflections for secondary suspension systems; whereas, on the other hand, it causes lower primary suspension system deflections than those deflections caused by a higher setting of the coefficients of the shock absorbers.

M_s	=	22630. kg
I_s	=	3000000. kg·m^2
M_{p_i}	=	210. kg
K_{p_i}	=	600000. N/m
K_{0_i}	=	200000. N/m
C_i	=	10640. N·sec/m
K_i	=	RIGID
ℓ_{s_1}	=	13.68 m
ℓ_{s_2}	=	9.12 m
ℓ_{s_4}	=	9.12 m
ℓ_{s_5}	=	13.68 m

Table 5.1 Original Recommended Values of Constants of the Canadian MAGLEV [5, 6].

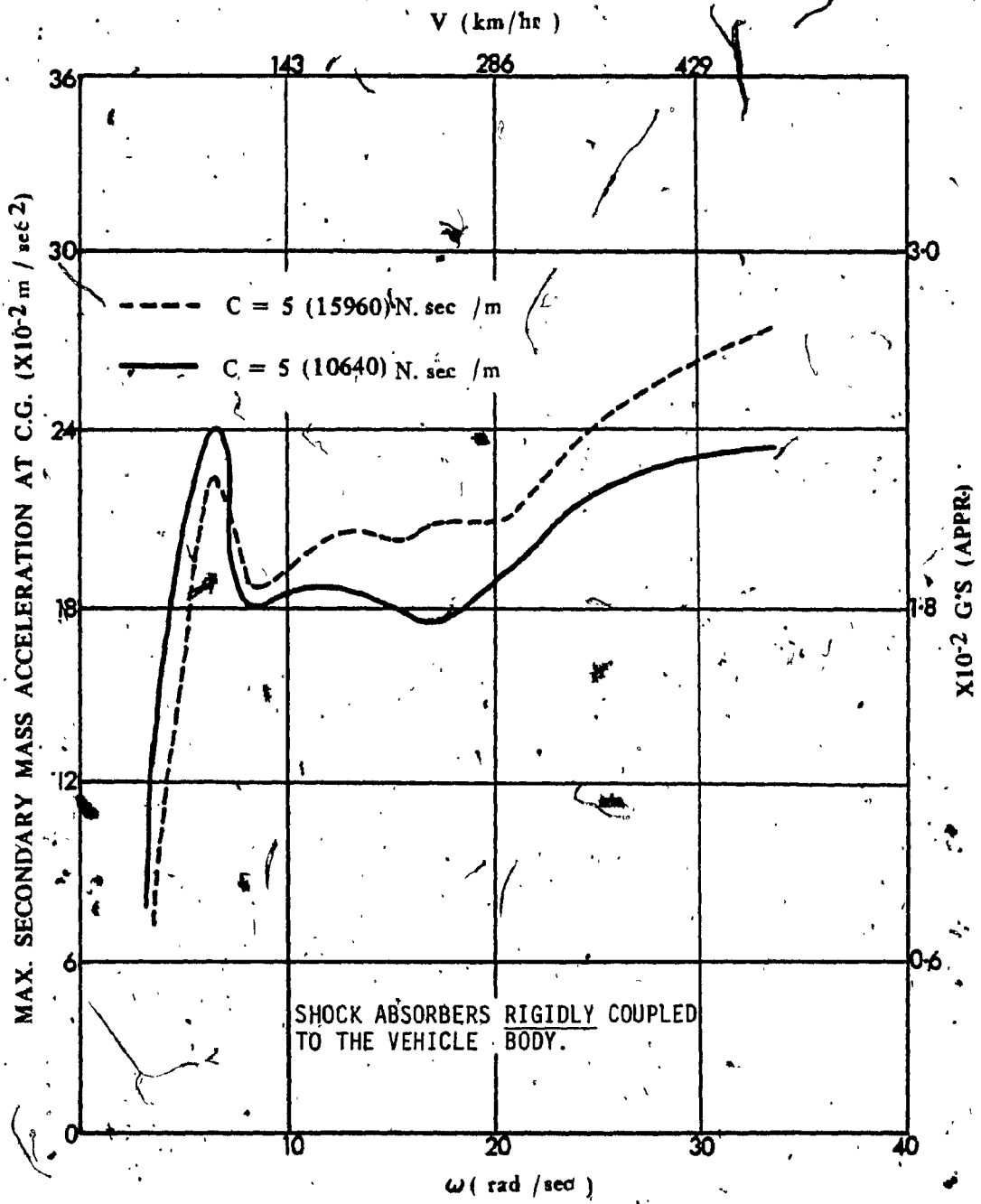

Fig. 5.3. Effect of Varying the Coefficient C_i of the Viscous Dampers on the Vehicle Body Bounce Acceleration.

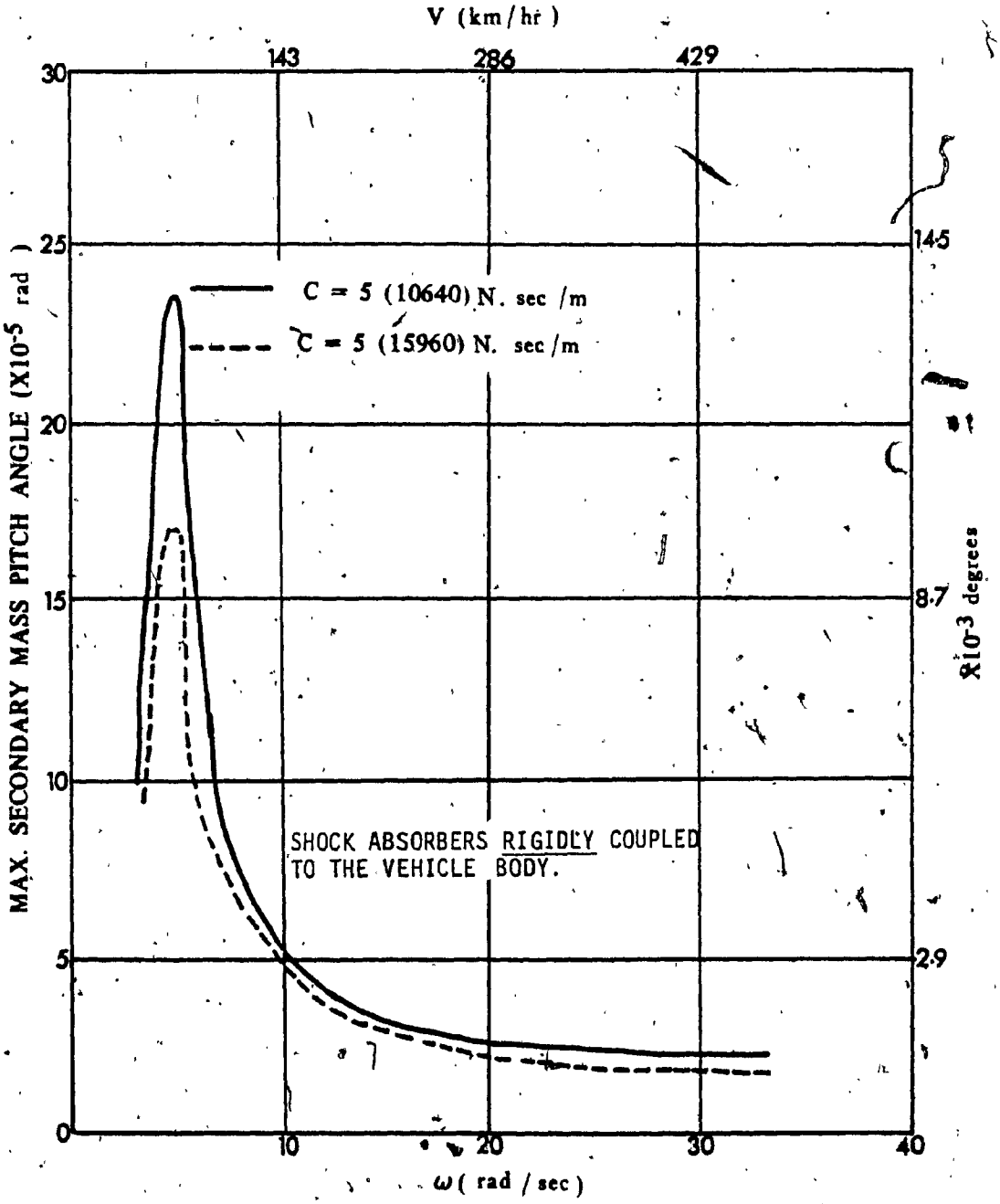

Fig. 5.4. Effect of Varying the Coefficient C_i of the Viscous Dampers on the Vehicle Pitch Response.

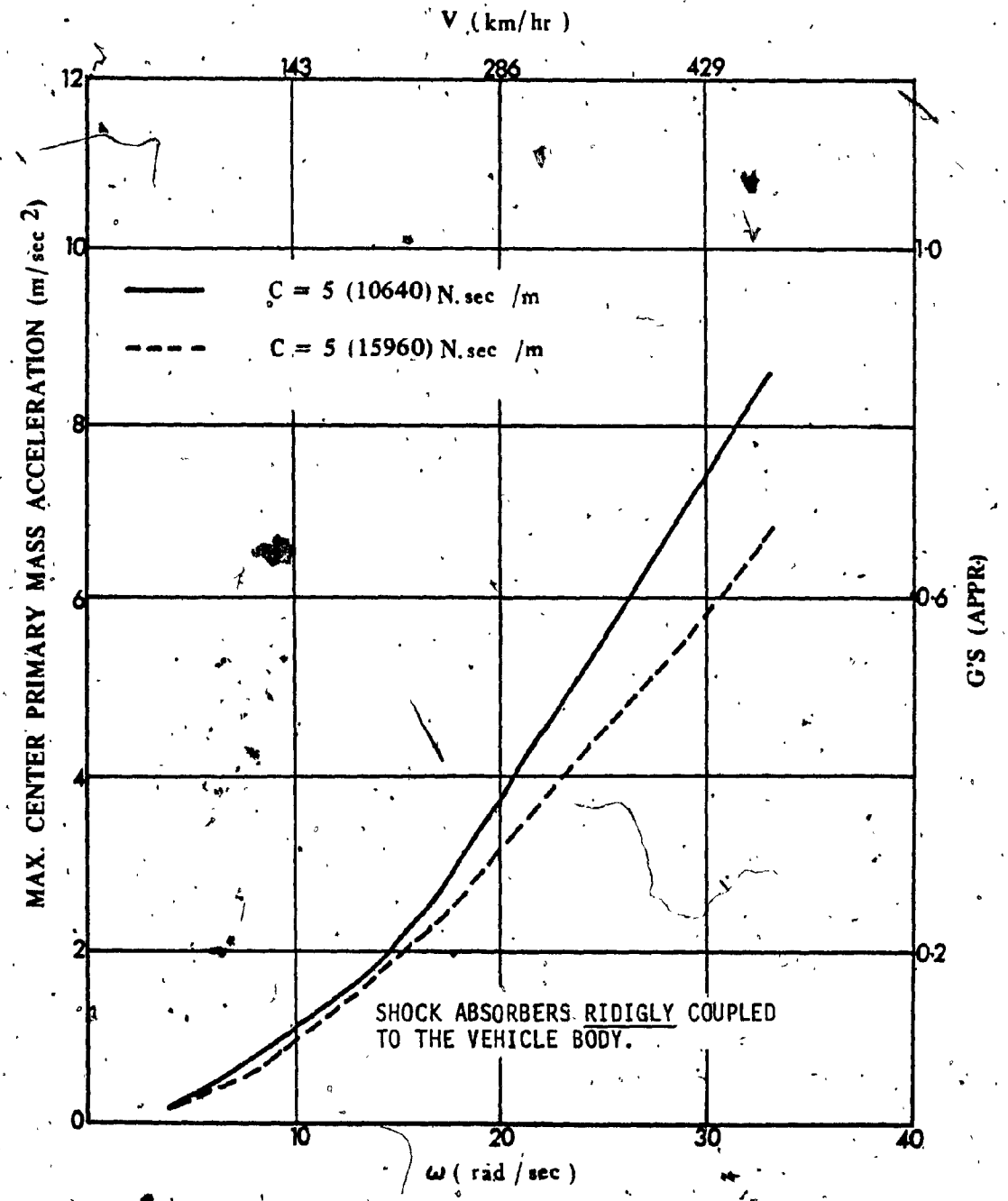

Fig. 5.5. Effect of Varying the Coefficient C_i of the Viscous Dampers on the Center Levitation Magnet Bounce Acceleration.

5.3.2 Stiffness Elements. Figs. 5.6, 5.7, and 5.8 show the effect of reducing the stiffness of the spring situated in parallel with the viscous damper, with the shock absorbers being rigidly coupled to the vehicle body. From Figs. 5.6 to 5.7, it may be seen that softer springs produce lower bouncing and pitching response of the vehicle body, and has very little effect on the levitation magnet bounce response. But, on the other hand, soft springs cause very large initial deflection to occur for both primary and secondary suspension systems and, thus, for practical reasons, and in order to prevent large suspension system initial deflections, the spring setting cannot be solely selected on the basis of system response alone, and any suspension system design should take this seriously into consideration.

The effect of adding a spring element in series with the shock absorbers cannot be readily illustrated since the main advantage of adding such an element is to allow for a variation in the viscous damper coefficients and in the stiffness coefficients of the springs in parallel with the shock absorbers, without producing an ill effect on the suspension systems deflections.

Variations in the value of K_i was found to affect the stability of the system in the sense that, as the value of K_i approached the value of K_{0_i}, it was found that the system became marginally stable, and furthermore, the system became unstable for all values of K_i less than K_{0_i}. Therefore, throughout this study, and in order to determine the near optimum values of the suspension elements which yield minimum vehicle body bounce acceleration response it was observed that the value of K_i must always be kept higher than the value chosen for K_{0_i}.

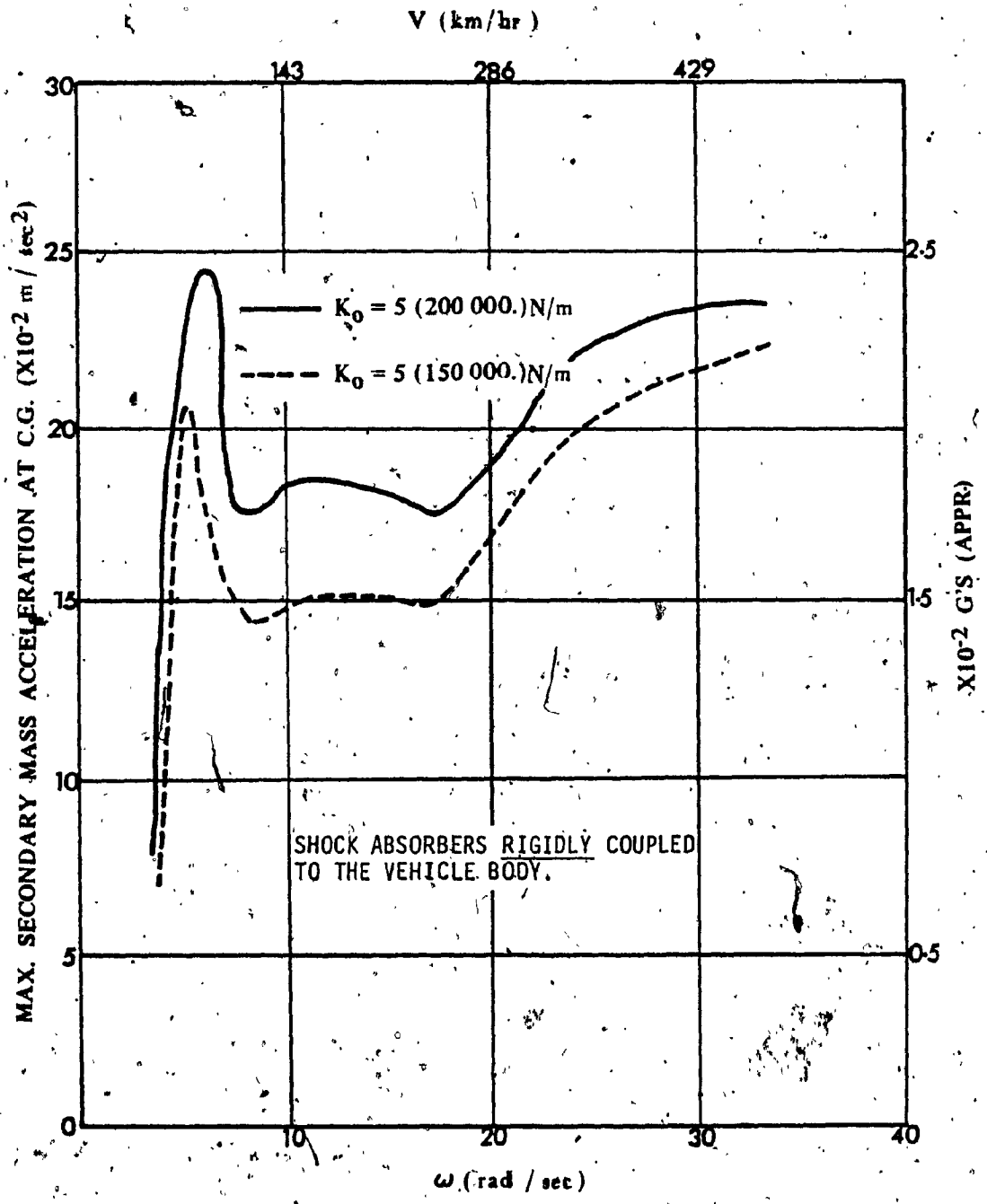

Fig. 5:6. Effect of Varying the Stiffness K_{0_i} of the Springs in Parallel with the Shock Absorbers on the Vehicle Body Bounce Acceleration.

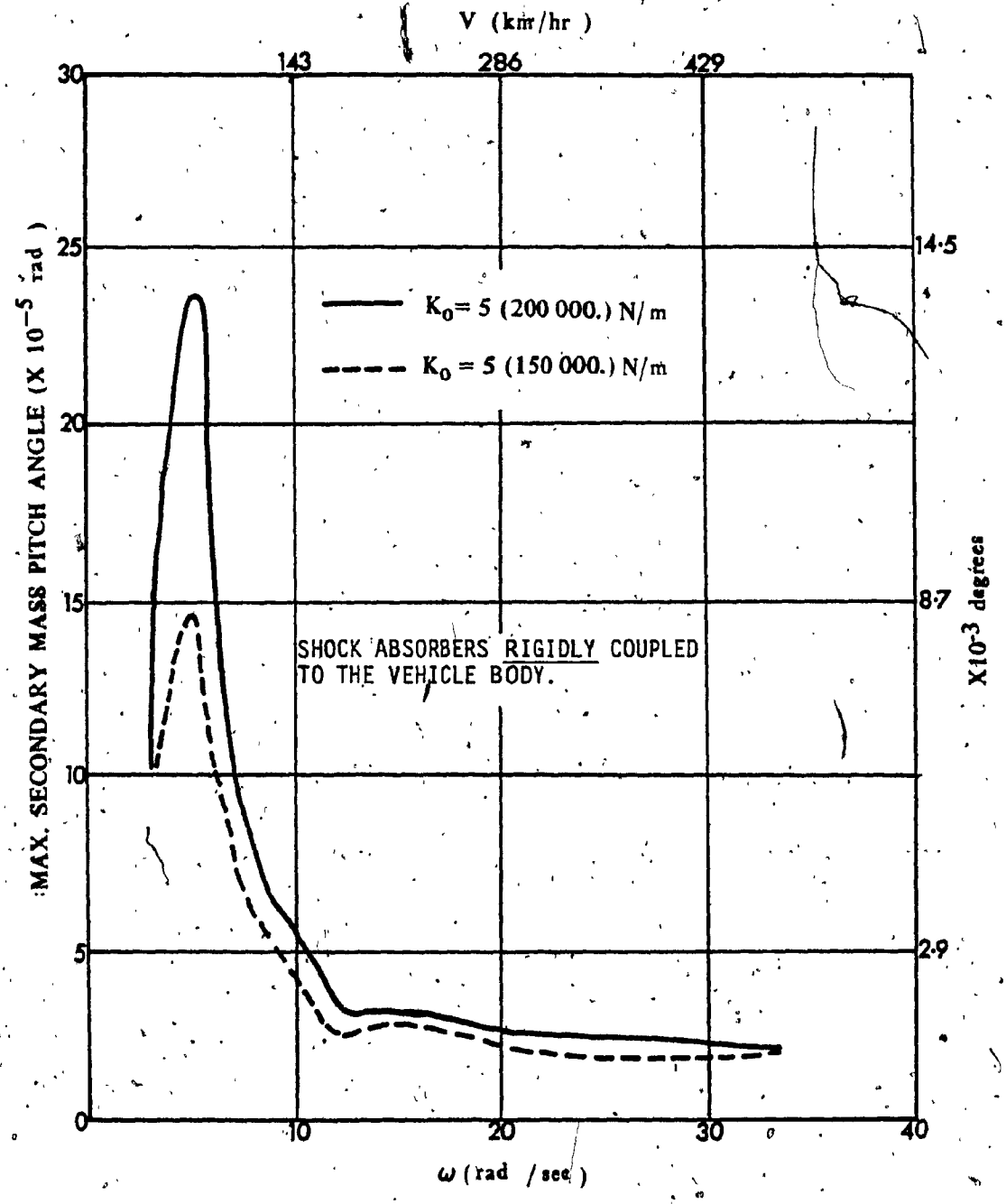

Fig. 5.7. Effect of Varying the Stiffness K_{0_1} of the Springs in Parallel with the Shock Absorbers on the Vehicle Body Pitch Response.

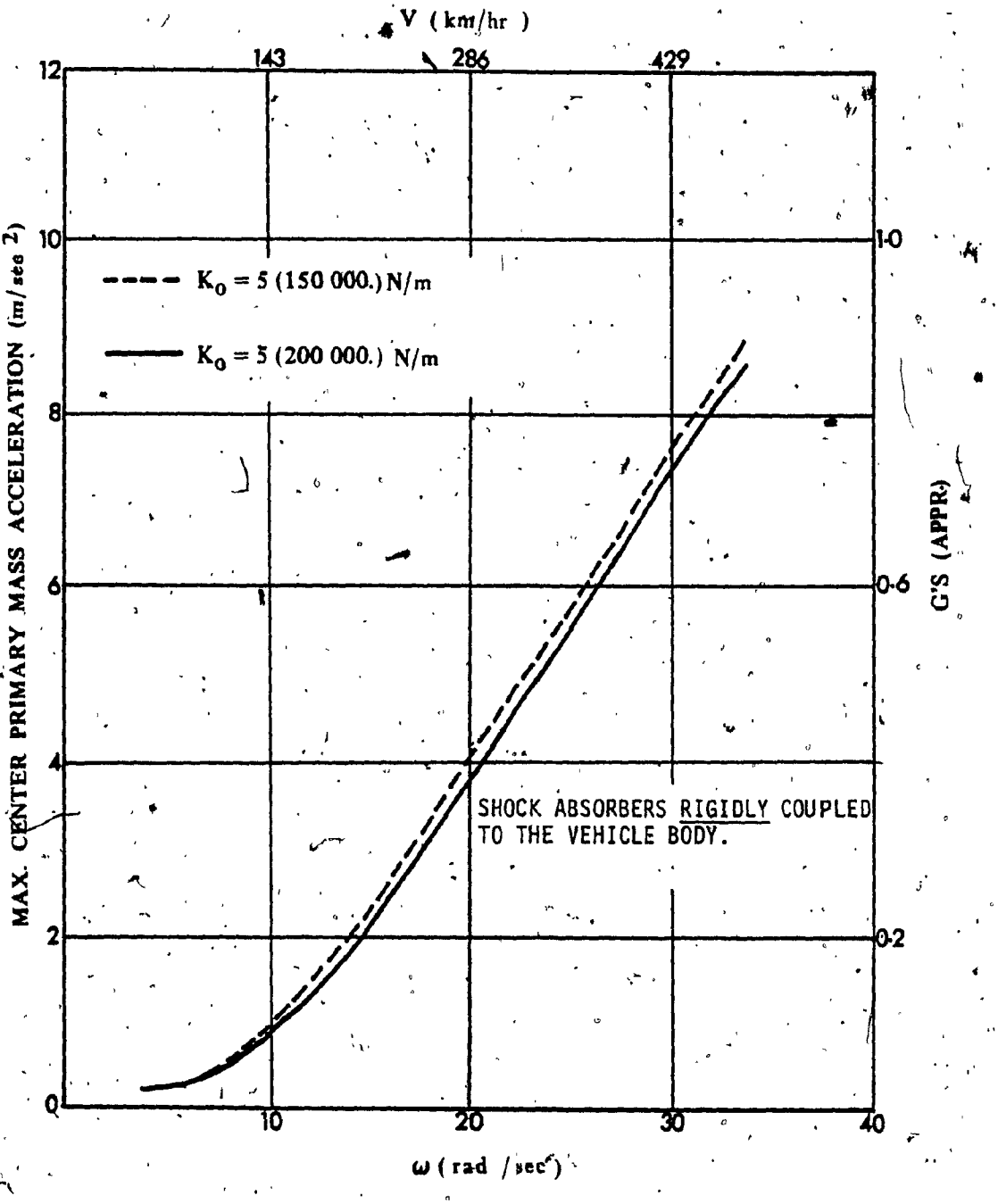

Fig. 5.8. Effect of Varying the Stiffness K_{0_i} of the Springs in Parallel with the Shock Absorbers on the Center Levitation Magnet Bounce Acceleration.

The effect of varying the suspension system parameters on the system response, with the shock absorbers being elastically coupled to the vehicle body is shown in Figs. 5.9 through 5.17. From Figs. 5.9, 5.10, and 5.11 it may be seen that a higher setting of K_i would yield better dynamic response for the vehicle body bounce and pitch modes and for the center levitation magnet bounce mode. As for the effect of varying the stiffness coefficients of the springs in parallel with the shock absorbers, given Figs. 5.12, 5.13, and 5.14 it is found that a lower value of K_{0i} yield better system response with acceptable suspension systems deflections. Figs. 5.15 to 5.17 show the effect of varying the shock absorbers setting for the case when the dampers are elastically coupled with the vehicle body. From a detailed study of these figures, similar conclusions to those made in the previous subsection can be drawn for the suspension specifications.

5.3.3 Vertical Alignment. It is also possible to reduce the vehicle bounce response by properly controlling the guideway input. The effect of guideway deflections on the vehicle bounce response is shown in Fig. 5.18. A reduction in the vertical deflection of the guideway beams by a factor of five causes a decrease in the vehicle body bounce response by the same order. However, since the purpose of this investigation is to find an optimum suspension system which would minimize the vehicle bounce, this investigation is not concerned with the structural aspects of guideway design for MAGLEV trains.

5.3.4 Conclusions of Parametric Study. In summary, the vehicle body bounce response can be minimized by:

i) Using soft springs in parallel with the shock absorbers; but

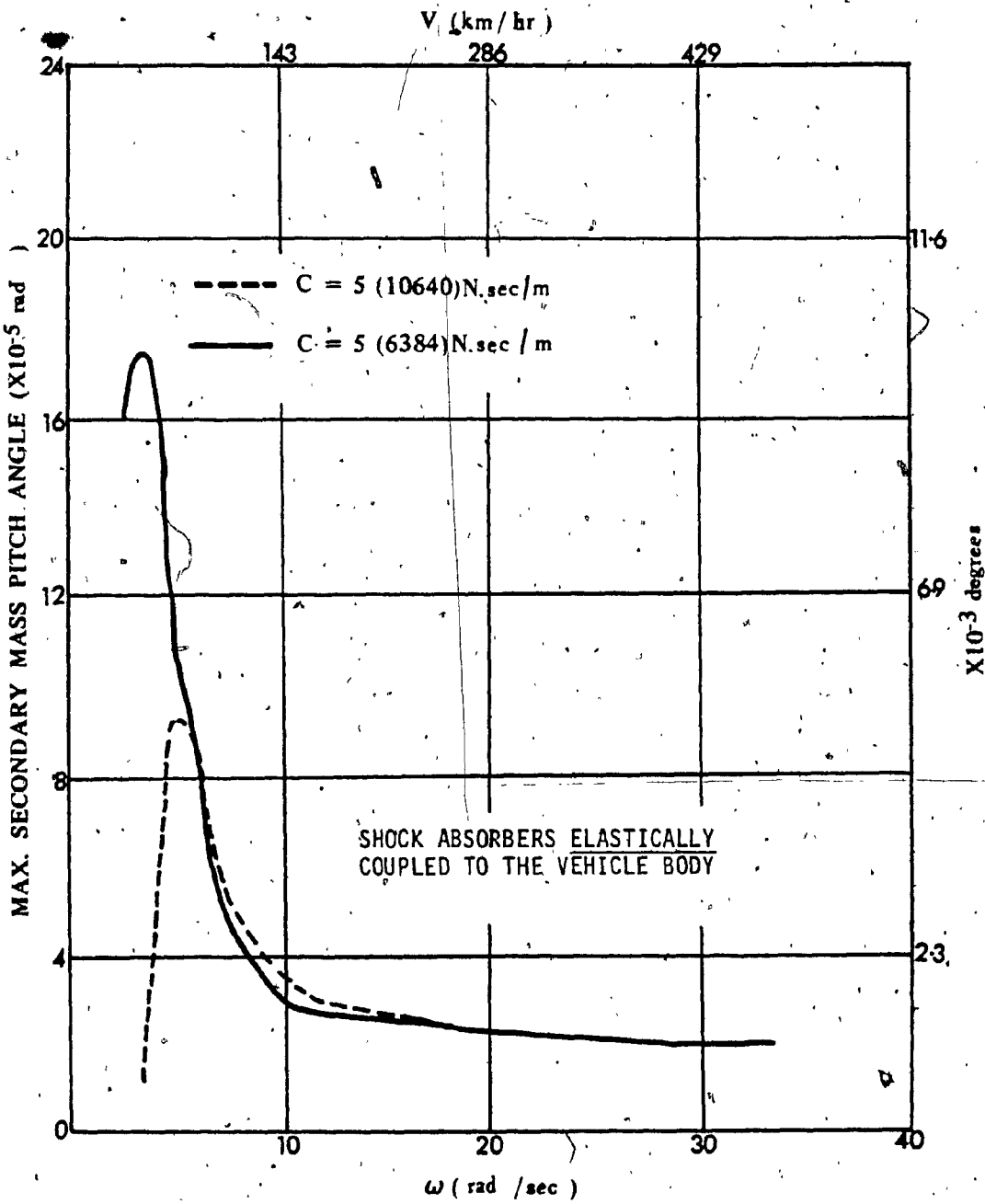

Fig. 5.16. Effect of Varying the Coefficient C_i of the Viscous Dampers on the Vehicle Body Pitch Response.

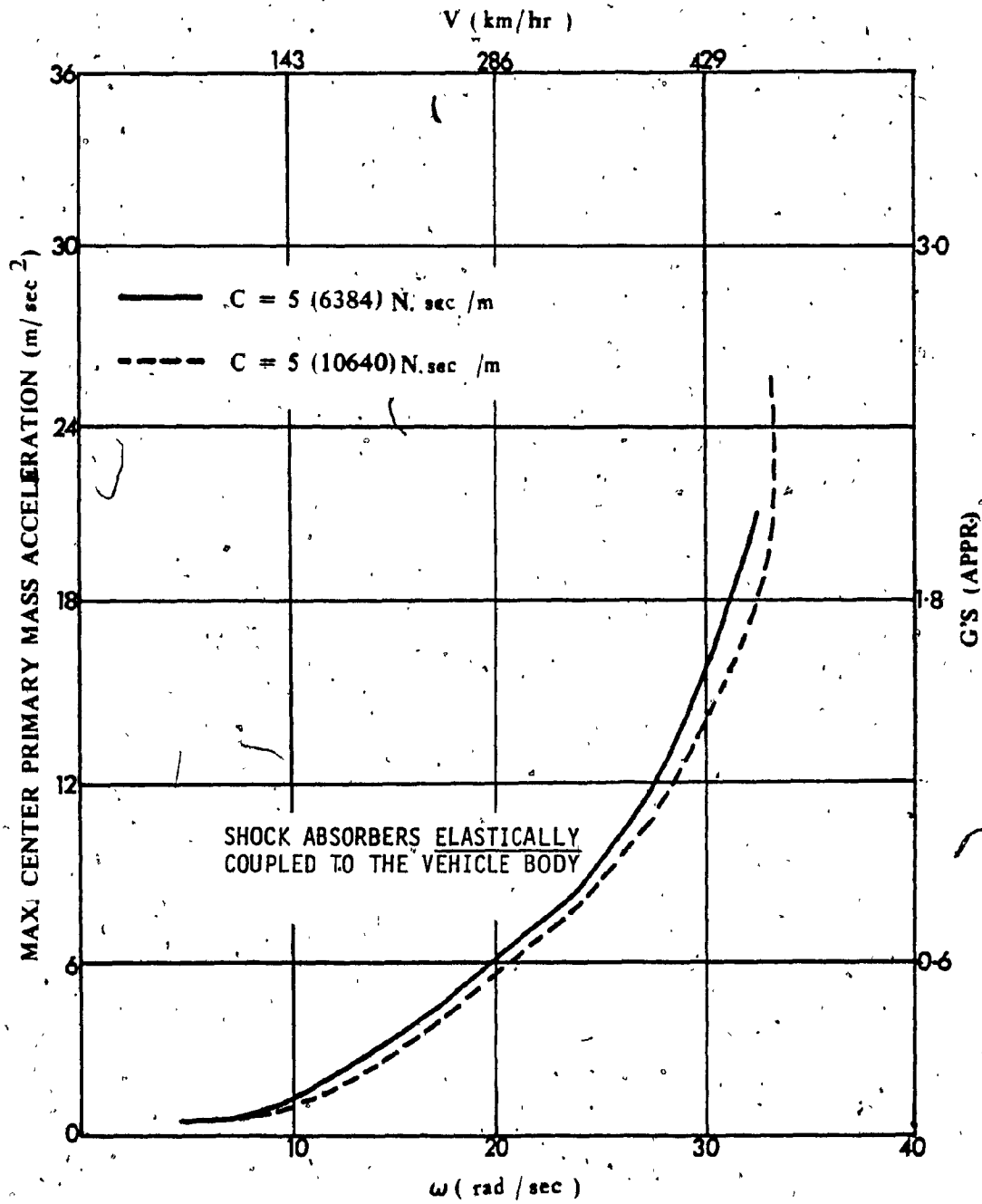

Fig. 5.17. Effect of Varying the Coefficient C_i of the Viscous Dampers on the Center Levitation Magnet Bounce Acceleration.

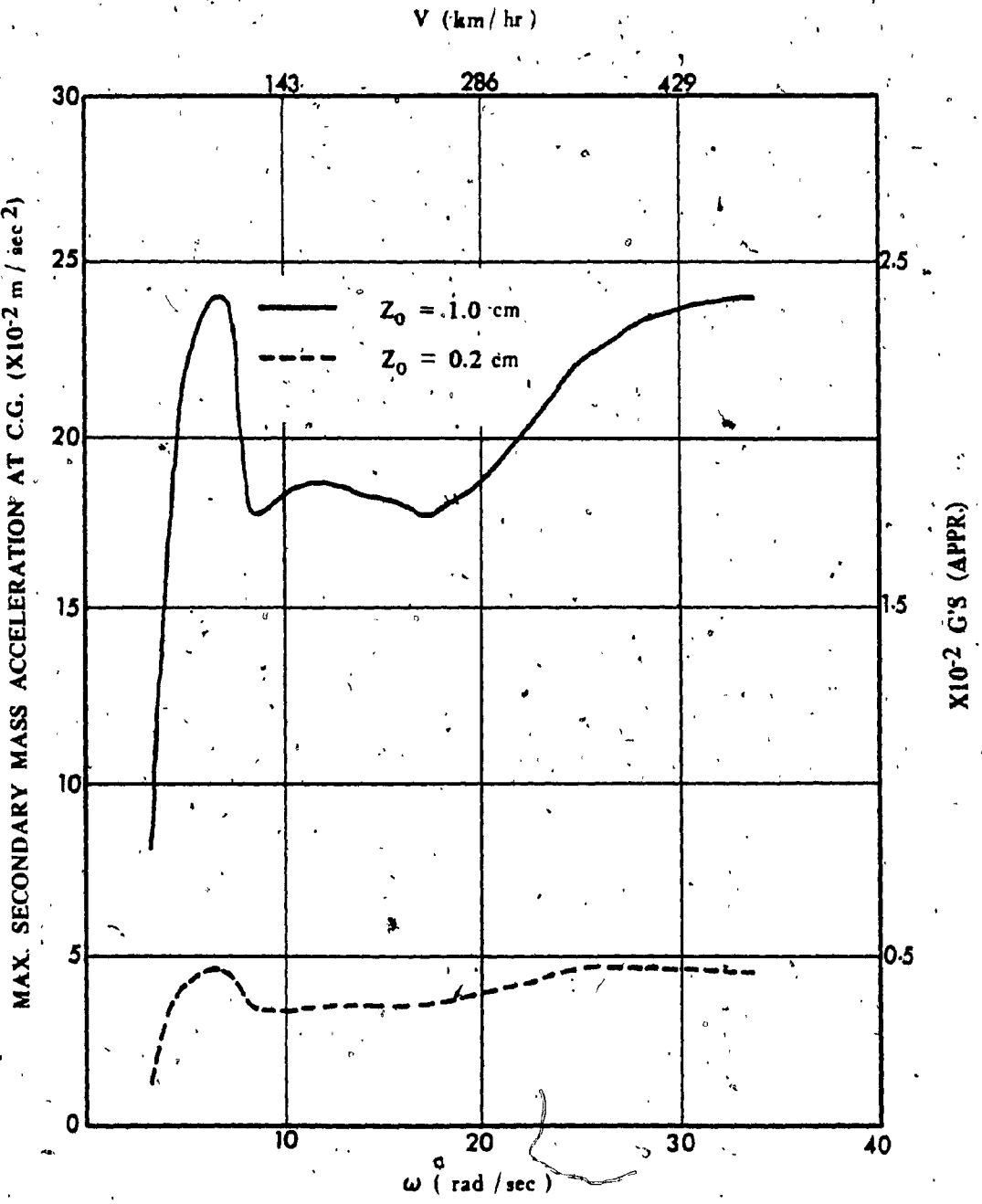

Fig. 5.18. Effect of Vertical Misalignment in Terms of Guideway Deflection on the Vehicle Body Bounce Response.

this would create large suspension system initial deflections.

ii) Adding stiffness elements in series with the shock absorbers in order to allow for variation in the stiffness elements in parallel with the shock absorber; in which case, it is found to improve the vehicle body bouncing and pitching responses, but is found to cause an increase in the levitation magnets bouncing responses.

Due to the above contradictions in the design recommendations arrived at from the parametric study carried out, the solution to the problem of specifying best suspension values demands further investigation using multivariable optimization techniques, as described in the following section.

5.4 Suspension Optimization

As previously stated, the transient bounce response in the frequency domain, as shown in Fig. 4.8, obtained from a series of time responses provides a suitable basis for comparing the system performance. However, such behavioral representation is not very convenient for carrying out a program of suspension optimization because of the large computer time required to generate the system time response at each frequency level for different sets of values of suspension system parameters. Taking advantage of the linearity of the system, a quick efficient solution for the steady state response of the system under harmonic excitation can be generated using methods of complex algebra [28]. A comparison between the transient and steady state responses of the system under guideway periodic excitation is shown in Fig. 5.19. As expected, the magnitude of the vehicle body acceleration at all frequency levels is higher in the transient state than it is in the steady state. However,

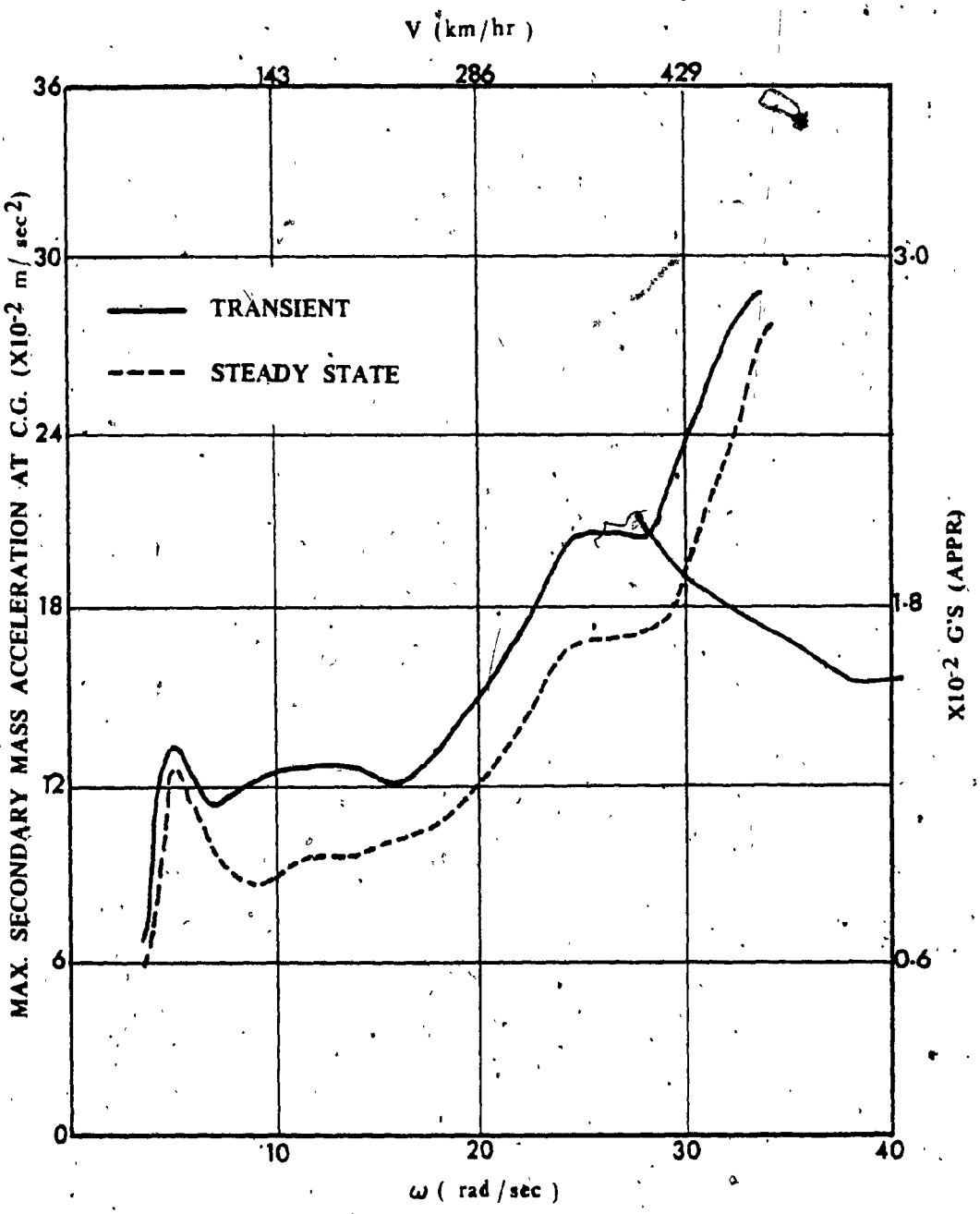

Fig. 5.19. Transient and Steady State Vehicle Bounce Responses.

both curves exhibit the essential behavior of the system response and therefore it is appropriate to apply optimization techniques to either the transient or the steady state response of the system, whichever convenient.

In order to be able to apply the complex algebra method of solution, as proposed by ElMaraghy et al [28], to the problem under investigation, the periodic excitation to the system needs to be approximated by a harmonic excitation. However, for simplicity, only the first harmonic term in Equation (3.2) is considered to represent the system input excitation, and all higher order terms are neglected. Fig. 5.20 shows the frequency responses of the vehicle body acceleration at the center of gravity when the system is subjected to either periodic or purely harmonic excitations from the guideway. These frequency response curves are generated from a series of time response curves at different vehicle speeds for both periodic and harmonic input excitations. As expected, it can be seen from the figure that at low frequency values the system response to periodic excitation is only slightly higher than its response to purely harmonic excitation; while at high frequency levels where the higher order terms of the Fourier series approximation to the periodic excitation become more significant, the difference between the responses due to harmonic and periodic excitations becomes dominant. Nevertheless, both curves exhibit the same system characteristics and show that the vehicle body acceleration will reach a peak at a frequency level of approximately 6 rad/sec, which corresponds to the pitch natural frequency of the system, after which it will decay and then gradually builds up as the vehicle velocity is increased.

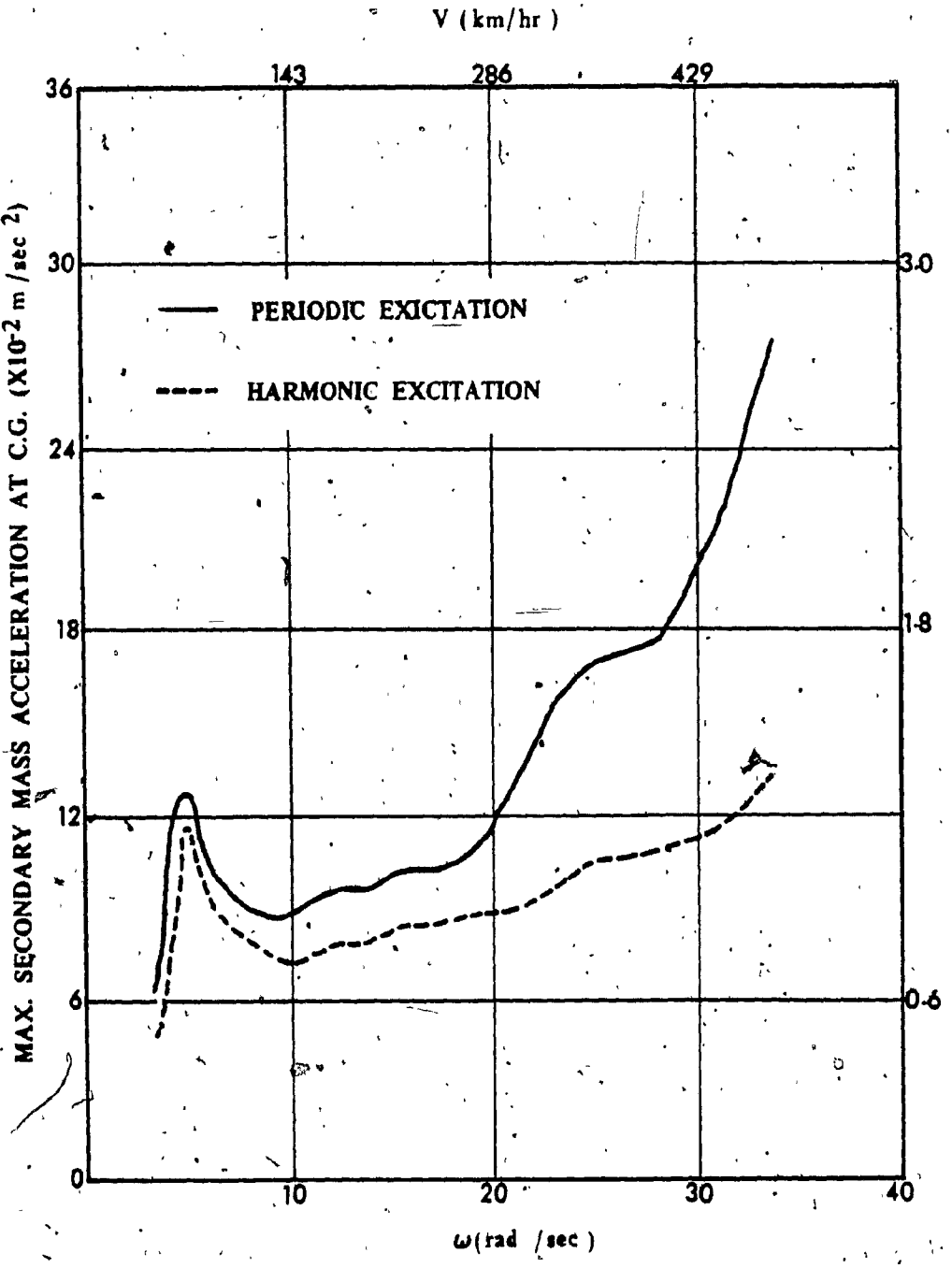

Fig. 5.20. Comparison of Vehicle Body Bounce Responses Under Periodic and Harmonic Input.

The method of complex algebra used to determine the steady-state response of the vehicle system is based on the fact that for a linear system where the impressed force is harmonic, the steady-state solution is also harmonic with the same frequency and in the presence of damping in the system there is a phase difference between the resulting motions and the input excitation. In principle, the method of solution can be summarized as follows:

1) The forcing function $\underset{\sim}{E}$ is expressed in a vector harmonic form

$$\underset{\sim}{E} = \underset{\sim}{E}_0 e^{i\omega t} \tag{5.1}$$

2) The resulting displacement $\underset{\sim}{z}$ of the system will have the same angular speed ω as that of the input forcing function but will be lagging by a phase angle ϕ and can be expressed as:

$$\underset{\sim}{z} = \underset{\sim}{Z} e^{i(\omega t-\phi)} = \underset{\sim}{Z} e^{-i\phi} e^{i\omega t} \tag{5.2}$$

where $\underset{\sim}{E}_0$ and $\underset{\sim}{Z}$ are the vectors representing the forcing function and the system response respectively.

Equation (5.2) can also be written as:

$$\underset{\sim}{z} = \underset{\sim}{\bar{Z}} e^{i\omega t}$$

where $\underset{\sim}{\bar{Z}} = \underset{\sim}{Z} e^{-i\phi}$ is the complex amplitude designating the response angular position with respect to the excitation amplitude $\underset{\sim}{E}_0$.

Applying the same complex notation to the vehicle system dynamic equations in state form:

$$\dot{\underset{\sim}{Z}} = \underset{\sim}{F}\underset{\sim}{Z} + \underset{\sim}{E}(t) \tag{5.3}$$

Substituting for $\dot{\underset{\sim}{Z}}$ by:

$$\dot{\underset{\sim}{Z}} = i\omega \underset{\sim}{Z}$$

Equation (5.3) can be written in the form:

$$\bar{Z} = (i\omega I - F)^{-1} E \qquad (5.4)$$

The system steady state response can then be obtained by solving Equation (5.4) for increasing values of the input frequency ω.

To check the validity of this method of solution, the steady state system response curves for increasing input frequency obtained from solving the system equations using numerical integration techniques as well as the method of complex algebra are plotted in Fig. 5.21. The data obtained from both methods of solution agree very closely with each other, and the two curves almost match as can be seen.

The steady state system response in the frequency domain obtained from solving Equation (5.4) for increasing values of input frequency is used for carrying out a multivariable optimization process which is explained in the following subsection.

5.4.1 Definition of the Optimization Problem. A statement of the optimization problem is to be defined through the objective of the optimization; which, in this case, is to find the suspension parameters X_d that minimize the objective function B that is defined to be the maximum value of an arbitrary function $f(Z(X_d))$ of the steady state response of the vehicle within the frequency domain of interest. Here, Z is the independent generalized coordinates of the system as defined in Chapter 4. In other words, it is required to find

$$\min \cdot B = \min_{\omega_i} \cdot \max \cdot f[Z(\omega_i(X_d), X_d)]$$

subjected to the following constraints

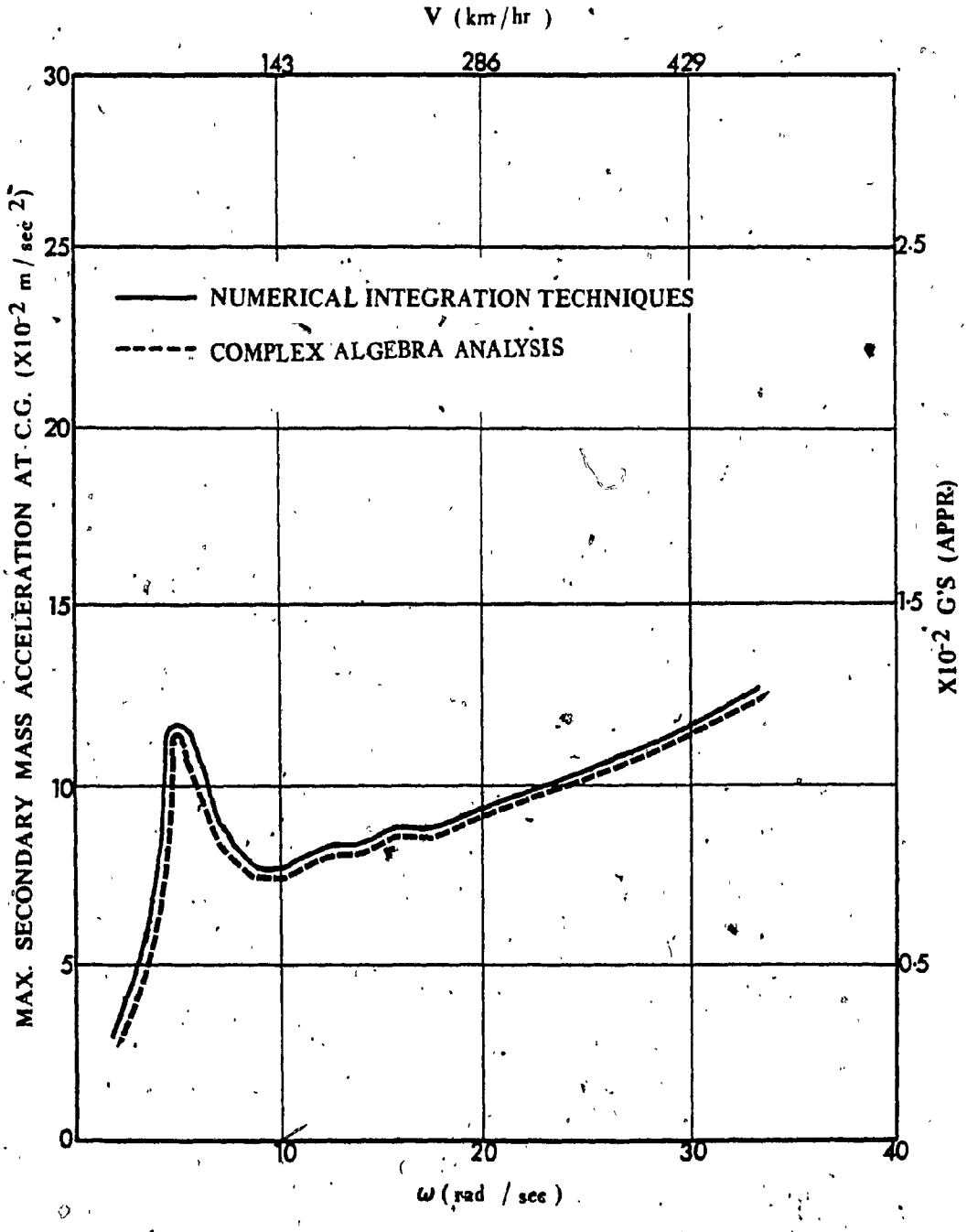

Fig. 5.21. Comparison of Steady State Vehicle Bounce Responses Generated Using Numerical Integration Techniques and Method of Complex Algebra.

$$\underset{\sim}{a} \leq \underset{\sim}{X}_d \leq \underset{\sim}{b}$$

where $\underset{\sim}{a}$ and $\underset{\sim}{b}$ define the practical region for the design variables.

5.4.2 Design Variables for Optimization. The independent design variables chosen for the optimization are as follows:

i) The five shock absorbers damping coefficients $(C_1, C_2, C_3, C_4, C_5)$

ii) The five stiffness elements that are situated in series with the shock absorbers $(K_1, K_2, K_3, K_4, K_5)$

iii) The five stiffness elements that are in parallel with the shock absorbers $(K_{0_1}, K_{0_2}, K_{0_3}, K_{0_4}, K_{0_5})$

The steady state vehicle body bounce response with the frequency domain of interest is chosen as the objective function here. The lower and upper bound frequencies that determine the frequency range in which optimization is carried are taken to be the frequencies corresponding to the vehicle lift-off speed of 50 km/hr (31.25 mph), that is the speed at which the vehicle becomes levitated on the primary magnetic suspension systems, and that corresponding to the proposed maximum cruising speed of 480 km/hr (300 mph) respectively. The optimization procedure and method of analysis employed are described in the following subsections.

5.4.3 Description of the Optimization Procedure. The optimization scheme used in this analysis is outlined through a flow chart detailed in Fig. 5.22. The step by step procedure used can be restated as follows:

i) An initial guess of the design variable vector $\underset{\sim}{X}_d$ is used to start the program.

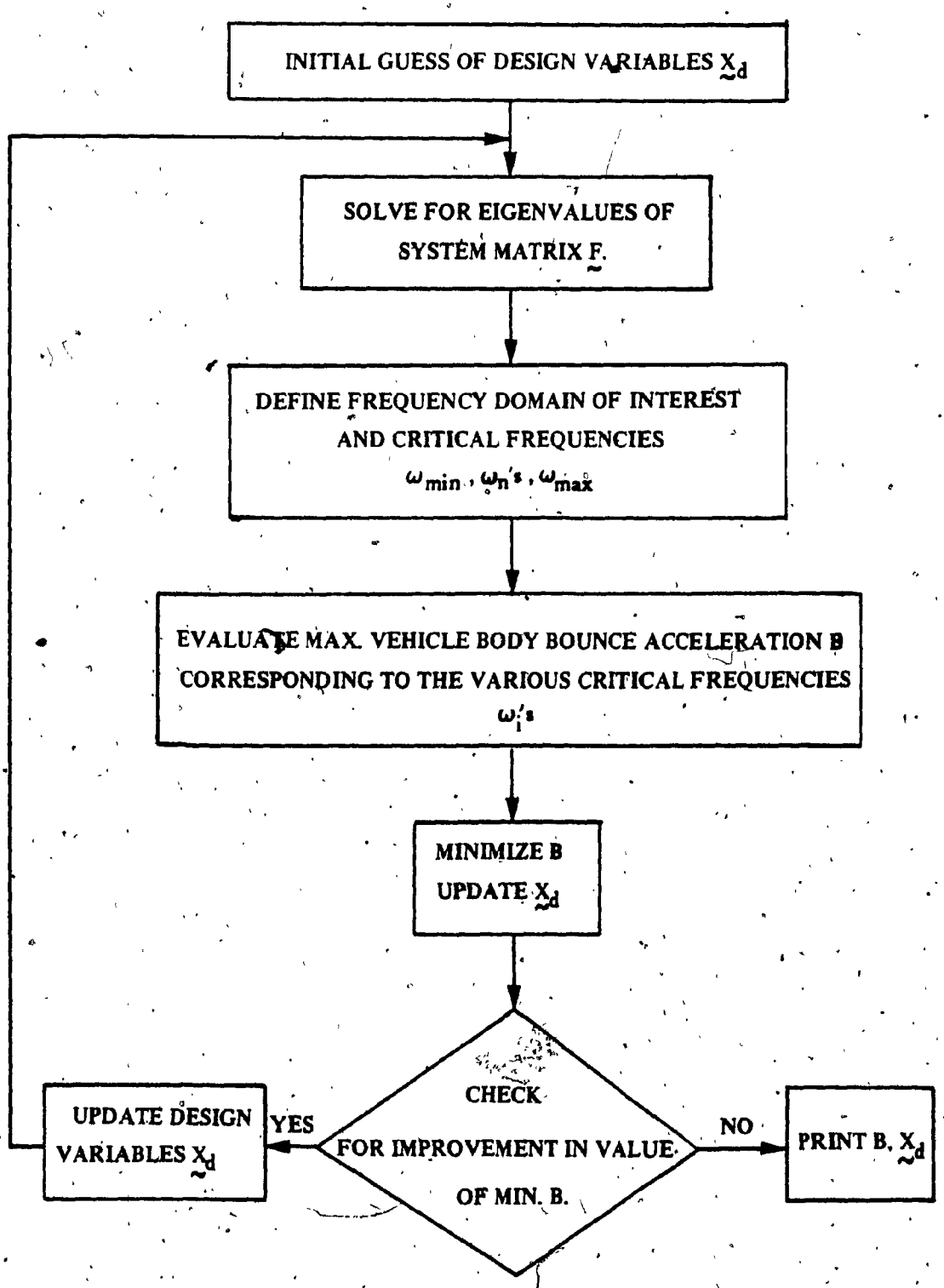

Fig. 5.22. The Optimization Scheme.

ii) The lower and upper bounds of the frequency range of interest are determined such that the solution will be determined for $\omega_{min} \leq \omega \leq \omega_{max}$.

iii) The eigenvalues of the system F are solved for, and the critical frequencies of the system are then defined to be ω_{min}, ω_{max}, as well as those natural frequencies ω_n such that $\omega_{min} < \omega_n < \omega_{max}$.

iv) For each given critical input frequency, the system equations, Equation (5.4), are solved for the steady state bounce response.

v) The maximum value of the bounce response is evaluated and is then defined to be the objective function B.

vi) A direct search method of multivariable optimization is applied to minimize B.

5.4.4 The Optimization Technique. A computer algorithm based on Hooke and Jeeves optimization technique [30, 34] is used to carry out the multivariable optimization. In this algorithm, a direct search method followed by a random search check is used. The search proceeds by incrementing the value of each design variable along the direction which improves the objective function B, with the practical design range set by the constraints specified. Near the optimum value of B, the incremental values are halved, and the search is repeated until an assumed optimum is arrived at. The optimum value found is then checked by conducting a random search within the vicinity of the assumed optimum. The algorithm is stopped when no improvements along the optimum line can be reached.

5.4.5 Results of Optimization. The optimization procedure described in the flow chart in Fig. 5.22 is first started with an initial guess of the design variables $\underset{\sim}{X}_d$ being the original suspension parameters of the MAGLEV vehicle in which the shock absorbers are rigidly connected to the vehicle body, as seen in Table 5.1 No improvement was found along the optimization line, hence it is assumed that these values of the parameters are optimum, and they are referred to as the optimum suspension parameters with rigid K.

The optimization procedure is then repeated with the initial guess of the vector $\underset{\sim}{X}_d$ being the near optimum values for the suspension parameters obtained from the results of the parametric study; these values are essentially:

$K_0 = 5(100000.)N/m$, $K = 5(800000.)N/m$, $C = 5(10640.)N\cdot sec/m$.

The results obtained from the multivariable optimization procedure shows that the vehicle bounce response reaches an optimum value with the following set of design variables:

$K_0 = 5(100000.)N/m$, $C = 5(10640.)N\cdot sec/m$, $K_2 = K_3 = 800000.\ N/m$,

$K_1 = K_4 = K_5 = Rigid.$

This set of parameters will be referred to as optimum with flexible K, that is to designate the optimal suspension parameters of the vehicle model in which the shock absorbers are coupled to the vehicle body through spring elements with stiffness K.

It is to be noted at this point that a minimum value of K_0 will give better bounce response but will cause very high suspension system deflections; therefore, the design constraints set on the allowable

suspension systems deflections are the major factor in determining the values of the spring stiffnesses K_0's. Also, as for the shock absorbers setting, optimization could not be achieved along the proposed optimal line since changing the values of C would have a reversible effect on the vehicle bounce response as the input frequency is increased. This trend was previously discussed in section 5.3.

The optimum bounce responses for the two sets of optimum parameters, with rigid K and with flexible K, are plotted in Fig. 5.23. It can be seen that allowing K to be flexible reduces the peak response occurring around 5 rad/sec, by almost 50% and gives rise to a lower bounce acceleration levels for the entire frequency range of interest. The maximum suspension systems deflections were observed in both cases and were found to be acceptable. The effect of making a flexible connection between two of the shock absorbers and the vehicle body on the vehicle pitching response and the center levitation magnet bounce response is illustrated in Fig. 5.24 and Fig. 5.25 respectively. From Fig. 5.24, one can see that the optimal set of suspension parameters with a flexible K would yield lower values of the pitching angle at all frequency levels. However, from Fig. 5.25, it can also be seen that at high frequency levels, the system response for the suspension parameters with such flexible K produces higher levels of levitation magnet acceleration. Therefore, in selecting the values of the suspension systems parameters for design adaptation for the vehicle, all these conflicting aspects of the overall design problem should be considered.

5.5 Summary

In this chapter, a detailed parametric study is carried out to

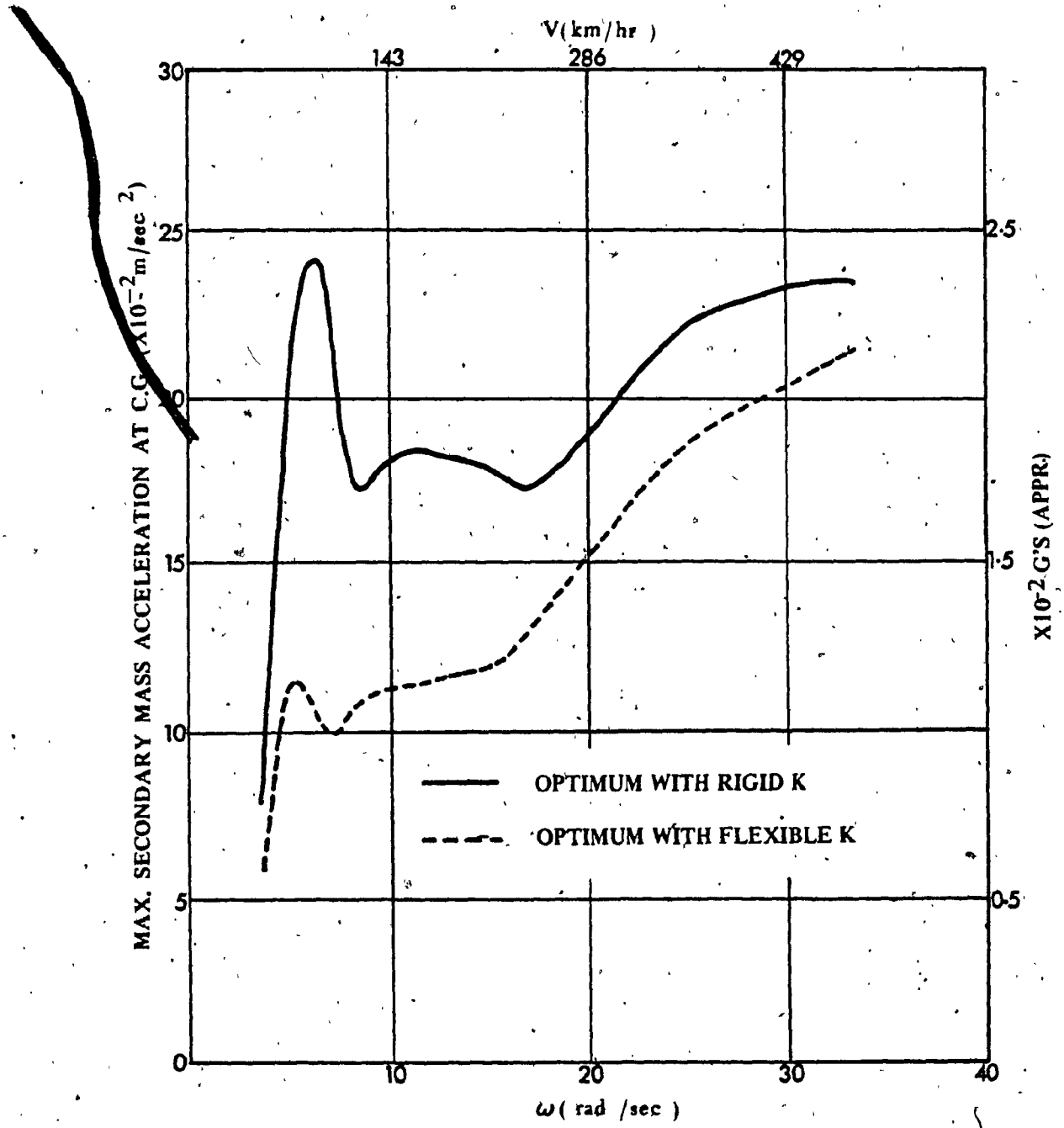

Fig. 5.23. Bounce Response of the Vehicle Body with the Optimum Suspension Parameters.

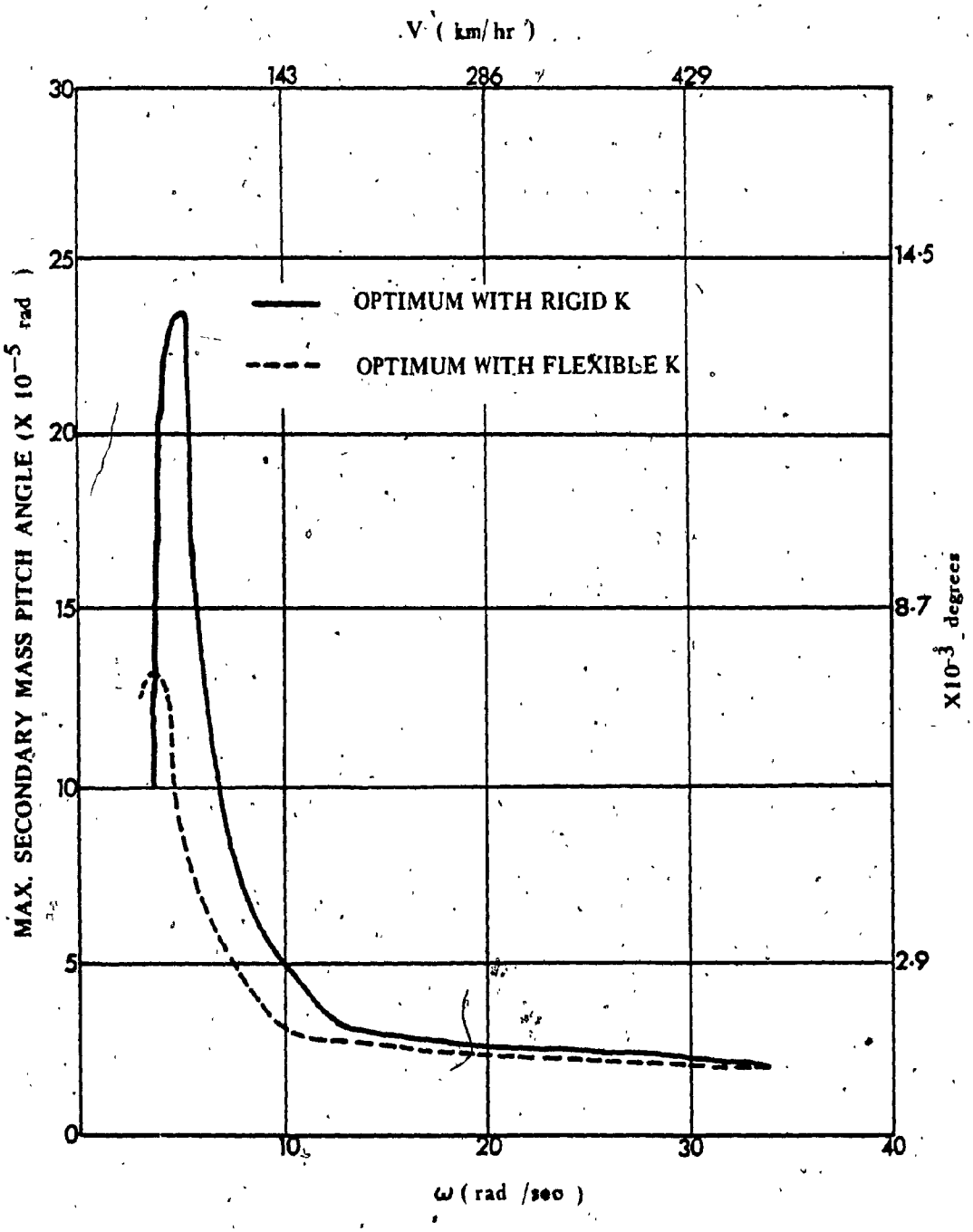

Fig. 5.24. Pitch Response of the Vehicle Body with the Optimum Suspension Parameters.

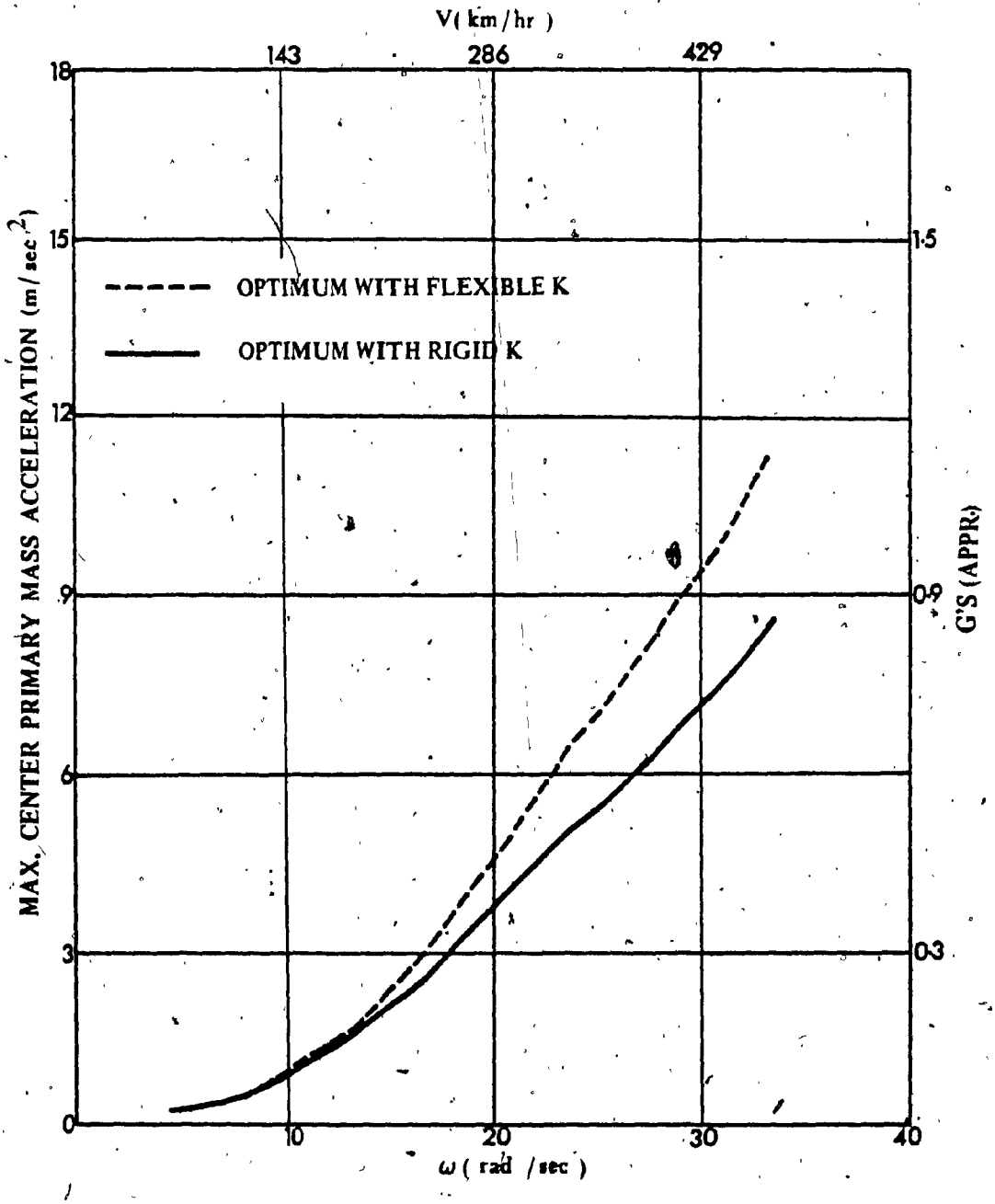

Fig. 5.25. Bounce Response of the Center Levitation Magnet with the Optimum Suspension Parameters.

find the sensitivity of the bounce acceleration response of the Canadian MAGLEV vehicle to different variations of the suspension constants. Also, the effect of varying the suspension systems parameters on the vehicle pitching response as well as the levitation magnets bouncing acceleration was observed. From the parametric study, the near optimum set of suspension parameters is found. Although useful, design recommendations made about the system are conflicting. Because of such conflict in the recommendations, a solution to the problem is sought by using rigorous multivariable optimization techniques. The results of the optimization show that the vehicle bounce acceleration levels can be minimized by installing spring elements between some of the shock absorbers and the vehicle body; however, this solution imposes a penalty of a 30% increase in the levitation bounce accelerations at the maximum vehicle cruising speed. Therefore, in choosing the values of the suspension systems parameters for design adaptation for the MAGLEV vehicle, all the conflicting aspects of the overall design problem should be assessed simultaneously. Up to this point, in this investigation, the input guideway excitation to the system was considered to be of a purely periodic form. An overall assessment to the vehicle dynamic response can only be made by considering the reality of the input forcing function to the vehicle as a combination of periodic and random processes and is discussed briefly in the following chapter.

CHAPTER 6

THE STOCHASTIC BOUNCE RESPONSE OF THE MAGLEV VEHICLE SYSTEM

6.1 Introduction

In the previous chapters the bounce response of the MAGLEV vehicle system was analysed using a deterministic approach and the effect of the vehicle input due to random guideway irregularities was neglected. For the vehicle bounce response problem, deterministic solution is only approximate since for the range of vehicle speeds considered the random component generated as excitation from the guideway irregularities becomes important. Therefore, for an accurate and complete investigation, the input excitation on the model should be described stochastically to include both the random as well as the periodic guideway irregularities and the stochastic bounce responses are to be described probabilistically.

6.2 Definition of the Stochastic Problem

The stochastic response of the vehicle system is derived in this chapter using the previously established linear model subjected to specified stochastic forcing function. To obtain the stochastic response of the system, the equations of motion are to be expressed in terms of state variables. The filter dynamic Equations (3.11) derived earlier, are incorporated into the vehicle Equation (4.17) in state form, in order to arrive at the state equation of the complete system that would now be subjected to a pure white noise input. This mathematical procedure, given in the study [29], is developed for nonlinear analysis of

freight cars and described in the following form.

The system Equations (4.17) in state form can be restated in the general form:

$$\dot{\underline{X}} = \underline{F}\underline{X} + \underline{B}_V \underline{U} \tag{6.1}$$

where

$\underline{X}$ is the vehicle response state vector,

$\underline{F}$ is the system matrix,

$\underline{B}_V$ is the associated system matrix, elements of which are defined in such a way that the product of $\underline{B}_V$ and $\underline{U}$ yields the vector representing the guideway input disturbance vector to the vehicle system in terms of a filtered white noise.

and

$\underline{U}$ is the vector of input forcing functions to the vehicle system in terms of a filtered white noise.

The input forcing function, $\underline{U}(t)$, to the system consists of both the periodic and random processes and was modeled in Chapter 3 as the output of a second order filter with a white noise input. The filter dynamic Equations (3.11) were given earlier and can be restated as:

$$\begin{aligned} \dot{\underline{\psi}}_{(10x1)} &= \underline{A}_{F(10x10)}\underline{\psi}_{(10x1)} + \underline{B}_{F(10x5)}\underline{W}_{(5x1)} \\ \underline{U}_{(5x1)} &= \underline{C}_{F(5x10)}\underline{\psi}_{(10x1)} + \underline{D}_{F(5x5)}\underline{W}_{(5x1)} \end{aligned} \tag{6.2}$$

Incorporating the filter Equations (6.2) into the system state Equations (6.1), the state equations of the complete system with a white noise input can be obtained in the following manner:

$$\begin{aligned} \dot{\underline{X}} &= \underline{F}\underline{X} + \underline{B}_V\underline{C}_F\underline{\psi} + \underline{B}_V\underline{D}_F\underline{W} \\ \dot{\underline{\psi}} &= \underline{A}_F\underline{\psi} + \underline{B}_F\underline{W} \end{aligned} \tag{6.3}$$

or in an alternate form:

$$\begin{bmatrix} \dot{X} \\ \dot{\psi} \end{bmatrix} = \begin{bmatrix} F & B_V C_F \\ 0 & A_F \end{bmatrix} \begin{bmatrix} X \\ \psi \end{bmatrix} + \begin{bmatrix} B_V D_F \\ B_F \end{bmatrix} W \qquad (6.4)$$

Equation (6.4) can be restated to represent the complete linear system in state variable form:

$$\dot{q}_0 = A_0 q_0 + B_0 W \qquad (6.5)$$

where W is the white noise input vector having a covariance matrix D defined in Equation (3.11).

6.3 The Instantaneous Response Covariance Matrix

Since the input white noise vector $W(t)$ to the complete system, Equation (6.5), is stationary and gaussian, then the response process will also be stationary and gaussian. Therefore, the response process is completely specified by the mean response vector and the instantaneous correlation matrix. The instantaneous covariance matrix for the system given in Equation (6.5) is defined by

$$P = E[q_0(t)\, q_0^T(t)] \qquad (6.6)$$

where the diagonal elements of P are the mean square values of the vector q_0.

For a linear system of equations forced by a white noise input, such as Equation (6.5), the differential equation for the covariance is [35]

$$\dot{P} = A_0 P + P A_0^T + Q \qquad (6.7)$$

If $\underset{\sim}{A}_0$ and $\underset{\sim}{Q}$ are constant matrices, the steady state solution to Equation (6.7) is found by setting $\dot{\underset{\sim}{P}} = \underset{\sim}{0}$, and therefore:

$$\underset{\sim}{A}_0\underset{\sim}{P} + \underset{\sim}{P}\underset{\sim}{A}_0^T = -\underset{\sim}{Q} \tag{6.8}$$

where $\underset{\sim}{Q}$ is a modified constant input covariance matrix defined by

$$\underset{\sim}{Q} = \underset{\sim}{B}_0 \underset{\sim}{D} \underset{\sim}{B}_0^T \tag{6.9}$$

The numerical solution of Equation (6.8) for the unknown elements of $\underset{\sim}{P}$, in terms of the elements of the matrices $\underset{\sim}{A}_0$ and $\underset{\sim}{Q}$, is detailed in the following section using the method described in [36].

6.4 Numerical Solution for the Response

The set of linear algebraic Equation (6.8), appears in many engineering applications and a fast and efficient solution for it has often been sought. An efficient numerical method for solving this equation, classically referred to as the Lyapunov's equation, was proposed by Davison [36], and is employed in the present analysis. The method assumes a solution for $\underset{\sim}{P}$ by a limiting process. That is:

$$\underset{\sim}{P} = \lim_{K\to\infty} \underset{\sim}{P}_K$$

where

$$\underset{\sim}{P}_{K+1} = (\underset{\sim}{\Gamma}^T)^{2^K} \underset{\sim}{P}(\underset{\sim}{\Gamma})^{2^K} + \underset{\sim}{P}_K, \quad K = 0,1,2,3....$$

and

$$\underset{\sim}{P}_0 = h_0 \underset{\sim}{Q}$$

where h_0 is the integration step size suggested to be 10^{-4} to 10^{-6}, and $\underset{\sim}{\Gamma}$ is the state transition matrix for the discrete homogeneous form of Equation (6.5), i.e., $\underset{\sim}{P}_{K+1} = \underset{\sim}{\Gamma}\underset{\sim}{P}_K$. Davison [36] shows that a good approximation for the state transition matrix $\underset{\sim}{\Gamma}$ is the Crank-Nicholson

expression:

$$\underset{\sim}{\Gamma} = \left(\underset{\sim}{I} - \frac{h_0}{2}\underset{\sim}{A}_0 + \frac{h_0^2}{12}\underset{\sim}{A}_0^2\right)^{-1}\left(\underset{\sim}{I} + \frac{h_0}{2}\underset{\sim}{A}_0 + \frac{h_0^2}{12}\underset{\sim}{A}_0^2\right)$$

Once Lyapunov's equation is solved on the digital computer, the diagonal elements of the matrix $\underset{\sim}{P}$ are the mean square values of the state variables. It is to be noted at this stage, that the acceleration of the passenger's compartment was not defined as a state; however, it is a linear combination of the states, that is:

$$\text{Acceleration} = \underset{\sim}{b}^T \underset{\sim}{q}_0$$

and

$$\overline{(\text{Acceleration}^2)} = \underset{\sim}{b}^T \underset{\sim}{P}\, \underset{\sim}{b}$$

where $\underset{\sim}{b}^T$ is a row of the $\underset{\sim}{A}_0$ matrix and $\overline{(\quad)^2}$ represents the RMS value.

The eigenvalues of the $\underset{\sim}{A}_0$ matrix are important as the values of their real parts give indications about the system stability. To ensure the stability of the system, the complex eigenvalues of the overall system real matrix $\underset{\sim}{A}_0$ are determined using a computer library subroutine EIGRF [37] for evaluation of complex eigenvalues of real matrices.

6.5 Evaluation of the Response Power Spectral Density

Performance specifications for the vehicle ride quality are commonly written in terms of acceleration power spectral density and so, in this case, the vehicle body acceleration power spectral density must be determined. For an acceptable ride quality, the suspension systems parameters must be chosen so that the passengers' compartment acceleration power spectral density falls within the specifications limit suggested.

For the system described by Equation (6.5), the state spectral density matrix $\underset{\sim}{S}_{qo}(\omega)$ can be expressed in terms of the input spectral density matrix $\underset{\sim}{S}_W(\omega)$ using the following expression:

$$\underset{\sim}{S}_{qo}(\omega) = (j\omega\underset{\sim}{I} - \underset{\sim}{A}_0)^{-1}\underset{\sim}{S}_W(\omega)(-j\omega\underset{\sim}{I} - \underset{\sim}{A}_0^T)^{-1} \qquad (6.10)$$

where the input white noise spectral density $\underset{\sim}{S}_W(\omega)$ is defined by:

$$\underset{\sim}{S}_W(\omega) = \frac{1}{2\pi}\underset{\sim}{Q} ,$$

$\underset{\sim}{Q}$ being the modified input covariance matrix defined in Equation (6.9).

The diagonal elements of $\underset{\sim}{S}_{qo}(\omega)$ are the spectral densities of the state variables. Since the velocity of the center of gravity is a state, then the acceleration density can be defined by:

$$S_{acc}(\omega) = \frac{2\pi}{(g)^2}(2\pi\omega)^2 S_{vel}(\omega) \qquad (6.11)$$

where S_{acc} is expressed in g^2/Hz units, V is expressed in m/sec, and ω is expressed in Hz.

A numerical solution for Equation (6.10) is obtained using computer library subroutines VMULFF [38] for matrix multiplications and LINV2F [39] for matrix inversion from the International Mathematical Subroutine Library (IMSL), for each frequency value ω within the bandwidth of human body sensitivity of about 0.1 to 60 Hz. The numerical values of the velocity power spectral density obtained from the solution of Equation (6.10) are then used to calculate the bounce acceleration power spectral density through proper substitutions in Equation (6.11). The bounce response power spectral density is generated through this procedure for different sets of suspension systems parameters, the results obtained are plotted and analysed in the following section.

6.6 Discussion of the Results

In order to evaluate the dynamic response of the vehicle under random excitation or a combination of periodic and random track input, a single parameter describing the bounce response under stochastic excitation should be selected to represent the true performance of the system. This parameter can be chosen to be either the mean square bounce acceleration evaluated over the entire range of the vehicle speeds or just the power spectral density of the vehicle body bounce acceleration. Since the ride quality specification adopted for the design of the Canadian MAGLEV vehicle are those recommended by the U.S. Department of Transport, which is the originally defined as Urban Tracked Air Cushion Vehicle (U.T.A.C.V.) specifications, they are given in terms of vertical acceleration power spectral density for the bounce mode of vibration. Hence, it may be recommended that it is suitable to evaluate the bounce response of the vehicle in terms of its acceleration power spectral density rather than the mean square response of the acceleration.

The bounce acceleration power spectral density of the vehicle under random excitation is plotted in Figs. 6.1, 6.2, and 6.3 for different values of suspension systems parameters. From these figures, it may be observed that the bounce acceleration power spectral density responses exhibit two peak values, the first one occurring at a frequency of about 0.87 Hz corresponding to the pitching natural frequency of the vehicle, and the other peak occurring at a frequency band around the breakpoint frequency of 5.3 Hz corresponding to a vehicle speed of 480 km/hr (300 mph) and a guideway span length of 25 m (82 ft). It can also be observed

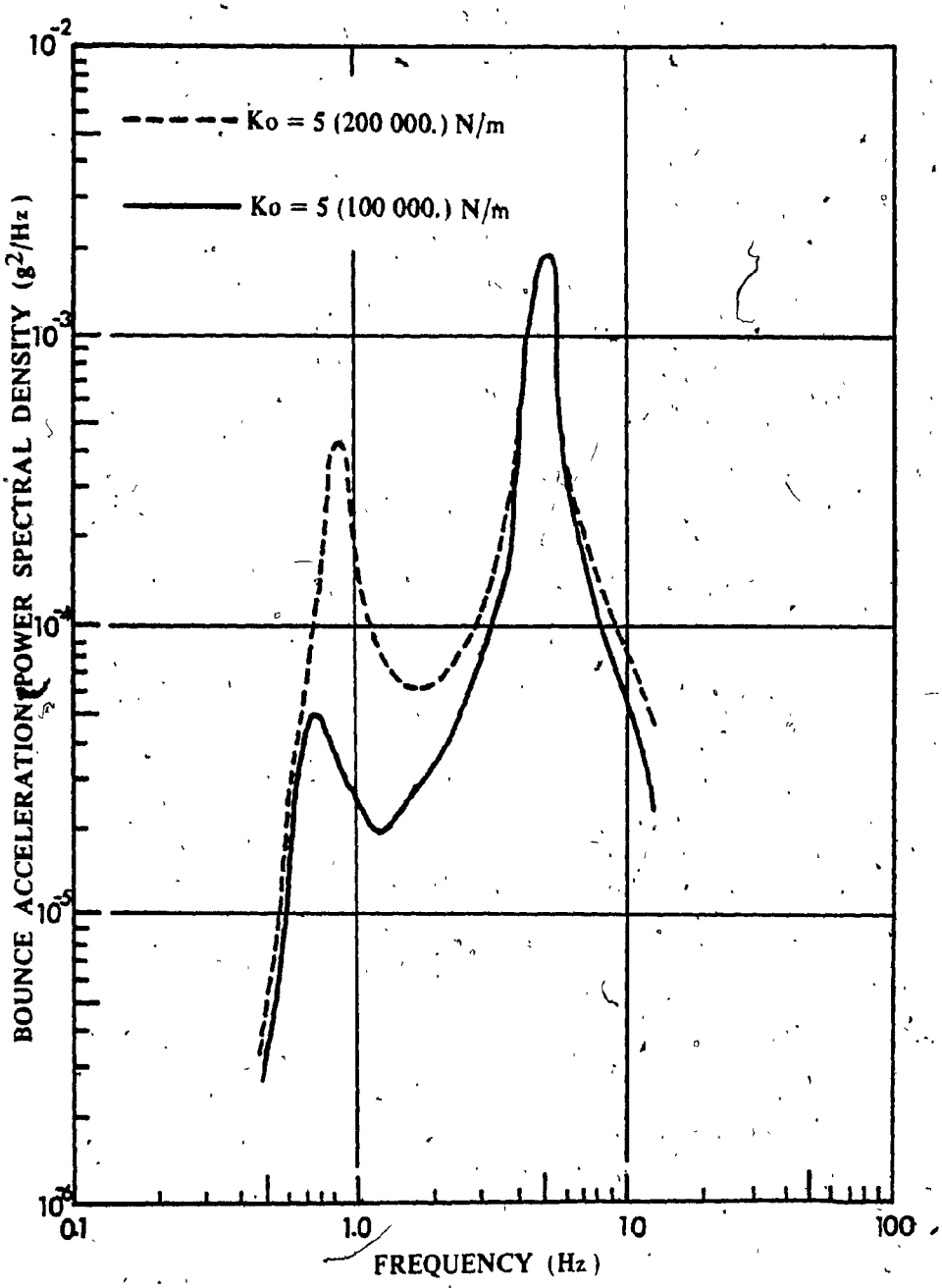

Fig. 6.1. Effect of K_0 on the Vehicle Bounce Acceleration Power Spectral Density.

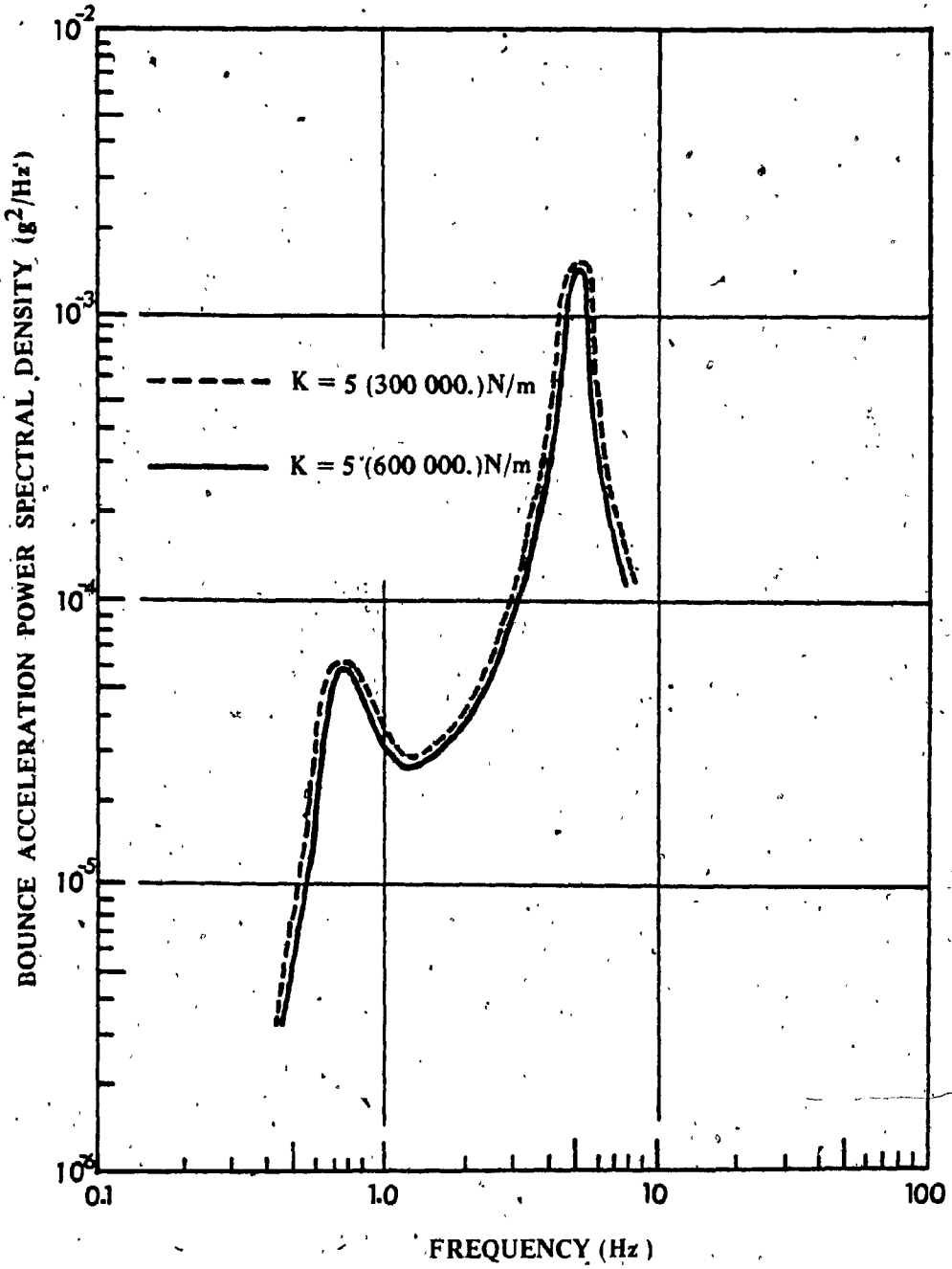

Fig. 6.2. Effect of K on the Vehicle Bounce Acceleration Power Spectral Density.

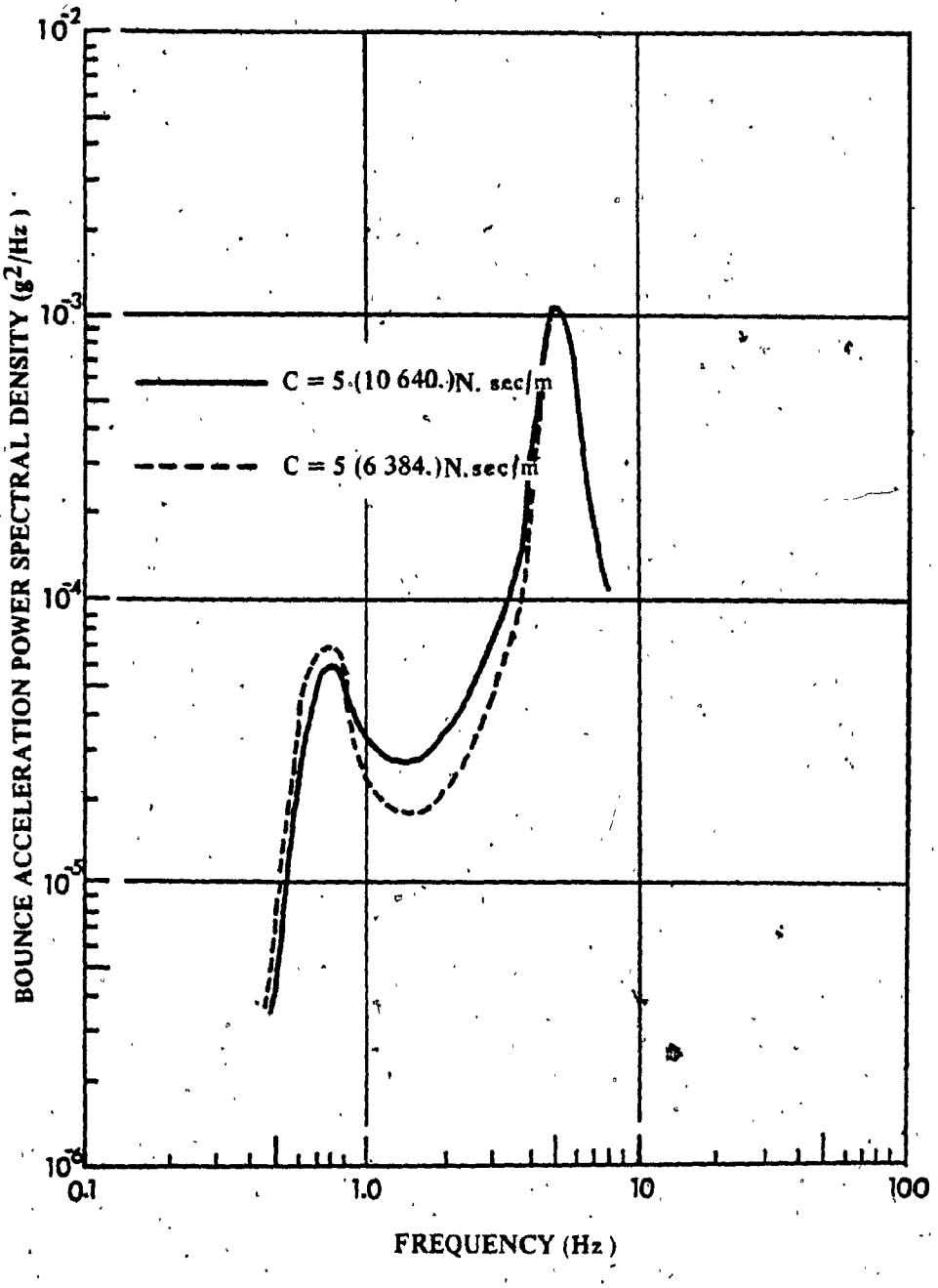

Fig. 6.3. Effect of C on the Vehicle Bounce Acceleration Power Spectral Density.

that the effect of varying the suspension system parameters on the system response with the system under stochastic input excitation is consistent with the results observed in Chapter 5 when the system response was obtained for purely periodic input excitation. Therefore, the same design approach can be adopted for specifying suspension elements and the optimum set of suspension parameters obtained from multivariable optimization techniques for the deterministic analysis may also be considered to be optimum for the case of conclusions based on the stochastic study. Optimum response curves for the vehicle body bounce acceleration power spectral density are generated, using the mathematical procedure outlined in section 6.5, for different guideway span lengths and are shown in Figs. 6.4, 6.5, and 6.6. Also plotted on these curves are the U.T.A.C.V. ride quality specifications as recommended by the U.S. Department of Transport. From Fig. 6.4, it can be seen that for a standard guideway span length of 25 m the vehicle response exceeds the U.T.A.C.V. specifications in the frequency bandwidth of about 5.4 to 10.5 Hz, and hence it can be concluded that a totally acceptable ride quality cannot be achieved for all speeds with the deployment of passive suspension systems only. The National Research Council of Canada [5], considered guideway spans of up to 45 m in their dynamic analysis of the vehicle system bounce response under stochastic input excitations and they recommended the use of passive suspension systems employing a simplified two-degree-of-freedom vehicle model. Their recommendations contradict the results shown in Fig. 4.5 which indicate that the vehicle response under purely random excitations is well within the ride quality specifications, while the response under a combination of periodic and random input processes becomes marginally acceptable. This contradiction

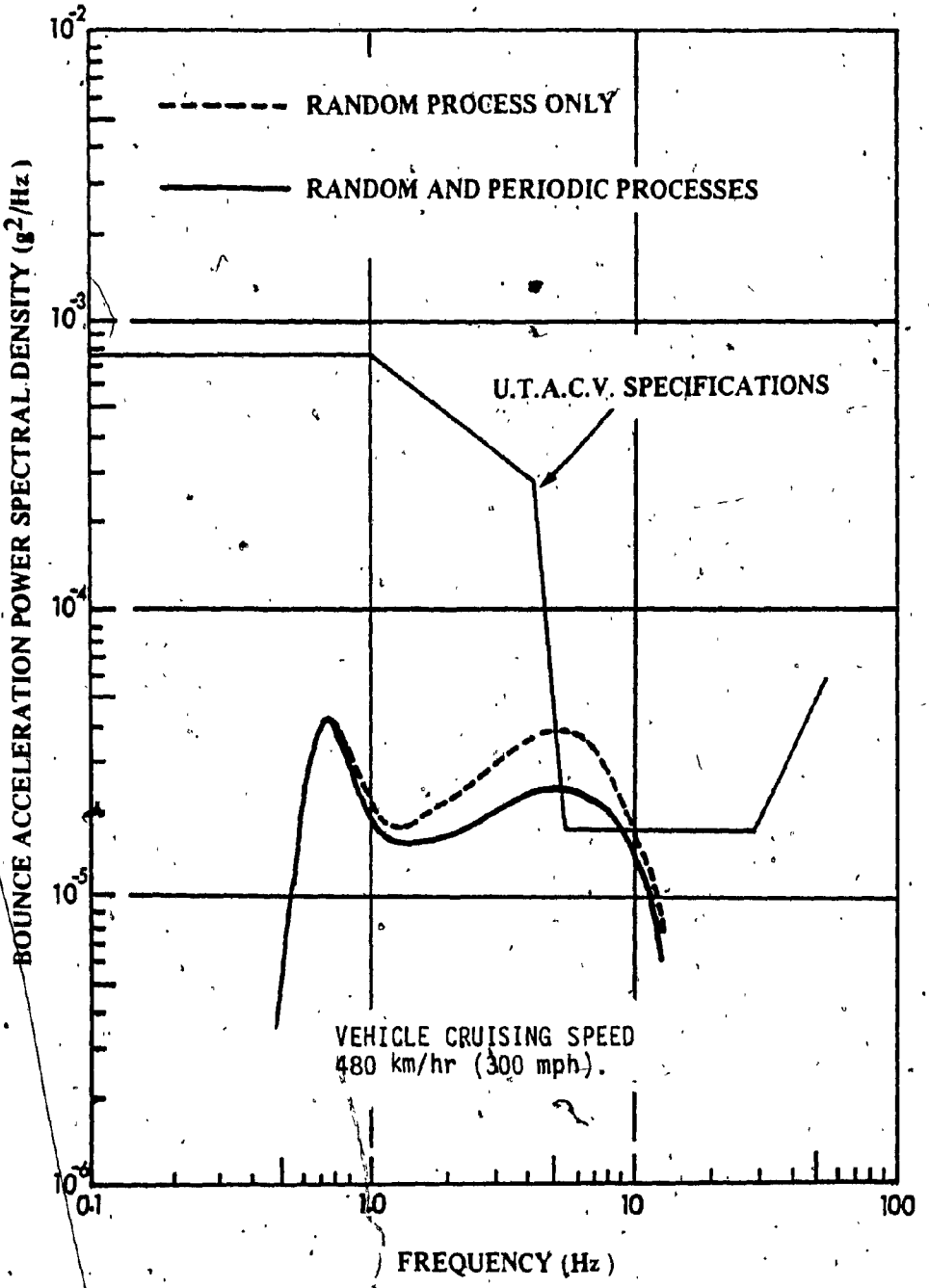

Fig. 6.4. The Power Spectral Density of the Vehicle Bounce Acceleration with Guideway of 25 m for Optimal Suspension Values.

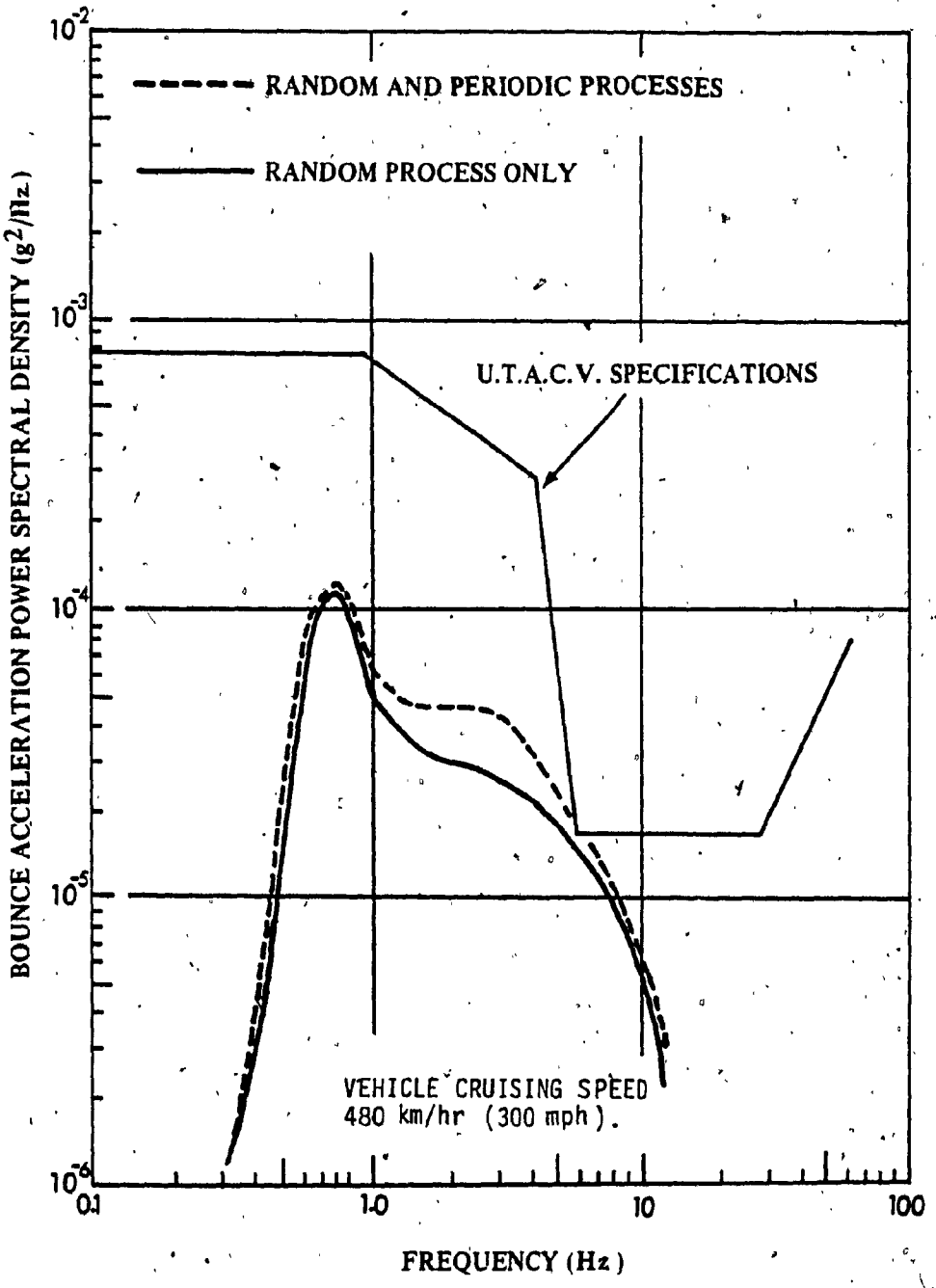

Fig. 6.5. The Power Spectral Density of the Vehicle Bounce Acceleration with Guideway Span of 45 m for Optimal Suspension Values.

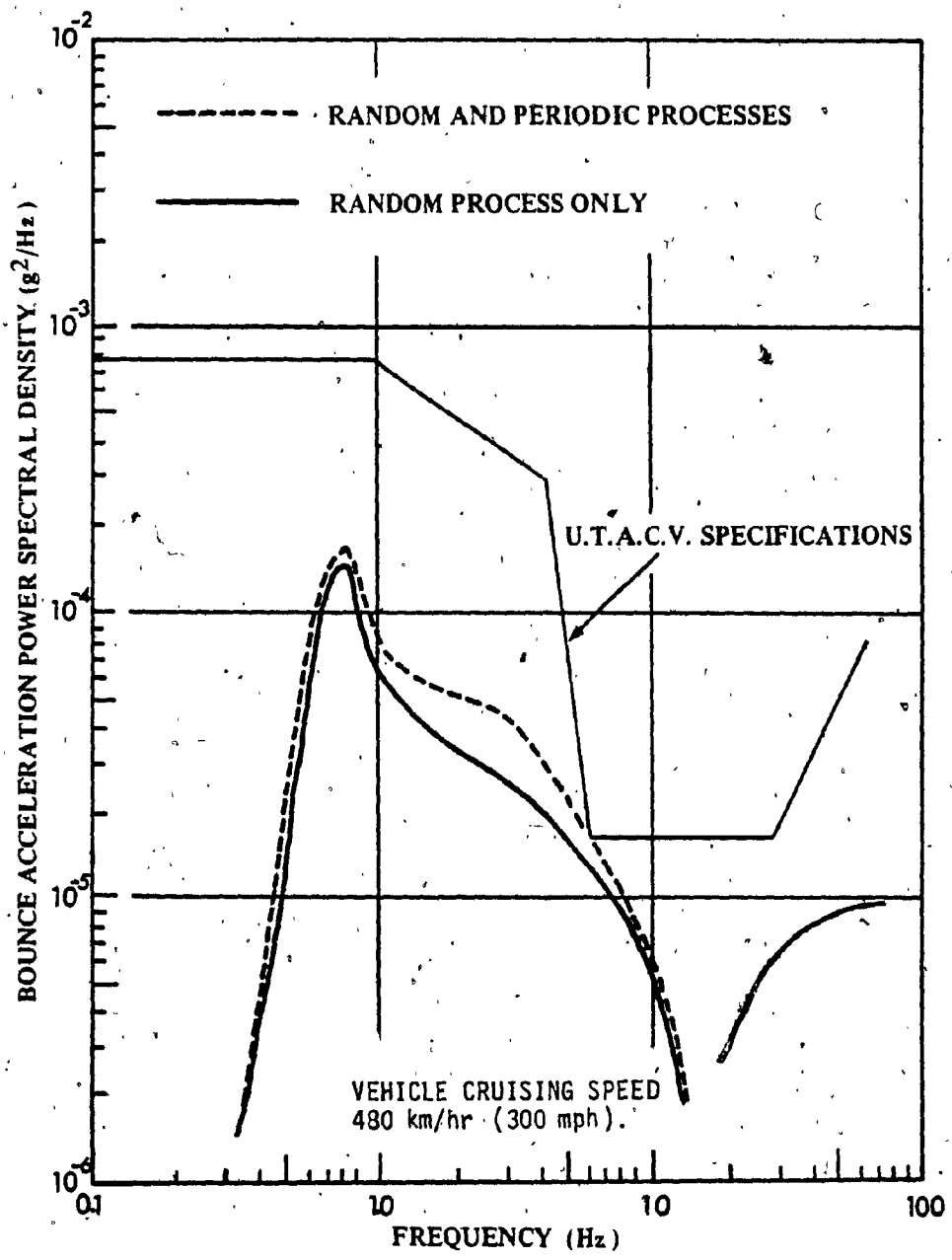

Fig. 6.6. The Power Spectral Density of the Vehicle Bounce Acceleration with Guideway Span of 50 m for Optimal Suspension Values.

in the recommendations is attributed to the facts that the model used in [5] was oversimplified and does not truly represent the actual vehicle behavior; also the use of the modified mechanical suspension system proposed in this investigation yields a limited bounce response of the vehicle system for all input options, namely, purely periodic, purely random, or a combination of periodic and random processes. Further, it can be seen from Fig. 6.6 that with a further increase in the guideway span length, say to 50 m, the vehicle response can be brought well within the limits for achieving an acceptable ride quality under both random and a combination of periodic and random input excitations induced by the guideway.

6.7 Summary

For deriving a complete description of the vehicle dynamic response, the system excitation is modeled to include both the periodic and the random guideway irregularities. Numerical techniques used to generate the response power spectral density are outlined. Ride quality limits according to previous governmental specifications are set for specifying optimal suspensions. A parameter sensitivity analysis is carried out and the optimal suspension parameters that would yield a minimum of the maximum bounce acceleration response are determined. The optimum bounce acceleration response is studied for different guideway span lengths and appropriate design recommendations are made.

CHAPTER 7

CONCLUSIONS AND RECOMMENDATIONS

7.1 Highlights of the Investigation

This investigation has attempted to provide a detailed study on those aspects of the design performance of the mechanical suspension systems controlling the bounce response of the Canadian MAGLEV vehicle under all forms of input excitations from the guideways. The analytical approach employed in this study can be generally applied to the dynamic analysis of any similar high speed vehicles.

Based on an improved linear mathematical model, the dynamic responses of the MAGLEV vehicle are determined when the vehicle is subjected to either a purely periodic or a combination of periodic and random input excitations from the guideways. The analysis is focused particularly on the bounce mode of vibration of the vehicle body since the bounce acceleration level of the passenger compartment is a primary indication of the vehicle ride quality. Additional attention is also given to the pitching response of the vehicle body as well as to the bounce responses of the levitation magnets. The equations of motion of the system under deterministic and stochastic inputs are solved using standard techniques for the state variables representing the system response. Both parameter sensitivity analysis and multivariable optimization technique are applied in order to ascertain the optimal mechanical suspension parameters that would minimize an objective function representing the maximum vehicle body bounce acceleration response over the frequency range of interest.

The major contributions of the investigation presented in this thesis can be summarized as follows:

i) An effective linear physical model is developed for describing the bounce response of the Canadian MAGLEV vehicle more accurately than before. A modified mechanical suspension system is considered in this model to allow for some flexibility in the choice of suspension arrangements.

ii) The input excitations to the vehicle are realistically modeled through a purely periodic process or a combination of periodic and random processes, to account for any particular dominant guideway irregularities.

iii) The bounce acceleration and the pitching angle of the vehicle body along with the bounce acceleration of the levitation magnets are evaluated as a function of the vehicle speed and for different suspension configurations when the vehicle is subjected to guideway excitations modeled as a periodic process.

iv) A complete parameter sensitivity analysis and, further, a multivariable optimization technique are employed to yield optimum values of the suspension system that would minimize the bounce acceleration of the vehicle body under deterministic input process.

v) The combined periodic and random excitation from the guideways is modeled in the form of input spectral density using available data [5]. A linear filter was designed in such a way to produce the required output (actual input to the vehicle) for

a specified white noise input. The dynamic equations of the filter are combined with the state equations of the vehicle to determine the response power spectral density describing the bounce acceleration.

vi) The effect of the optimal suspension values arrived at under (iv) on the bounce acceleration power spectral density of the vehicle is studied to determine the ride quality when the vehicle is subjected to a combination of periodic and random guideway induced excitations.

7.2 Discussion of the Results

In this investigation, two different mechanical suspension system configurations for the Canadian MAGLEV vehicle are considered. The first arrangement couples the vehicle body to the levitation magnets through suspension systems represented by a parallel connection of a shock absorber with a stiffness element. In the second model, the suspension system is represented by a shock absorber connected in series with a stiffness element and the combination is in turn connected in parallel with another stiffness element. Response curves generated for the two suspension models exhibit similar dynamic characteristics for the vehicle. The bounce responses of the vehicle in the frequency domain, generated over the vehicle operating speed range, show that the bounce acceleration builds up to a peak level occurring at a frequency value corresponding to the pitch natural frequency of the vehicle system after which it decays to a minimum value; thereafter, this response oscillates around this minimum value and then builds up again with an increasing vehicle speed thus indicating a beat phenomenon.

The study of the sensitivity of the system response to variations in a single suspension parameter at a given time shows that, for the entire frequency domain of interest, the system bounce response can be improved by lowering the spring stiffness of the element connected in parallel with the shock absorbers. A disadvantage of this arrangement would be to cause large initial deflections of the vehicle, particularly during loaded stationary states and perhaps may lead to inefficient braking. The effect of the variations in the different suspension parameters on the vehicle body pitch response, the levitation magnets bounce responses as well as on the initial deflections of the suspension systems were also further studied. Useful but somewhat conflicting parameter sensitivity analysis and hence a further investigation techniques was taken up. The results of the optimization program clearly showed that the bounce response of the vehicle can be improved using the proposed modified mechanical suspension system configuration in which the shock absorbers are elastically coupled to the vehicle body through a series connection with a stiffness element.

For a better evaluation of the vehicle ride quality, the analysis was extended to the case when the vehicle is subjected to a purely random or a combination of periodic and random input processes and a method for obtaining the vehicle bounce acceleration power spectral density is outlined. The bounce acceleration power spectral density responses exhibit two peak values; one occurring at a frequency of 0.87 Hz that corresponds to the pitch natural frequency of the vehicle, and the other peak occurs at 5.3 Hz which is the breakpoint frequency due to the segmented nature of the multispan guideway structure. All aspects of

the power spectral density response are generated for different values of the suspension parameters.

The parameter sensitivity analysis and the quasi-optimization study reported in this case employed an objective to minimize the bounce acceleration power spectral density over the frequency range of interest. The results obtained from this study basically confirmed the conclusions arrived at from the previous deterministic analysis and optimization. The bounce acceleration power spectral density responses with the optimum suspension parameters are then used to evaluate the vehicle ride quality for different guideway spans for comparison with the U.T.A.C.V. specifications. It is found that for a standard guideway span (25 m) the ride quality is unacceptable for the frequency bandwidth of 5.4 to 10.5 Hz. Also for a guideway span of 45 m as in the case of the National Research Council of Canada [5], the ride quality is only marginally acceptable indicating slightly longer span requirement. As expected, the response envelope is well within the specifications for a guideway span of 50 m. All the responses were generated for a standard vehicle cruising speed of 480 km/hr (300 mph).

7.3 Recommendations for Future Study

The investigation presented in this thesis provides useful design information on the bounce dynamics of the Canadian MAGLEV vehicle. The mathematical model and the analytical solutions of this analysis is formulated on a general basis and could be easily extended for the investigation of the lateral vibrations of the vehicle particularly when the aerodynamic excitations due to cross wind gusts become significant.

The mathematical model developed in this analysis considered all

suspension systems to behave linearly by assuming small oscillations of the vehicle about its equilibrium position. A more general and perhaps realistic approach would be to include the nonlinear characteristics of some of the suspension elements and evaluate the vehicle responses based on a nonlinear mathematical model.

Lastly, this investigation has considered the guideway and support structures to provide essentially a rigid foundation for vehicle support. Although this is a reasonable assumption, accuracy of the results may be improved if the pertinent details of the guideway structural design leading to a formulation of the different guideway parameters that affect the vehicle responses are taken into account. This means that the flexibility of the guideway, its pier supports and their foundations are to be included in the dynamic analysis of the vehicle, particularly in view of the coupling effects between the vehicle and the guideway structure.

REFERENCES

1. Richardson, H.H. and Wormley, D.N., "Transportation Vehicle/Beam - Elevated Guideway Dynamic Interactions: A State-of-the-Art Review", Trans. ASME, Journal of Dynamic Systems, Measurement, and Control, Vol. 96 G, June 1974, pp. 169-179.

2. Limbert, D.A., Richardson, H.H. and Wormley, D.N., "Controlled Dynamic Characteristics of Ferromagnetic Vehicle Suspensions Providing Simultaneous Lift and Guidance", Trans. ASME, Journal of Dynamic Systems, Measurement, and Control, Vol. 101 G, September 1979, pp. 217-222.

3. Ooi, B.T., "Electromechanical Stiffness and Damping Coefficients in the Repulsive Magnetic Levitation System", IEEE Transactions on Power Apparatus and Systems, Vol. PAS-95, No. 3, May/June 1976, pp. 936-943.

4. Milner, J.L., "Dynamics of Magnetic Levitation Suspension Systems for High Speed Ground Vehicles", Surveys of Research in Transportation Technology, AMD - Vol. 5, Trans. ASME, 1973.

5. Hayes, W.F., "High Speed Electrodynamic MAGLEV Guided Ground Transportation System Conceptual Design Study", National Research Council Laboratories, Report No. LTR-CS-176, September 1977.

6. "Superconducting Magnetic Levitation and Linear Synchronous Motor Propulsion for High Speed Ground Transportation", Phase III Final CIGGT Report No. 77-13, Canadian Institute of Guided Ground Transport, Queen's University, Kingston, Ont., September 1977.

7. Laithwaite, E.R., "Transport Without Wheels", ELECK Science, London, 1977.

8. Ward, J.D., "The Future Roles for Tracked Levitated Vehicle Systems", Trans. ASME, Journal of Dynamic Systems, Measurement, and Control, Vol. 96 G, June 1974, pp. 117-127.

9. "Superconducting Magnetic Levitation and Linear Synchronous Motor Propulsion for High Speed Ground Transportation", Phase III CIGGT Report No. 75-5, Canadian Institute of Guided Ground Transport, Queen's University, Kingston, Ont., March 1975.

10. "Superconducting Linear Synchronous Motor Propulsion and Magnetic Levitation for High Speed Guided Ground Transportation", Phase III Interim CIGGT Report No. 76-7, Canadian Institute of Guided Ground Transport, Queen's University, Kingston, Ont., March 1976.

11. Atherton, D.L., Bélanger, P.R., Burke, P.E., Dawson, G.E., Eastham, A.R., Hayes, W.F., Ooi, B.T., Silvester, P. and Slemon, G.R., "The Canadian High Speed Magnetically Levitated Vehicle System", Canadian Electrical Engineering Journal, Vol. 3, No. 2, 1978.

12. Howell, J., "A Consideration of Some Aerodynamic Problems Related to Advanced Ground Transport", Magnetic Levitation Group, Department of Engineering, University of Warwick, Coventry, March 1979.

13. Bélanger, P.R. and Guillemette, R., "Passive Suspension Design for a Magnetically Levitated Vehicle", Trans. ASME, Journal of Dynamic Systems, Measurement, and Control, Vol. 99 G, December 1977, pp. 277-283.

14. Biggers, S.B. and Wilson, J.F., "Dynamic Interactions of High Speed Tracked Air Cushion Vehicles with Their Guideways Part I of a Parametric Study", Trans. ASME, Journal of Dynamic Systems, Measurement, and Control, Vol. 95 G, March 1973, pp. 76-85.

15. Chung, Y.I. and Genin, J., "Stability of a Vehicle on a Multispan Simply Supported Guideway", Trans. ASME, Journal of Dynamic Systems, Measurement, and Control, Vol. 100 G, December 1978, pp. 326-332.

16. Smith, C.C., Gilchrist, A.J. and Wormley, D.N., "Multiple and Continuous Span Elevated Guideway - Vehicle Dynamic Performance", Trans. ASME, Journal of Dynamic Systems, Measurement, and Control, Vol. 97 G, March 1975, pp. 30-41.

17. Doran, A.L. and Mingori, D.L., "Periodic Motion of Vehicles on Flexible Guideways", Trans. ASME, Journal of Dynamic Systems, Measurement, and Control, Vol. 99 G, December 1977, pp. 268-277.

18. Chiu, W.S., Smith, R.G. and Wormley, D.N., "Influence of Vehicle and Distributed Guideway Parameters on High Speed Vehicle-Guideway Dynamic Interactions", Trans. ASME, Journal of Dynamic Systems, Measurement, and Control, Vol. 93 G, March 1971, pp. 25-34.

19. Snyder, III J.E. and Wormley, D.N., "Dynamic Interactions Between Vehicles and Elevated, Flexible Randomly Irregular Guideways", Trans. ASME, Journal of Dynamic Systems, Measurement, and Control, Vol. 99 G, March 1977, pp. 23-33.

20. Wilkie, D.F., "Dynamics, Control and Ride Quality of a Magnetically Levitated High Speed Ground Vehicle", Transportation Research, Vol. 6, 1972, pp. 343-369.

21. Katz, R.M., Nene, V.D., Ravera, R.J. and Skalski, C.A., "Performance of Magnetic Suspensions for High Speed Vehicles Operating Over Flexible Guideways", Trans. ASME, Journal of Dynamic Systems, Measurement, and Control, Vol. 96 G, June 1974, pp. 204-212.

22. Hullender, D.A., Wormley, D.N. and Richardson, H.H., "Active Control of Vehicle Air Cushion Suspensions", Trans. ASME, Journal of Dynamic Systems, Measurement, and Control, Vol. 94 G, March 1972, pp. 41-49.

23. Margolis, D.L., Tylee, J.L. and Hrovat, D., "Heave Mode Dynamics of a Tracked Air Cushion Vehicle with Semiactive Airbag Secondary Suspension", Trans. ASME, Journal of Dynamic Systems, Measurement, and Control, Vol. 97, December 1975, pp. 399-407.

24. Crosby, M.J. and Karnopp, D.C., "The Active Damper - A New Concept for Shock and Vibration Control", The Shock and Vibration Bulletin, Part 4, June 1973, pp. 119-132.

25. Hedrick J.K., Billington, G.F. and Dreesbach, D.A., "Analysis, Design, and Optimization of High Speed Vehicle Suspensions Using State Variable Techniques", Trans. ASME, Journal of Dynamic Systems, Measurement, and Control, Vol. 96 G, No. 2, June 1974, pp. 193-203.

26. Samaha, M. and Sankar, T.S., "Dynamic Rocking Response and Optimization of the Nonlinear Suspension of a Railroad Freight Car", Trans. ASME, Journal of Mechanical Design, Vol. 102, No. 1, January 1980, pp. 86-93.

27. Samaha, M. and Sankar, T.S., "An Analog Simulation Study of the Rocking Response of a Railroad Freight Vehicle", Journal of Sound and Vibration, 1979, pp. 109-124.

28. Elmaraghy, W.H., Dokainish, M.A. and Sidall, J.N., "Minimax Optimization of Railway Vehicle Suspension", ASME Paper No. 74-WA/RT-3, November 1974.

29. Samaha, M.A., "Dynamic Response and Optimization of a Railroad Freight Car under Periodic and Stochastic Excitations", D.Eng. Thesis, Concordia University, March 1978.

30. Sidall, J.N., "OPTISEP", Designers Optimization Subroutines, McMaster University, Hamilton, Ontario, 1970.

31. Young, J.W. and Wormley, D.N., "Optimization of Linear Vehicle Suspensions Subjected to Simultaneous Guideway and External Force Disturbances", Trans. ASME, Journal of Dynamic Systems, Measurement, and Control, Vol. 95 G, June 1973, pp. 213-219.

32. Hullender, D.A., "Analytical Models for Certain Guideway Irregularities", Trans. ASME, Journal of Dynamic Systems, Measurement, and Control, Vol. 97 G, December 1975, pp. 417-423.

33. Scientific Subroutine Package, "HPCG", Computer Center, Concordia University, Montreal.

34. Jacoby, S.L.S., Kowalik, J.S. and Pizzo, J.T., "Interative Methods for Nonlinear Optimization Problems", Prentice-Hall, New Jersey, 1972, pp. 71-79/

35. Gresch, W., "Mean-Square Responses in Structural Systems", Journal of the Acoustical Society of America, Vol. 48, No. 1, Part 2, July 1970, pp. 403-413.